International
Progress Report

IPR-02-26

Äspö Hard Rock Laboratory

TRUE Block Scale Project

Investigation of effect of structural model updates on response to simulated tracer tests

Xavier Rachez
Daniel Billaux

Itasca Consultants S.A.

October 2002

Svensk Kärnbränslehantering AB
Swedish Nuclear Fuel
and Waste Management Co
Box 5864
SE-102 40 Stockholm Sweden
Tel +46 8 459 84 00
Fax +46 8 661 57 19

Äspö Hard Rock
Laboratory

Report no.
IPR-02-26
No.
F56K
Author
Xavier Rachez
Daniel Billaux
Date
Oct 2002
Checked by
Anders Winberg
Date
Jan 2003
Approved
Christer Svemar
Date
June 2003

Äspö Hard Rock Laboratory

TRUE Block Scale Project

Investigation of effect of structural model updates on response to simulated tracer tests

Xavier Rachez
Daniel Billaux

Itasca Consultants S.A.

October 2002

Keywords: Evolution, fracture, hydrostructural, model, numerical, response, simulation, tracer test

Abstract

ANDRA has been involved for over 4 years in the TRUE Block Scale project, an integrated flow and transport program including in situ experiments and modeling, run at the Äspö Hard Rock Laboratory, in Sweden. This experiment has been using an iterative approach to characterisation: one borehole is drilled, data is obtained from this borehole and integrated into the model of the block, and then a new borehole is discussed : is it needed? If yes, where should it be drilled and with what geometry? This approach, together with reprocessing of previously acquired data and with further testing in existing boreholes, has resulted in a number of successive updates of the hydrostructural model for the block, in order to accommodate incompatibilities between the new-incoming data and the « old » model. One may question how much the model upgrades contributed to enhancing their predictive and explanatory power with regard to tracer transport : suppose one had to give a blind prediction of an experiment to be performed later. What would have been the prediction for this experiment at each stage of model upgrading? How much would this have changed? Finally, how much better would a prediction based on our current knowledge, embodied in the latest model, turn out compared to ones using prior versions of the model? In order to address these questions, four successive numerical models of the TRUE Block Scale volume were constructed with *3FLO*, the 3D flow and transport code developed by ITASCA Consultants SA, corresponding to four successive stages of the characterisation process: Scoping stage, Preliminary Characterisation stage, Detailed Characterisation stage and Tracer test stage. Three tracer tests were simulated. The models take into account both deterministic structures, and stochastic background fractures, with conditioning where data are available.Twelve “forward” simulations (three tracer tests per model) were carried out, using the properties specified by the hydrostructural models available at each stage, choosing the injections points, in the earlier models, to represent the real injection points as closely as possible. In these tests, we could see how the variation of the transport path geometry, from model to model, progressively looses similarity with the test responses, until the Scoping Characterisation model response has very little to do with the based on the Tracer test stage model response.The transport parameters of the Tracer test stage model were calibrated simultaneously to the three tests, by changing the properties of Structures # 13, 19 and 23. This resulted in a significantly improved, if not perfect, fit between the simulated and measured tracer breakthrough. On the other hand, using the new properties in the older models essentially did not improve their response, which still were degraded when going back in time.In addition, ten “synthetic” injection points were simulated. These “synthetic” points do not correspond to any real experimental result, but comparing the behaviour of the tracers injected there from model to model shows that the four successive hydrostructural models are clearly very different in their response to tracer tests performed in the area of interest, while the change in properties imposed during calibration has a small influence on the overall response.In this work, we could see clearly how, in the TRUE Block Scale site, the response to tracer tests is strongly conditioned by the hydrostructural model used. Because most of the tracers travel along a limited number of interpreted deterministic structures, proper knowledge of their geometry is a requisite for being able to represent the actual in situ network behaviour were realistically.

Sammanfattning

TRUE Block Scale, ett integrerat program för undersökning av flöde och transport som innefattar både *in situ* försök och numerisk modellering, har genomförts i Äspölaboratoriet. Projektet har utnyttjat en iterativ metodik i den utförda karakteriseringen: ett borrhål borras och karakteriseras, resultaten integreras i en beskrivande strukturmodell av den undersökta bergvolymen. Ett nytt karakteriseringsborrhål övervägs därefter. Behövs ett nytt borrhål över huvud taget?! Om svaret är ja, var skall det borras och med vilken geometri (lutning och längd)? Den utnyttjade metodiken sammantaget med utnyttjande av tidigare insamlad information har resulterat i ett antal uppdateringar av den beskrivande modellen i tre dimensioner. Detta för att hantera inkonsistenser mellan nya karakteriseringsdata och den existerande ”äldre” modellen. Det kan vara på sin plats att ställa frågan hur mycket den genomförda modelluppdateringen har bidragit till att öka motsvarande numeriska modellers prediktiva och förklarande förmåga med avseende på transport av lösta substanser. Om en ”blind” förutsägelse skulle lämnas för ett försök som skall genomföras senare – hur skulle en sådan förutsägelse se ut för modelluppgarderingar med olika grad av ”mognad”? Hur mycket skulle dess förutsägelser förändras med tiden? Slutligen, hur mycket bättre skulle en modellförutsägelse baserad på vår nuvarande kunskap vara i förhållande till en som är baserad på tidigare versioner av den beskrivande modellen? För att besvara dessa frågor har fyra numeriska modeller av TRUE Block Scale-volymen kostruerats med hjälp av 3FLOW (utvecklad av Itasca), motsvarande fyra väldefinierade steg i karakteriseringsprocessen, i vilka tre olika spårförsök simulerades. Modellerna inkluderar både deterministiskt modellerade strukturer samt stokastiskt beskrivna bakgrundssprickor. För de genomförda simuleringarna (tre per modell) utnyttjades de olika materialegenskaper som tillskrevs modellerna vid de aktuella tidpunkterna. I resultatet av dessa simuleringar kan man se en klar variation i geometrin hos de utvecklade transportvägarna. Vidare kan man notera en successivt försämring i överensstämmelsen mellan mätta resultat (genombrottskurvor) och simulerade resultat när successivt äldre modeller utnyttjades. Transportparametrarna för den senaste beskrivande modellen kalibrerades simultant relativt mätta resultat genom att justera egenskaperna hos Strukturerna #13, #19 och #23. Detta resulterade i signifikant förbättrad överensstämmelse mellan simulerade och mätta genombrottskurvor. Utnyttjande av dess kalibrerade transportparametrar i de äldre modellerna förbättrade inte deras responser i förhållande till mätta data Vidare simulerades genombrott från tio fiktiva injiceringspunkter. Dessa fiktiva punkter är inte kopplade till några faktiska experimentresultat. En jämförelse mellan simulerade genombrott visar dock att responserna skiljer sig markant mellan de olika underliggande modellerna. På motsvarande sätt har en förändring av materialegenskaperna liten betydelse för den övergripande responsen. Resultaten av den utförda studien visar klart att i fallet med den undersökta i bergvolymen TRUE Block Scale så är responsen av simulerade spårförsök starkt betingad av den utnyttjade hydrostrukturella modellen som använts. Givet att huvuddelen av spårämnena transporteras i ett fåtal deterministiskt tolkade strukturer så är kunskap om deras geometri en förutsättning för att realistiskt kunna beskriva hur ett nätverk av strukturer fungerar i transporthänseende.

Contents

List of figures

List of tables

1 Introduction

ANDRA has been involved for over 4 years in the TRUE Block Scale project, an integrated flow and transport program including in situ experiments and modeling, now in its final stage, run at the Äspö Hard Rock Laboratory, in Sweden. This experiment has been using an iterative approach to characterisation: one borehole is drilled, data is obtained from this borehole and integrated into the model of the block, and then a new borehole is discussed : is it needed? If yes, where should it be drilled and with what geometry?

This approach, together with reprocessing of previously acquired data and with further testing in existing boreholes, has resulted in a number of successive updates of the hydrostructural model for the block (cf. Anderson et al., 2002a), in order to accommodate incompatibilities between the new-incoming data and the « old » model. One may question how much the model upgrades contributed to enhancing their predictive and explanatory power with regard to tracer transport : suppose one had to give a blind prediction of an experiment to be performed later. What would have been the prediction for this experiment at each stage of model upgrading? How much would this have changed? Finally, how much better would a prediction based on our current knowledge, embodied in the latest model, turn out compared to ones using prior versions of the model?

In order to address these questions, numerical simulations of actual in situ experiments using the successive models are performed and interpreted, and then compared to the experimental results. These runs use “a priori” geometry and properties as described by the successive models, without attempting a calibration. Then, after transport properties are calibrated to obtain a realistic representation of tests with the given model, runs using these calibrated properties and the preceding hydrostructural models to older models are used to test the possible degradation of the tracer transport simulations.

Four successive models were analysed, that were chosen after discussion between ANDRA and SKB. The first one embodies the prior knowledge of the site (i.e. used for scoping calculations), before the Preliminary Characterisation, the second one is the output of the Preliminary Characterisation phase, the third one is the “March 1999 model”, which uses detailed characterisation results, then the fourth one essentially accounts for our current knowledge about this volume of rock “March 2000 model”. Three tracer tests, chosen from the B-2 stage (Anderson et al., 2000b), are simulated in each model. Also, 10 synthetic tracer tests are simulated, that do not correspond to real tests, in order to explore more broadly on the variability of test response when the model of the site is changed.

Chapter 2 below describes the way the models are built, and give the data sources used. The four models are described in chronological order, to help see how they evolved with time. In chapter 3 are presented and discussed the results of the “forward” simulations, that used directly the parameters described in chapter 2. Here, an inverse chronological order is used, to point on the “degradation” of the prediction results from the latest to the oldest model. In chapter 4 the results of the “calibrated” simulations are presented and discussed. Chapter 5 is a comparison between the synthetic tests. Conclusions are presented in Chapter 6.

2 Description of the models used for the forward simulations

2.1 Preamble

The characteristics of the four analysed numerical models of the TRUE Block Scale experimental site are based on the different structural geological models and preceding studies undertaken for ANDRA. Although only a few structures have changed or have been added between the successive stages, all the characteristics are presented in this report for completeness and easy accessibility.

The size of each model is identical. According to the interpreted deterministic structures and the volume of interest for the tracer experiments discussed hereafter, the model of the TRUE Block Scale experimental site is restricted to the following volume :

- box limited by Äspö local coordinates :
  X : 1820 to 2040 m
  Y : 7080 to 7260 m
  Z : -550 to –360 masl
- volume further bounded by three planes representing structures 7, and fracture zones NE-1 and Z.

All simulations are run using *3FLO*, a 3D flow and transport code for fractured and continuum media, developed by Itasca during the last 10 years. A short description of *3FLO* is presented in Appendix.

2.2 Scoping stage

The network characteristics of this first model are based on the studies undertaken by Itasca Consultants for ANDRA in 1997, essentially based on the "scoping stage" period (Hermanson et al., 2001a)

2.2.1 Interpreted deterministic structures

Due to the position of the deterministic structures in relation to the grouted zone, 12 large structures are selected out of the 18 structures interpreted at the Äspö site (Hermanson et al., 2001a).
The three boreholes considered in the Scoping Characterisation Stage study are defined in the *3FLO* model by the coordinates of their initial (collar) and end points.
For each of the 12 structures, we define which well(s) it is known to intersect, and which it is not.

Table 2-1 records the selected structures as well as the boreholes these structures are intersected by. Table 2-2 gives the strike and dip of the structures, as well as the coordinates of points belonging to them.

In the scoping stage, the structures are allowed to extend accross the entire model and are not limited to certain smaller areas by given corners, like in later studies. We calculate from the data given in Table 2-2 the end points (or corners) of the structures corresponding to the intersections between these structures and the boundaries of the numerical model. We then define the structures according to their corners.

Table 2-1 : Scoping stage - Intersection of selected interpreted structures with boreholes

structure number	borehole KA3510A	borehole KA2563A	borehole KA2511A
2	Loc	X	
3	Loc	X	
4	X	Loc	
5	X	Loc	
6	X	Loc	
7	X	Loc	
8	Loc	X	
10	Loc		
16		Loc	X
17		Loc	X
18		Loc	X

Loc : structure intersects borehole at a specified location
X : structure intersects borehole

Table 2-2 : Scoping stage – Coordinates of two points A & B for interpreted structures in KA3510A & KA2563A (from IPR-01-41)

structure	X_A	Y_A	Z_A	X_B	Y_B	Z_B	Dip	Strike
2	1983,18	7244,35	-386,98	1944,10	7258,36	-454,53	88	113
3	1982,96	7244,44	-386,99	1920,98	7252,50	-468,35	78	113
5	1961,48	7231,15	-409,74	1914,27	7250,83	-472,35	77	293
4	1967,27	7234,70	-403,68	1943,11	7258,11	-455,11	90	293
6	1931,30	7212,91	-440,92	1913,17	7250,55	-473,01	86	158
7	1929,08	7211,58	-443,19	1888,22	7244,41	-487,87	90	128
8	1883,52	7184,76	-488,96	1937,97	7256,79	-458,2	90	36
10	1810,96	7133,42	-574,77	1856,34	7099,10	-468,62	89	126
16	1983,43	7244,38	-386,73	1966,06	7173,70	-379,42	19	199
17	1957,15	7227,45	-415,38	1934,78	7151,64	-404,66	29	206
18	1906,95	7195,10	-470,10	1856,49	7096,41	-467,84	17	203

The transmissivities of the structures, estimated from pressure build-up tests, are given in Table 2-3. For the pipes representing flow in a given structure, a lognormal conductivity distribution with a mean computed is used, as discussed below from the transmissivity value given in Table 2-3, a standard deviation taken as 1.3 times the mean, and a minimum taken as zero.

In the study performed in 1997 for ANDRA, one square grid of channels on each structure was put. In order to increase accuracy in the flow paths in our current model, a second square grid of channels is superimposed, oriented at 45 degrees from the first square grid as shown in Figure 2-1. The spacing for the first square grid of channels is 6 m (the spacing for the second square grid of channels is then $6/(2)^{1/2}$).

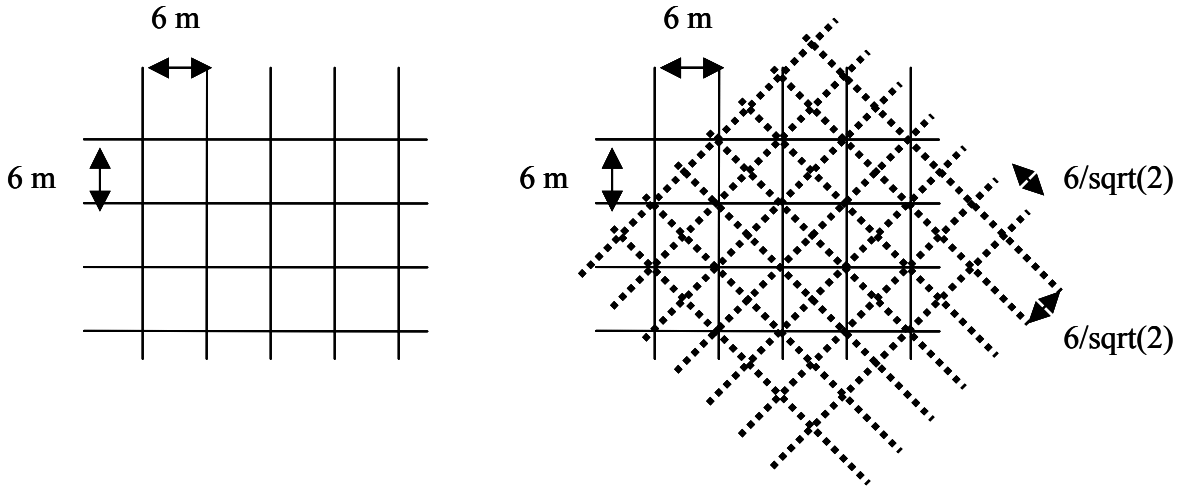

Figure 2-1 : *Scoping stage model – 2 square grids of channels on each structure*

Table 2-3 : Scoping stage - Transmissivities of interpreted structures	
structure name	**Mean transmissivity used in model (m²/s)**
S2	$1.0\ 10^{-6}$
S3	$1.0\ 10^{-6}$
S4	$1.5\ 10^{-5}$
S5	$1.0\ 10^{-4}$
S6	$3.2\ 10^{-5}$
S7	$3.1\ 10^{-5}$
S8	$1.0\ 10^{-6}$
S10	$1.0\ 10^{-6}$
S16	$1.0\ 10^{-6}$
S17	$1.0\ 10^{-6}$
S18	$1.0\ 10^{-6}$

Varying conductivities are generated for the pipes in a given structure. The mean conductivity ***C*** is computed from the mean structure transmissivity ***T***, using the following equation:

$$C=T*\frac{g}{shapef}$$

Where:

g is the grid size (length of the square edges, here 6 m), and

shapef is a shape factor, with a value of "1" for a simple square grid, and of "$1+\sqrt{2}$" for the "squares plus diagonals" grid that is used here(two superimposed square grids, with relative spacings 1 and $\sqrt{2}$).

It can easily be verified that the transmissivity – conductivity relationship above yields, for a homogeneous regular grid, flow properties equivalent to those of a continuum with transmissivity ***T*** *(*Billaux et Guérin, 1993).

In order to calibrate the transport results, the aperture of channels in each structure can be independently modified. Once channel conductivities have been generated, channel cross sections S are chosen so that conductivities are proportional to the cube of sections (cubic law) :

$S = \alpha * C^{1/3}$, where α is constant for all the channels in a structure

This corresponds to flat "ribbons" within which Poiseuille's law may be applied. For the forward simulations, before the transport parameters are calibrated to the three tracer tests considered, the coefficient α is equal to 0.05 for all the structures so that the total porosity of the structures is around 0,5%.

2.2.2 Background fractures

These small fractures are separated into 3 sets (Table 2-4). A pseudo-normal distribution is used (i.e. the angle between the given mean and a generated orientation is normally distributed with mean zero).

Table 2-4 : Scoping Characterisation stage - Orientation distributions for 3 background fractures sets

Set	Mean Pole (Trend, Plunge in degrees)	Standard deviation of angular dispersion in degrees	Weight in %
1	(203.2 , 2.6)	20.	48.1
2	(290.4 , 8.5)	15.	33.1
3	(312.5 , 85.1)	15.	18.8

The linear intensity of fractures λ_l (area of fractures per cubic meter) is 1.3 m^2 / m^3.

The fracture radius distribution characteristics are :

- Lognormal,
- Mean radius = 6 m,
- Standard deviation = 2 m.

From the linear intensity λ_l and the mean area S of fractures, one can easily deduce the fracture volumetric density λ_v,:

$$\lambda_v = \lambda_l / S$$

yielding a volumetric density λ_v of 1.03 10^{-2} fractures/m^3.

With the density given above, generating the background fractures in the volume representing the considered Äspö rock volume is above our current computational capacity. Also, in a network generated from the above statistical characteristics, a large number of fractures would have essentially no effect on the overall properties : these are fractures with small radii.

We can assess the connectivity of the network by computing a "connectivity index" (Billaux and Guérin, 1993). This index is the mean number of intersections per fracture, weighted by fracture radius. A network is at the percolation threshold (i.e. it has the minimum density for which an "infinite" path exists) when the connectivity index is about 3, and is on the other hand well connected when the index is above 15.

If the fracture radii are distributed according to the lognormal law given above, without truncation, the network connectivity is around 22. By removing all the fractures with a radius less than 6 m, the network connectivity is around 17, which is still very connected. As nearly 63% of the fractures have a radius less than 6 m, we just have to generate the three fractures sets with a total fracture density of 0.38 10^{-2} fractures/m^3 while truncating them to 6 m to obtain a network equivalent to the one given above.

The fracture radius distribution used in the *3FLO* model is then :

- Lognormal,
- Mean radius = 6 m,
- Standard deviation = 2 m
- Truncation at 6 m, with a total density of 0.38 10^{-2} fractures/m^3

The spacing g for the square grid of channels on each fracture is 12 m (a smaller value of the spacing g for the background fractures would be above our computational capacity).

The fracture transmissivity distribution characteristics are :

- truncated lognormal,
- log mean = -9.3,
- truncated at 10^{-9} m^2/s,
- log standard deviation of 1.

These values yield generated transmissivities in the range 10^{-9} m^2/s to 10^{-7} m^2/s, with a few fractures going as high as 10^{-6} m^2/s (Figure 2-2) .

In each fracture, the transmissivity T is supposed uniformly among channels. Each channel is assigned a conductivity C reproducing the overall transmissivity of the fracture:

$C = T * g$, where g is the spacing of the square channel grid.

The overall transport aperture e_t of each small fracture is :

$$e_t = T^{0.5}$$

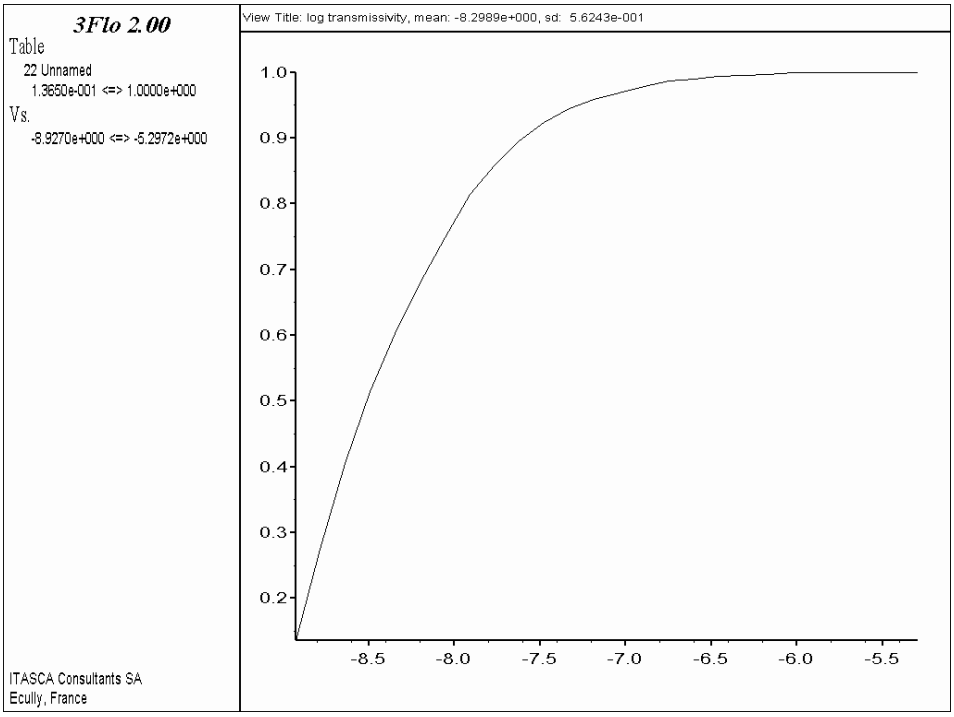

Figure 2-2 : *Scoping stage model - Cumulative lognormal transmissivity distribution used for the Background Fractures*

To get the order of magnitude of the large-scale permeability of the background fractures, we compute a "best fit" permeability tensor for a 80 m radius network generated with the above geometry and conductivity statistics. The procedure used is as follows (Billaux, 1990) :

- use a network with a spherical boundary;
- impose at the boundary linearly varying heads, yielding an overall unit gradient in the sphere;
- compute the flowrate across a disk perpendicular to the direction of the gradient and divide this flowrate by the area of the disk. This gives a "directional permeability".
- Repeat directional permeability computations, in the same network, for a large number of gradient directions.
- Perform a simple least squares regression to obtain the six coefficients of the permeability tensor that give the best match to these directional permeabilities.

Besides the tensor coefficients, the least square analysis yields a normalized mean square error, which is called the Variability Index (Iv). Parametric studies (Billaux and Guérin, 1993) have shown that a network can be considered equivalent to a continuous medium, at the scale of the sphere, only if the variability Index is lower that 10^{-3}.

Here, principal permeabilities are in the range of 8.8 10^{-10} m/s with a small anisotropy (factor of 1.40), and a Variability Index below 10^{-3} (5.5 10^{-4}).

2.3 Preliminary Characterisation stage

The network characteristics for this second model are taken from the studies undertaken by Itasca Consultants for ANDRA in 1999, essentially based on the Preliminary Characterisation stage (Andersson et al., 2002a).

2.3.1 Interpreted deterministic structures

Out of five wells used for the preliminary characterisation stage (KI0023B, KI0025F, KA2511A, KA2563A and KA3510A), only four cut the volume defined in our numerical model, so borehole KA2511A is not considered further.

The volume considered is intercepted by structures 6, 9, 13 and 20, which are therefore explicitly entered in the model. The equations of the planes of these structures, as well as their terminations, are given in Table 2-5.

Table 2-5 : Preliminary Characterisation Stage - Plane and Termination of selected structures

Struct.	DirectionVector, and distance				Strike (°)	Dip (°)	Average width (cm)	Type	Termination
	Nx	Ny	Nz	D					
6	-0.9051	-0.4218	0.0533	-4810.05	155	87	50	Frac-fault	#5 North of #20
7	**0.4973**	**0.8613**	**-0.1045**	**7216.54**	**120**	**84**	**40**	**Frac-fault**	**Boundary**
9	0.0868	-0.9924	0.0872	-7320.10	76	86	8	Frac-fault	West of #19 East of #20
13	0.7832	0.6179	-0.0698	5960.09	142	86	17	Fault	South of #15 North of NE-2
19	**-0.7924**	**-0.3751**	**-0.4810**	**-3948.95**	**335**	**61**	**30**	**Frac-fault-zone**	**Boundary**
20	-0.7409	-0.6643	-0.0987	-6147.39	318	84	100	Frac-swarm-fault	South of #15 North of NE-2
Z	**-0.4424**	**0.8682**	**0.2250**	**5158.48**	**243**	**77**	**550**	**zone**	**Boundary**

The structure written in **bold black** are boundary limits of the model.

For flow and transport runs, the same grids of channels as the Scoping Phase model are projected on the structures (regular 6 and 6/sqrt(2) meter-spaced grids oriented 45% from each other). In order to reproduce, in at least a crude fashion, the variability of transmissivity within each structure, we generate pipe conductivities using for each structure a truncated normal distribution estimated from the ranges of transmissivity given by Winberg (1999) in the same fashion explained for the Scoping Phase model.

The transmissivity distributions used for each structure are given in Table 2-6.

The channels sections S are chosen in the same way as for the Scoping Phase model ($S = \alpha . C^{1/3}$, with $\alpha = 0.05$ for all the structures for the forward simulations, before calibration).

Table 2-6 : Preliminary Characterisation Stage - Truncated normal distribution of the structures transmissivity (from Winberg, 1999)			
structure Id	**Transmissivity used in model (m^2/s)**		
	mean	standard deviation	Min
6	$1\ 10^{-7}$	$5.0\ 10^{-8}$	$1.25\ 10^{-8}$
9	$5\ 10^{-7}$	$2.5\ 10^{-7}$	$6.25\ 10^{-8}$
13	$1\ 10^{-7}$	$5.0\ 10^{-8}$	$1.25\ 10^{-8}$
19	$1\ 10^{-7}$	$5.0\ 10^{-8}$	$1.25\ 10^{-8}$
20	$2\ 10^{-7}$	$2.5\ 10^{-9}$	$2.50\ 10^{-9}$

2.3.2 Background fractures

A discrete stochastic fracture network, made of disk-shaped fractures, is created in two steps. First, semi-deterministic structures are placed along boreholes in order to reproduce the measured traces. In this way, the resulting fracture network will be conditioned to observations. Second, a stochastic fracture field is generated, discarding fractures that intersect the wells.

The intercept position and orientation of fractures cutting each well are taken from Hermanson et al. (2001b). For each of them, a fracture is introduced in the model. Two parameters for this fracture are unknown : its radius and centre position. The radius is generated from the same statistical distribution as the stochastic part of the network (see below) and the center position is chosen from a Poisson point process in the plane defined by the intercept with the well and the fracture orientation.

The parameters taken into account for the stochastic fracture network result from Hermanson et al. (2001a). There are three sets of fractures, with characteristics given in Table 2-7.

Table 2-7 : Preliminary Characterisation Stage - Parameters of the stochastics network (from Hermanson & al. 2001a)			
Fractures set	**Fisher distribution of orientations**		
	trend (°)	plunge (°)	K (concentration coefficient)
1	117.9	12.9	5.64
2	200.4	2.0	15.75
3	186.5	81.1	13.6

In order to be able to generate all the fractures in the volume considered for the Äspö site, only the larger fractures are generated, by using a higher truncation of the radius distribution and decreasing the density accordingly :

- Density $0.585\ 10^{-2}$ fractures/m^3 (instead of $1.48\ 10^{-2}$ previously)
- radii lognormal, mean = 4 m, σ = 2 m truncated at 4.5 m (instead of 3 m previously)
- transmissivity lognormal (-11, 1.7) truncated at 2.10^{-11} m^2/s

The resulting connectivity index is around 16.2: the network is still very well connected. The large-scale hydraulic conductivity (calculated in a 80 m-radius sphere) is in the range of 1.2 10^{-11} m/s, with a small anisotropy (factor of 1.40) and a Variability Index below 10^{-3} (5.8 10^{-4}).

2.4 Detailed Characterisation stage

The network characteristics of this third model are taken from the March 1999 structural model. The actual values used are found in Doe (2001).

2.4.1 Interpreted deterministic structures

The march 1999 structural model consists of a selection of possible conductive structures intersecting the studied rock volume at the TRUE Block Scale experimental site, based on data obtained from a new borehole, KI0025F02, and from new hydraulic tests.

The major features of the March 1999 structural model are structures 6, 7, 13, 19, and two new structures, 21 and 22. Their planes and terminations are given in Table 2-8 and Table 2-9 respectively. One can note that the geometrical characteristics of the structures have slightly changed from the Preliminary Characterisation Stage model.

The structure intersections with the boreholes are given in Table 2-10.

The same 6 and 6/sqrt(2) meter-spaced grids of channels as in the preceding models are projected on the structures. Channel conductivities are also generated using a truncated normal distribution in order to obtain the transmissivity estimated by Doe (2001).

The transmissivity distribution used for each structure is given Table 2-11.

The channel sections S are chosen in the same way as for the preceding models ($S = \alpha . C^{1/3}$, with $\alpha = 0.05$ for all the structures for the forward simulations, before calibration).

Table 2-8 : Detailed Characterisation model - Planes of selected structures (from Doe, 2001)

structure	Direction vector and distance				Strike (°)	Dip (°)
	Nx	Ny	Nz	D		
6	0.7946	0.6053	- 0.0471	5915.65	142.7	87.3
7	0.3659	0.9255	- 0.0976	7423.23	111.6	84.4
10	0.0916	0.9458	0.3116	6736.41	276.0	72.0
13	- 0.7477	- 0.6283	- 0.2149	- 5831.18	320.0	77.6
19	0.8351	0.5320	- 0.1395	5455.44	147.5	82.0
20	- 0.7349	- 0.6723	- 0.0891	- 6197.84	317.6	84.9
21	- 0.9752	- 0.1371	- 0.1736	- 2770.80	352.0	80.0
22	- 0.8914	- 0.4062	- 0.2011	- 4543.85	335.5	78.4

Table 2-9 : Detailed Characterisation model - Termination of selected structures, given in the form of coordinates of end points (from Doe, 2001)

structure	Coordinates	Corners			
		1	2	3	4
6	Easting	1911	1907	1941	1945
	Northing	7231	7229	7184	7186
	Elevation	-427	-527	-527	-427
7	Easting	1826	1820	2048	2054
	Northing	7262	7245	7155	7172
	Elevation	-350	-527	-527	-350
10	Easting	1800	1807	1931	1924
	Northing	7089	7121	7109	7077
	Elevation	-427	-527	-527	-427
13	Easting	1877	1894	1953	1936
	Northing	7193	7207	7137	7123
	Elevation	-427	-527	-527	-427
19	Easting	1872	1860	1955	1967
	Northing	7204	7196	7046	7054
	Elevation	-427	-527	-527	-427
20	Easting	1874	1881	1981	1975
	Northing	7227	7233	7123	7117
	Elevation	-427	-527	-527	-427
21	Easting	1906	1924	1933	1915
	Northing	7194	7196	7131	7129
	Elevation	-427	-527	-527	-427
22	Easting	1917	1935	1965	1947
	Northing	7191	7199	7134	7126
	Elevation	-427	-527	-527	-427

Table 2-10 : Detailed Characterisation model - Summary of identified conductive structures in the TRUE Block Scale volume (from Doe, 2001)

	KA2563A				KA2511A				KA3510A				KI0025F				KI0023B				KI0025F02				Width
Structures	Depth (m)	Width (cm)	Type	Strike/ dip	Depth (m)	Width (cm)	Type	Strike/ dip	Depth (m)	Width (cm)	Type	Strike/ dip	Depth (m)	Width (cm)	Type	Strike/ dip	Depth (m)	Width (cm)	Type	Strike/ dip	Depth (m)	Width (cm)	Type	Strike/ dip	Average width
1	12.5	0.2	Frac	335/82																					1
2	68.5	220	Zone	135/87					11.1	15	Frac	309/75													110
3	68.5	220	Zone	135/87					37.5	40	Zone	106/81													130
4	94.4	6	Frac	296/74	23.1	10	Frac	300/80	12.9	8	Fault	115/89													10
5	103	2	Frac	114/89					47.7	10	Fault	138/75	4.9	10	Frac	307/57	7.2	5	Frac	112/87					10
6	157	140	Frac	309/89	100.1	0.2	Frac	340/71					61.8	80	Frac	342/86	44.2	10	Fault	103/87	52.3	1	Frac	317/89	50
7	153	140	Fault	111/73	38	0.2	Frac	143/87					43.5	25	Frac	253/84	42.2	4	Frac	338/83	39.9	1	Frac	126/70	40
8	242	8	Fault	026/84					16.1	100	Zone	232/89													50
9	230	5	Fault	123/88																					8
10	351	25	Fault	124/80	240.5	0.5	Frac	127/85									170.7	30	Zone	298/83					20
11					258.2	15	Fault	288/88																	10
12																									
13	207	20	Fault	321/86													85.6	15	Fault	318/89	93.9	8	Fault	140/83	17
15									118	60	Fault	269/88													60
16	56.3	120	Zone	011/40	104.7	100	Zone	233/18																	110
		0.2				5																			3
17	109	(140)	Frac	222/34	132.4	(230)	Frac	270/16																	(190)
		0.1																							
18	194	(20)	Frac	012/18	242.5	10	Fault	155/9									75.5	80	Swarm	348/41					20
19	238	10	Fault	243/76	198.2	35	Frac	324/87					166.4	65	Zone	338/74	111.6	20	Fault	342/87	133	12	Fault	330/76	30
						0.2	Frac/																		
20	189	5 (60)	Fault	316/82	122	(100)	Swarm	336/67					87.7	0.2	Frac	336/77	69.8	20	Fault	157/82	74.7	10	Fault	138/90	100
21													(166.4)			338/74	71.1	10	Frac	123/86	97.9			354/77	
22													88.8			340/81					66.8			337/88	
Z													192.1	+550	Zone	243/77									+550

Table 2-11 : Detailed Characterisation model - Truncated normal distribution of the structures transmissivity (from Doe, 2001)			
structure name	**Transmissivity used in model (m²/s)**		
	mean	sd	Min
6	$2.0\ 10^{-7}$	$1.0\ 10^{-7}$	$1\ 10^{-8}$
7	$2.0\ 10^{-5}$	$1.0\ 10^{-5}$	$1\ 10^{-6}$
10	$5.0\ 10^{-7}$	$2.5\ 10^{-7}$	$5\ 10^{-8}$
13	$1.0\ 10^{-7}$	$1.0\ 10^{-7}$	$1\ 10^{-9}$
19	$1.5\ 10^{-5}$	$1.0\ 10^{-5}$	$1\ 10^{-7}$
20	$8.0\ 10^{-7}$	$2.0\ 10^{-8}$	$5\ 10^{-7}$
21	$1.0\ 10^{-8}$	$1.0\ 10^{-8}$	$1\ 10^{-9}$
22	$4.0\ 10^{-7}$	$2.0\ 10^{-7}$	$1\ 10^{-7}$

2.4.2 Background fractures

The same background fractures are used as in preceding model, based on the Preliminary Characterisation stage.

2.5 Tracer test stage

The network characteristics of this fourth model are taken from the March 2000 structural and hydraulic model. The actual values used are found in Andersson et al. (2002a).

2.5.1 Interpreted deterministic structures

The March 2000 structural model is updated from the March 1999 structural model with data obtained from the new borehole KI0025F03 and new hydraulic tests.

The main conductive structures selected in the March 2000 structural model are structures 6, 7, 13, 19, 20, 21, 22 and two new Structures 23 and 24. Their planes are given in Table 2-12. The terminations of the structures, used to generate the structures in the *3FLO* model, are given in Table 2-13 The structure intersections with the boreholes are given in Table 2-14.

The same 6 and 6/sqrt(2) meter-spaced grid of channels used for the preceding models are projected on the structures. Channel conductivities are also generated using a truncated normal distribution in order to obtain the corresponding transmissivity estimated by Doe (2001).

The transmissivity distribution used for each structure is given in Table 2-15.
Again, the channels sections S are chosen in the same way as for the preceding models ($S = \alpha . C^{1/3}$, with $\alpha = 0.05$ for all the structures for the forward simulations, before calibration).

Table 2-12 : Tracer test stage model - Planes of selected structures (from Anderson et al., 2002a)						
structure	DirectionVector, and distance				Strike (°)	Dip (°)
	Nx	Ny	Nz	D		
6	- 0.8429	- 0.5374	- 0.0253	5487.00	327.5	88.6
7	0.4404	0.8851	- 0.1504	-7299.84	116.5	81.4
13	- 0.7303	- 0.5535	- 0.4003	5172.72	322.8	66.4
19	- 0.8586	- 0.5125	- 0.0126	5285.73	329.2	89.3
20	- 0.7464	- 0.6596	- 0.0884	6129.78	318.5	84.93
21	0.8698	0.3739	- 0.3221	-4504.55	156.74	71.21
22	0.8437	0.3999	- 0.3580	-4672.57	154.64	69.02
23	0.7337	0.6794	0.0000	-6304.34	137.2	90.0
24	0.6391	0.7552	- 0.1457	-6753.70	130.24	81.62
10	- 0.0916	- 0.9458	- 0.3117	6736.05	275.53	71.84

Table 2-13 : Tracer test stage model - Termination of selected structures, given in the form of coordinates of end points (from Anderson et al., 2002a)							
structure	**Coordinate**	**Corner**					
		1	**2**	**3**	**4**	**5**	**6**
6	Easting	1784.327	1799.417	2118.921	2103.975	-	-
	Northing	7420.639	7420.527	6919.361	6919.26	-	-
	Elevation	-199.361	-700.79	-700.639	-199.507	-	-
7	Easting	1649.361	2150.793	2150.639	1649.45	-	-
	Northing	7392.688	7143.232	7058.112	7307.397	-	-
	Elevation	-199.361	-199.472	-700.639	-700.825	-	-
13	Easting	1842.699	2150.675	2150.66	1947.787	1649.385	1649.317
	Northing	7420.705	7014.25	6919.278	6919.305	7313.005	7420.613
	Elevation	-700.692	-700.551	-569.251	-199.295	-199.263	-347.88
19	Easting	1730.108	1737.527	2036.671	2029.388	-	-
	Northing	7420.649	7420.528	6919.351	6919.252	-	-
	Elevation	-199.351	-700.793	-700.649	-199.502	-	-
20	Easting	1678.12	1737.532	2150.532	2150.665	2121.151	-
	Northing	7420.609	7420.579	6953.287	6919.262	6919.338	-
	Elevation	-199.481	-700.692	-700.674	-447.995	-199.461	-
21	Easting	1915.555	2130.957	1945.342	1729.951	-	-
	Northing	7420.706	6919.275	6919.294	7420.487	-	-
	Elevation	-199.294	-199.517	-700.706	-700.73	-	-
22	Easting	1936.065	2150.537	2150.52	1960.907	1723.467	-
	Northing	7420.802	6968.196	6919.227	6919.378	7420.507	-
	Elevation	-199.417	-199.457	-254.175	-700.782	-700.68	-
23	Easting	1720.653	1720.748	2150.533	2150.601	-	-
	Northing	7420.575	7420.472	6956.347	6956.274	-	-
	Elevation	-199.379	-700.765	-700.621	-199.533	-	-
24	Easting	1753.722	1649.372	1649.422	2150.684	2150.684	-
	Northing	7420.443	7420.403	7411.863	6987.775	7084.454	-
	Elevation	-199.168	-656.728	-700.739	-700.518	-199.444	-

Table 2-14 : Tracer test stage model - Summary of identified conductive structures in the TRUE Block Scale volume (from Anderson et al., 2002a)

	KA2563A			KA2511A			KA3510A			KI0025F			KI0023B			KI0025F02			KI0025F03		
#	Depth	Strike	Dip	Depth	Strike	Dip	Depth	Strike	Dip	Depth	Strike	Dip	Depth	Strike	Dip	Depth	Strike	Dip	Depth	Strike	Dip
1	12.5	335	82																		
2	68.5	135	87				11.1	309	75												
3	68.5	135	87				37.5	106	81												
4	94.4	296	74	23.1	300	80	12.9	115	89												
5	103.0	114	89				47.7	138	75	4.9	307	57	7.2	112	87						
6	157.2	309	89	100.1	340	71				(61.8)	342	86	44.2	88	83	52.3	317	89	**51.9**	**136**	**81**
7	153.4	111	73	38	143	87				43.5	253	84	42.2	103	87	39.9	126	70	**43.0**	**88**	**84**
8	242.4	26	84				16.1	232	89												
9	230.0	123	88																		
10	351.3	124	80	240.5	127	85							170.7	298	83						
11				258.2	288	88															
12																					
13	207.0	321	86										85.6	318	89	93.9	140	83	**87.9**	**338**	**87**
15							118.0	269	88												
16	56.3	11	40	104.7	233	18															
17	108.9	222	34	132.4	270	16															
18	194.3	12	18	242.5	155	9							75.5	348	41						
19	237.9	343	76	198.2	324	87				166.4	336	84	111.6	342	87	133.0	334	87	**124.7**	**339**	**86**
20	188.7	316	82	122	321	73				87.7	336	77	69.8	157	82	74.7	134	89	**73.2**	**326**	**64**
21										(166.4)	338	74	71.1	123	86	97.9	354	77	**91.9**	**296**	**59**
22										88.8	340	81				66.8	337	88	**63.2**	**154**	**87**
23																59.2	125	80	**56.8**	**301**	**77**
24										**37.1**	**301**	**82**	**31.8**	**308**	**76**	**33.9**	**307**	**72**	**33.8**	**135**	**75**
Z										192.1	243	77									

Note : **Bold Black** text shows new intercepts and black test shows the unchanged March 1999 Structural model data.

Table 2-15 : Tracer test stage model - Truncated normal distribution of transmissivity structures (from Anderson et al., 2002a)			
structure	**Transmissivity used in model (m²/s)**		
	mean	sd	Min
6	$2.0\ 10^{-7}$	$1\ 10^{-7}$	$1\ 10^{-8}$
7	$2.0\ 10^{-5}$	$1\ 10^{-5}$	$1\ 10^{-6}$
13	$1.0\ 10^{-7}$	$1\ 10^{-7}$	$1\ 10^{-9}$
19	$1.5\ 10^{-5}$	$1\ 10^{-5}$	$1\ 10^{-7}$
20	$8.0\ 10^{-7}$	$2\ 10^{-8}$	$5\ 10^{-7}$
21	$1.0\ 10^{-8}$	$1\ 10^{-8}$	$1\ 10^{-9}$
22	$4.0\ 10^{-7}$	$2\ 10^{-7}$	$1\ 10^{-7}$
23	$6.0\ 10^{-9}$	$3\ 10^{-9}$	$3\ 10^{-9}$
24	$6.0\ 10^{-9}$	$3\ 10^{-9}$	$3\ 10^{-9}$

2.5.2 Background fractures

Dershowitz in Anderson et al. (2002a) undertook a study on the characterisation of the background fractures in the vicinity of the region where the TRUE Block Scale boreholes intersect Structures 13, 20, 21 and 22.

The background fractures are separated into 2 sets, with general characteristics given in Table 2-16.

Table 2-16 : Tracer test stage model – Parameters for 2 background fractures sets (from Anderson et al., 2002a)		
Parameter	Set # 1	Set # 2
Orientation & Distribution	Fisher distribution Mean Pole (Trend, Plunge) = (211, 0.6) Fisher dispersion k = 9.4	Fisher distribution Mean Pole (Trend, Plunge) = (250, 54) Fisher dispersion k = 3.8
Intensity	$\lambda_l = 0.16\ m^2/m^3$ (55.2% of fractures)	$\lambda_l = 0.13\ m^2/m^3$ (44.8% of fractures)
Transmissivity	Lognormal distribution with the following parameters values for the associated normal distribution : Mean = $-8.95\ \log_{10}$ (m²/s) St.dev = $0.93\ \log_{10}$ (m²/s)	Lognormal distribution with the following parameters values for the associated normal distribution : Mean = $-8.95\ \log_{10}$ (m²/s) St.dev = $0.93\ \log_{10}$ (m²/s)
Size equivalent radius	Lognormal distribution Mean = 6 (m) St.dev = 3 (m)	Lognormal distribution Mean = 6 (m) St.dev = 3 (m)

The linear intensity λ_l and the mean area S of fractures given above yield to a volumetric density λ_v of 2.05 10^{-3} fractures/m^3, smaller than the previous ones

The same spacing g = 12 m as the preceding models is used for the square grid of channels on each background fracture.

The fracture transmissivity distribution given above yields generated transmissivities in the range 10^{-12} m^2/s to 10^{-7} m^2/s, with one or two fractures going up to 10^{-6} m^2/s (Figure 2-3).

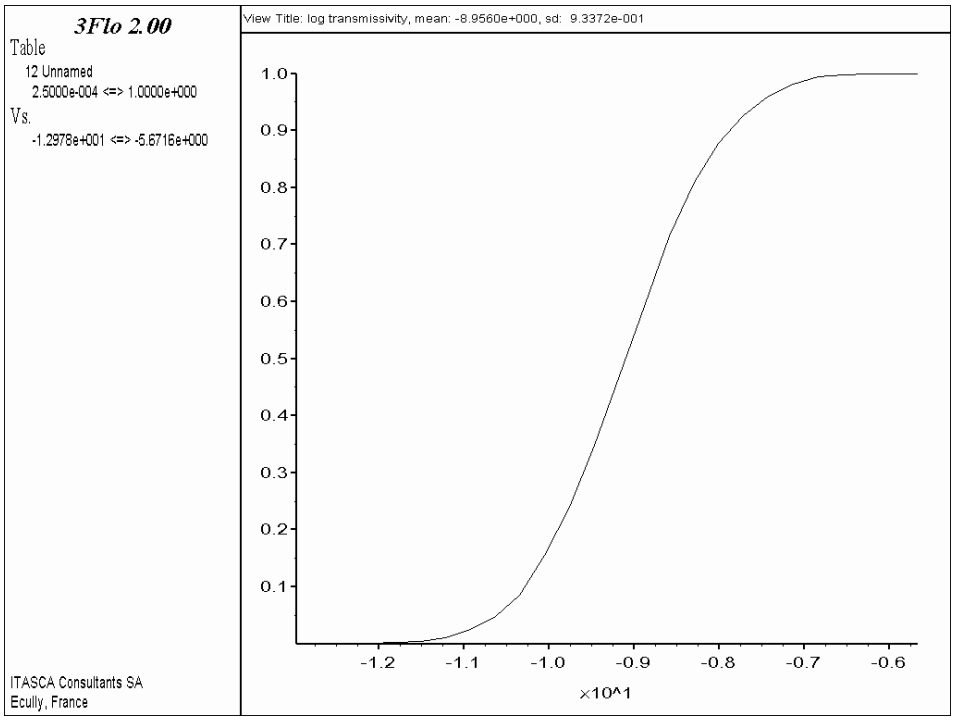

Figure 2-3 : *Tracer test stage model - Cumulative log10 transmissivity distribution used for the Background Fractures*

The connectivity index is around 6.4 which gives a relatively connected network.

The large-scale permeability (calculated in a sphere whose size is large enough compared to size of the background fractures ; here a 100 m-radius sphere) is in the range of 3.7 10^{-12} m/s with a small anisotropy (factor of 2.6), and a Variability Index above 10^{-3} (1.9 10^{-2}), indicating that at this 100 m-radius scale, the background fractures cannot be considered equivalent to a continuous medium, even for flow only.

Note that the background fracture studies, from Soping to the Tracer Test stage, have yielded quite variable results, with "equivalent permeability" going from 10^{-9} m/s for the Scoping stage model to 10^{-11} m/s for the Preliminary Characterisation stage model, to 10^{-12} m/s for the Tracer Test stage model. Because they rely on a relatively large number of Posiva flow logs (Anderson et al., 2002a), and are focussed on the specific volume in which the tracer tests are performed, the latter evaluations should be more reliable. Also more features have been put recently in the deterministic structure population, and some of the higher transmissivities which would have been earlier counted as "background" are now interpreted as "deterministic structures", which should effectively yield lower flow properties.

3 Simulation of injection tests, without calibration

3.1 Tracer tests

In agreement with ANDRA, the three following tracer tests are simulated (Anderson et al., 2000b) in the four models :

1. Equivalent to Test 1 (asymmetrical dipole flow geometry)
   B-2d : injection in borehole KI0025F03-P7 (borehole section : 55.0 – 58.5 m from collar)
2. Equivalent to Test 2 (radially converging tracer test)
   B-2c : injection in borehole KA2563A-S1 (borehole section: 242.0 – 246.0 m from collar)
3. Equivalent to Test 3 (radially converging tracer test)
   B-2b : injection in borehole KI0025F02-P3 (borehole section : 93.4 – 99.25 m from collar)

The pumping, which is the same for the three tracer tests, occurs in borehole KI0023B, section P6 (70.95-71.95 m from the borehole collar, in Structure # 21). The pumping rate is $3.433\ 10^{-5}$ m^3/s.

The data given in Table 3-1 were used for the three tracer tests are taken from Anderson et al. (2000a & 2000b).

Table 3-1 : Data used for the three tracer tests (from Anderson et al. 2000a & 2000b)

Test number	Test Name	Injection section	Interval in borehole (m)	structures included	Injection flowrate (m^3/s)	Injected mass (g)	Section volume (l)
1	B-2d	KI0025F03:P7	55.0-58.5	23	$1.667\ 10^{-7}$	2.323	4.98
2	B-2c	KA2563A:S1	242-246	19	$8.333\ 10^{-9}$	3.872	9.08
3	B-2b	KI0025F02:P3	93.4-99.25	13, 21	$2.667\ 10^{-8}$	2.917	8.42

For each test in each model, the injection sections are chosen such that:

- they are effectively cut by the specified structure(s), except if impossible (i.e. Structure 23, to be injected in test 1, does not exist in the Scoping Characterisation model)
- they are as close as possible to the real injection points.

The geometry injection section is explicitly simulated. The total mass of tracer is added to it at the start of the simulation. Then, the chamber is progressively flushed by the injection flowrate specified for the given test.

A series of 10 synthetic tracer tests is also simulated in each model. These synthetic tests do not correspond to any experimental test. Comparing the results obtained from these synthetic tests will help us understanding the effects of the model successive changes.

The real and synthetic injection points chosen for each model are given and discussed in chapter 5.

In order to do the calibration study, we necessarily started to work on the Tracer Test stage model, then "backed-up", using the calibrated parameters in the earlier models. For easier understanding and analysis, we therefore present the results hereafter in an inverse chronological order of the structural model evolution. We start then with the Tracer Test stage model and finish with the Scoping stage model.

3.2 Tracer test stage model

Figure 3-1 shows the shape in the *3FLO* model of the selected structures of the March 2000 structural model. Note that the grid used to visualize the structures in this Figure is not the real flow grid: for better readability, a single square grid is used, and the second square grid at a 45° angle that we use in the flow and transport simulations is not superimposed. The injection sections chosen in the *3FLO* model in order to include the correct structures are given in Table 3-2. One section had to be slightly moved: not surprisingly, modelled and real structure intersections are consistent.

Table 3-2 : Points selected in the 3FLO Tracer Test stage model for simulation of three tracer tests and comparison with hydrostructural model

Test number	Test Name	Injection section	*Real Interval in borehole (m)*	*Real structures included*	*3FLO* Interval in borehole (m)	*3FLO* structures included
1	B-2d	KI0025F03:P7	*55.0-58.5*	*23*	55.0-58.5	23
2	B-2c	KA2563A:S1	*242-246*	*19*	229-233	19
3	B-2b	KI0025F02:P3	*93.4-99.25*	*13, 21*	93.4-99.25	13, 21
Pumping well		KI0023B:P6	*70.95-71.95*	*21*	70.95-71.95	21

The three tracers tests described above are simulated. Figure 3-2 presents the logarithm of the concentration of tracer (Ln C) in the injection chamber versus time in hours. One can check that these three tracer injection functions correspond to the ones presented in Anderson, 2000b.

The breakthrough of the three tracers from the three injection sections are monitored in the pumping well KI0023B. Mass recoveries and breakthrough curves, respectively, are plotted Figure 3-3 and Figure 3-4. The breakthrough curves are plotted as mass flux versus time in hours, in a log-log scale. Figure 3-5 to Figure 3-10 also represent the flow paths along structures and the mean arrival time of tracer in each pipe along structures and background fractures for each of the three tracer tests.

There is a 100% recovery for Test 2 (B2-c) and Test 3 (B2-b) and a 74 % recovery for Test 1 (B2-d), the remaining mass of tracer being lost to the model boundaries.

The first arrivals for Test 1 (B2-d) are around 100 hours, and the peak breakthrough is around 250 hours. Most of the tracers from Test 1 arrive before 10 000 hours. The remaining part of the Test 1 tracers exit the model before 1 000 hours, reaching the boundary of the model through Structure #23 where particles are injected.

Figure 3-5, Figure 3-7, and Figure 3-9 show, for each of the three tests, the structures where transport effectively occurs (i.e. parts of the transport paths located within deterministic structures), colour-coded by structure number. The injection and pumping wells are also represented by two coloured crosses. In Figure 3-6, Figure 3-8, and Figure 3-10, for each test, all transport paths are shown (i.e. both paths within structures and paths within background fractures). By comparing the two corresponding figures on one page (Figure 3-5 and Figure 3-6 for example), one can assess the relative importance of the two types of flow paths. In these latter figures, each pipe is colour-coded for the mean arrival time of all particles that crossed the pipe.

Looking more precisely at the flow paths along structures for Test 1 (Figure 3-5), one can see that particles travel from Structure #23, to Structure # 22, then go through Structure #20 or #13 and finally arrive to Structure #21 where the pumping well is located. From the mean arrival time in pipes along the path plotted in Figure 3-6, one can see that the main and fastest transport path (blue coloured)is through Structures # 22, #20 and # 21 whereas particles transported through Structure # 13 arrive much later. Also, transport through background fractures is much slower, and accounts for only a fractional part of the masses.

For Test 2 (B2-c), first arrivals are around 6 000 hours ; the peak breakthrough is quite late, at around 16 000 hours, and most of the particles arrive before 60 000 hours (Figure 3-3 & Figure 3-4). The particles, injected in Structure #19, travel through Structure #13 before arriving into Structure # 21 (Figure 3-7). Most of the travel time is spent in Structure 19 (Figure 3-8): this transmissive structure sees very little perturbation from the pumping, since its connection to it is through relatively less transmissive structures, and its connection to the imposed head boundaries is more direct. Again, also here, background fractures seem to play only a minor role.

In Test 3 (B2-b), particles are injected in Structure #13 and # 21 and the pumping well is located in Structure # 21. It is not surprising that the first arrivals, around 25 hours, are faster compared to the two other tests. The peak breakthrough is around 100 hours and most of the tracers from Test 3 arrive before 1 000 hours. The transport paths involve mainly Structure # 21 (Figure 3-9), with some tracer being “retarded” by exploring the structure at depth before travelling up to the pumping point.

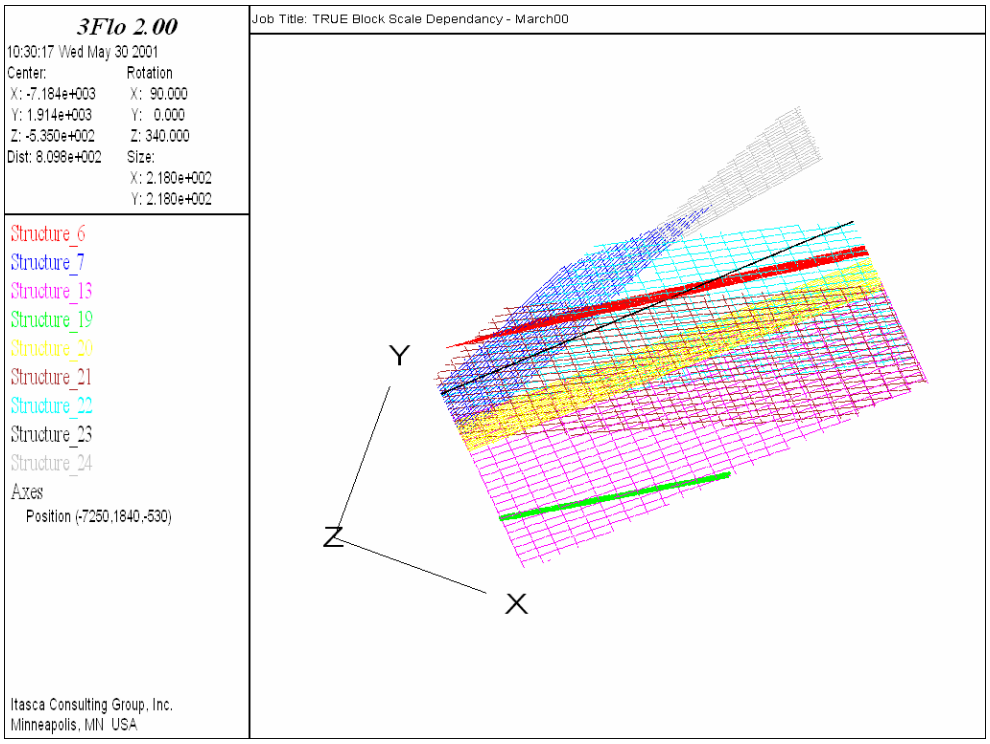

Figure 3-1 : *Tracer test stage model – Interrelation and shape of the structures (top view)*

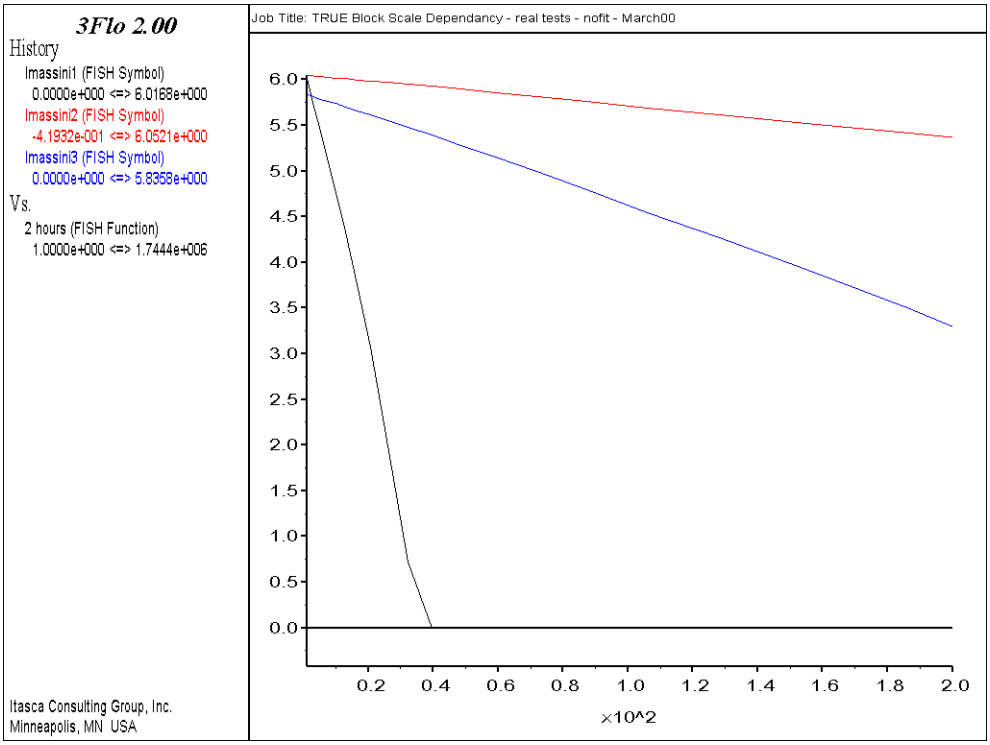

Figure 3-2 : *Tracer test stage model – Forward simulations*
Ln (concentration) in the three tracer tests vs time (hours)
(legend : black curve ⇔ Test 1, red curve ⇔ Test 2, blue curve ⇔ Test 3)

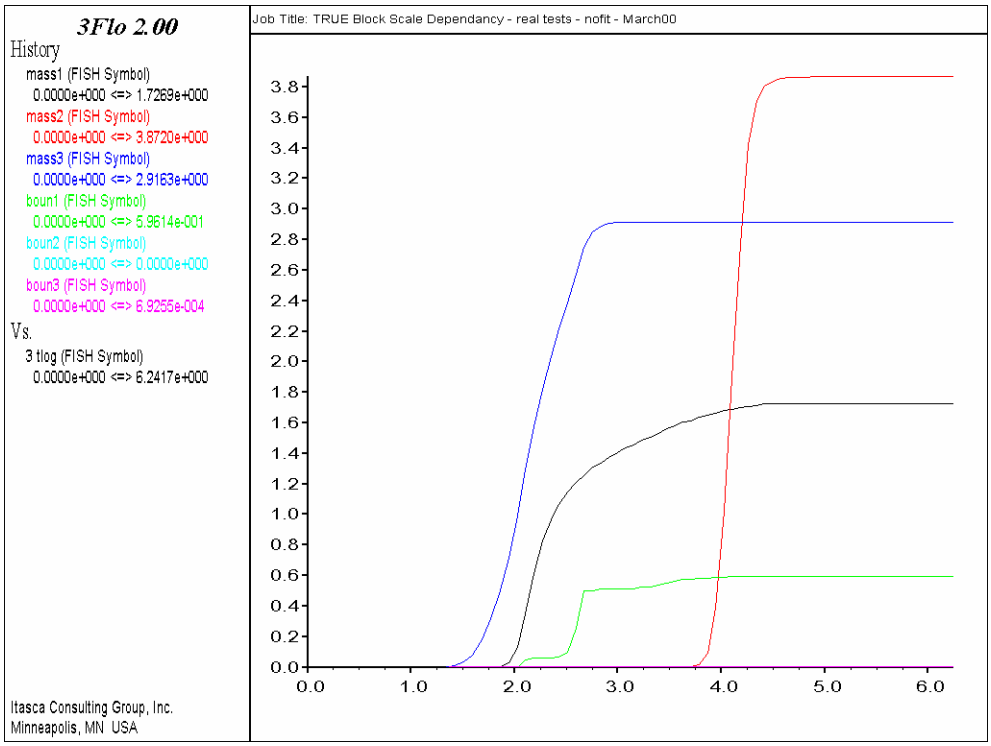

Figure 3-3 : *Tracer test stage model – Forward simulations*
Cumulative mass arrival (g) for the three tracer tests vs log (time in hours)

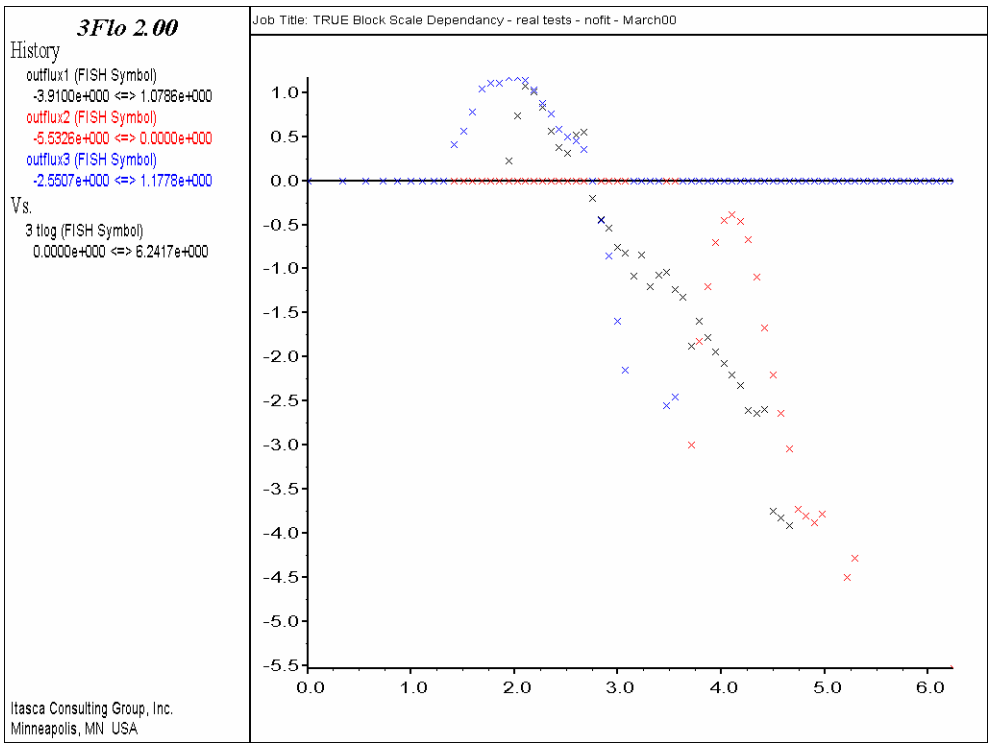

Figure 3-4 : *Tracer test stage model – Forward simulations*
Mass flux (mg/h) for the three tracer tests vs time in hours (log-log)

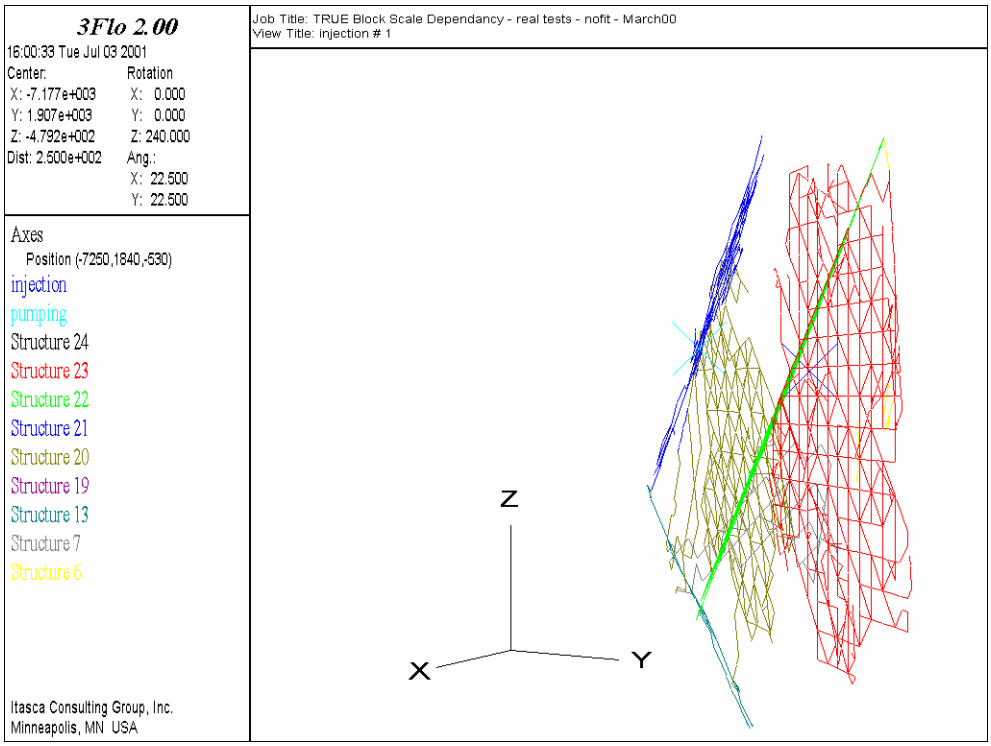

Figure 3-5 : *Tracer test stage model – Forward simulations*
Flow path for the simulated tracer Test 1

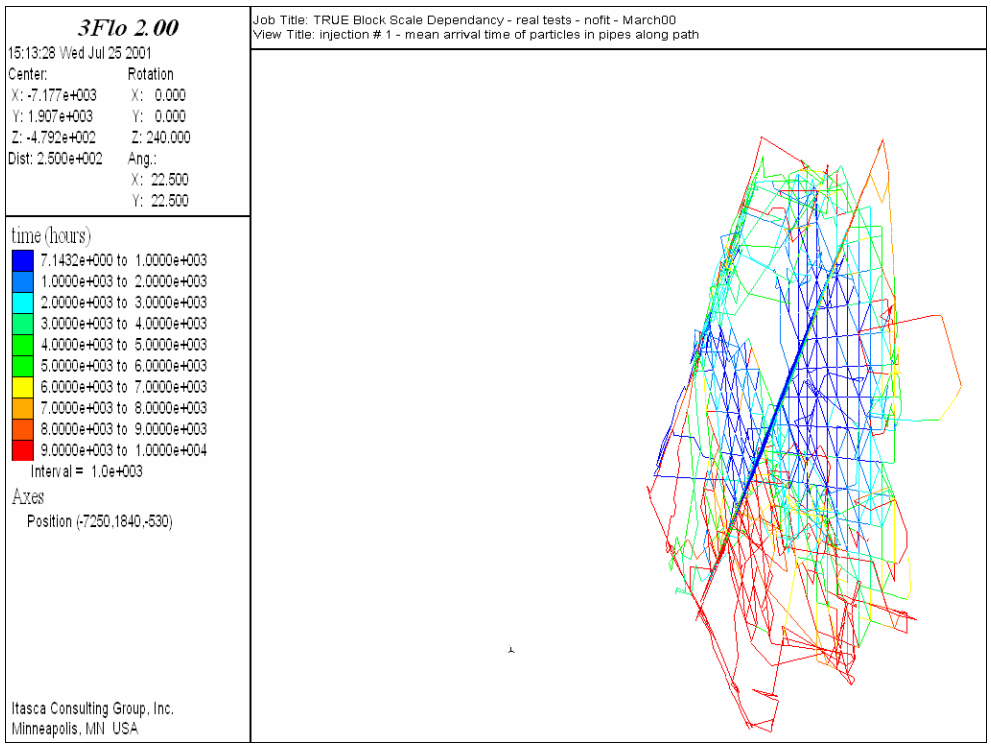

Figure 3-6 : *Tracer test stage model – Forward simulations*
Mean arrival time in hours of tracers in pipes along path for the simulated tracer Test 1

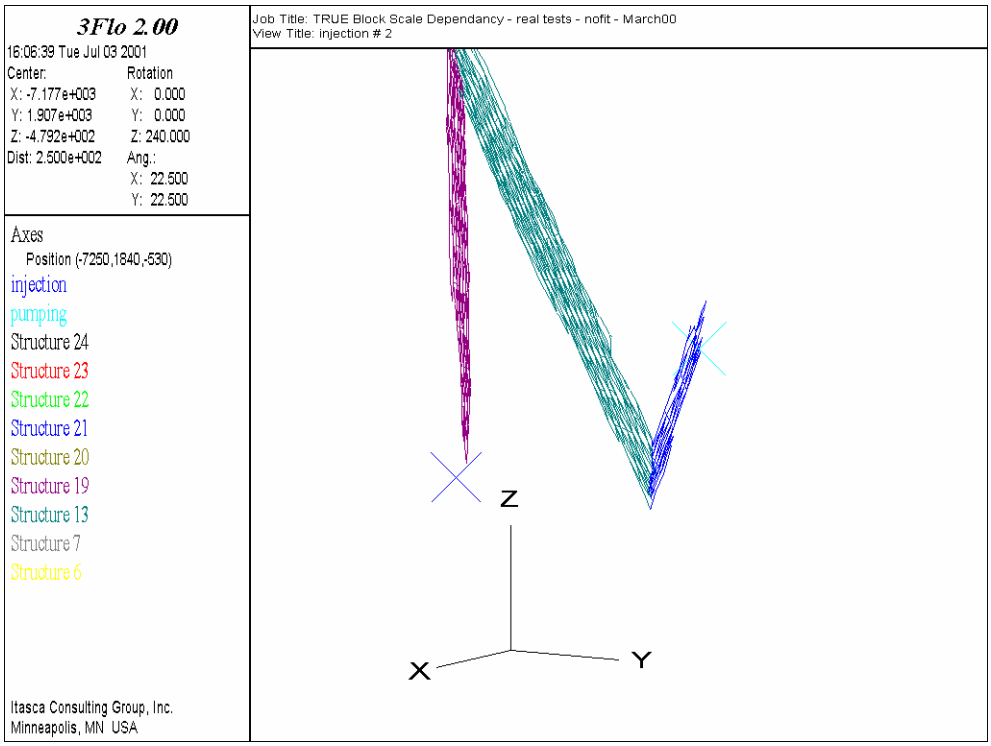

Figure 3-7 : *Tracer test stage model – Forward simulations*
Flow path for the simulated tracer Test 2

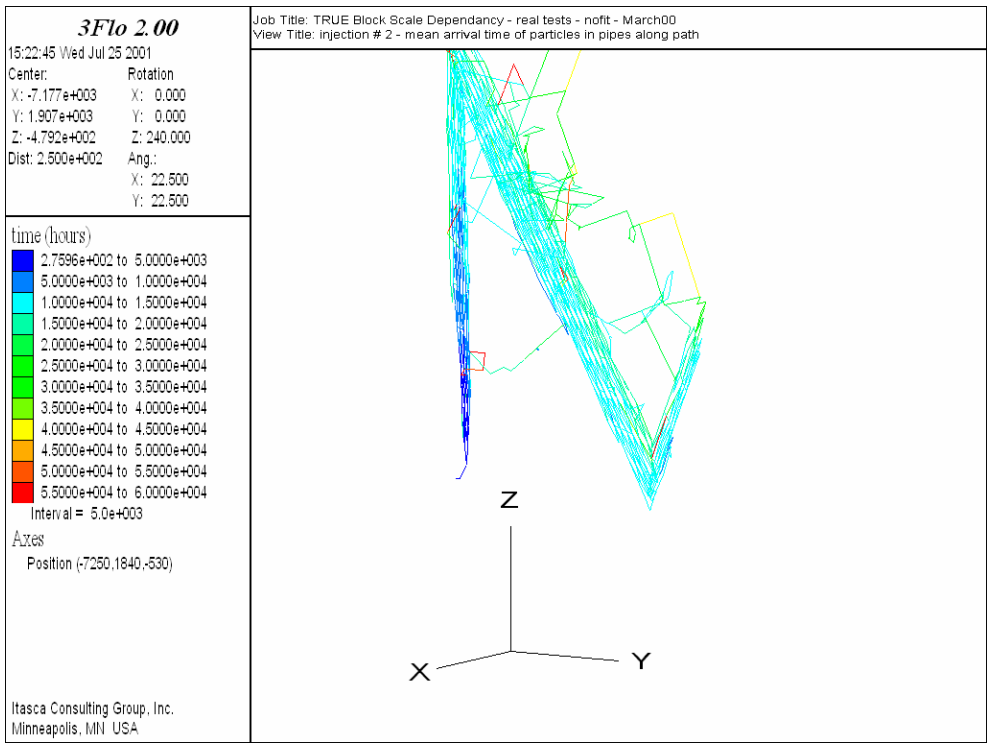

Figure 3-8 : *Tracer test stage model – Forward simulations*
Mean arrival time in hours of tracers in pipes along path for the simulated tracer Test ***2***

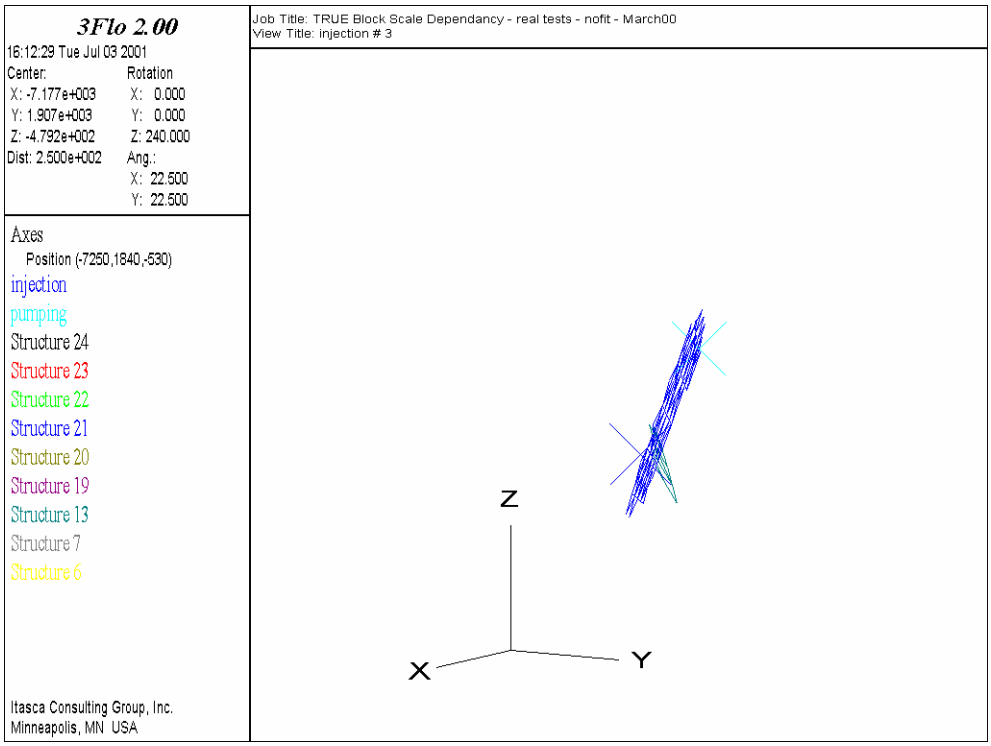

Figure 3-9 : *Tracer test stage model – Forward simulations*
Flow path for the simulated tracer Test 3

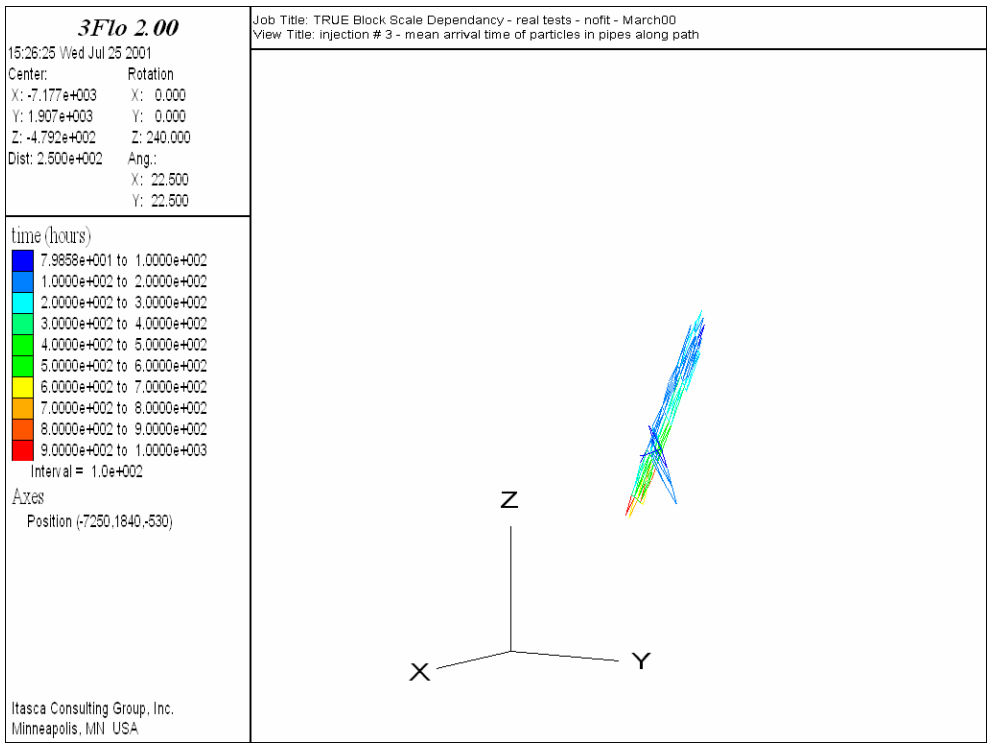

Figure 3-10 : *Tracer test stage model – Forward simulations*
Mean arrival time in hours of tracers in pipes along path for the simulated tracer Test 3

3.3 Detailed Characterisation stage model

Figure 3-11 shows the shape in the *3FLO* model of the structures of the March 1999 structural model (with a square grid-only for visualization, as previously employed), from a point of view slightly different from the one used in Figure 3-1 for the March 2000 model. We can still observe that besides the addition of Structures 23 and 24, the March 2000 model geometry is very close to the March 1999 model.

Table 3-3 gives the injection sections and the pumping point chosen in the March 1999 structural model. For Test 1 (B-2d), as Structure #23 does not exist, the interval along the borehole is slightly modified in order to cut a structure instead of cutting only the background fractures. The structure closest along the borehole is Structure #22.

Table 3-3 : Points selected in the 3FLO Detailed Characterisation stage model for simulation of three tracer tests

Test number	Test Name	Injection section	*Real Interval in borehole (m)*	*Real structures included*	*3FLO* Interval in borehole (m)	*3FLO* structures included
1	B-2d	KI0025F03:P7	*55.0-58.5*	*23*	50.0-61.0	22
2	B-2c	KA2563A:S1	*242-246*	*19*	230-236	19
3	B-2b	KI0025F02:P3	*93.4-99.25*	*13, 21*	93.4-99.25	13, 21
Pumping well		KI0023B:P6	*70.95-71.95*	*21*	70.0-71.0	21

Mass recoveries and breakthrough curves, respectively, are plotted in Figure 3-12 and Figure 3-13. Figure 3-14 to Figure 3-19 also represent the flow paths along structures and the mean arrival time of tracer in pipes along paths for each of the three tracer tests.

There is a 100% recovery for the three tests. A comparison of Figure 3-12 and Figure 3-3 shows that the behaviours to the three tracer tests of the Tracer test stage model and of the Detailed Characterisation stage model are somewhat similar. Each of the three tracer tests respond in the same way for the two models analysed. The differences between the three tests are also of the same magnitude for the two models.

The first arrivals for Test 1 (B-2d) are around 200 hours and the peak breakthrough is around 550 hours, instead of 100 and 250 hours for the March 2000 model. Most of the tracers from Test 1 arrive before 1 600 hours. The peak breakthrough is later than the one obtained in the March 2000 model, but “late” arrivals are faster. In the March 1999 model, Structure # 23 does not exist, and the tracer Test 1 is performed in Structure #22 instead. From the flow paths along structures plotted Figure 3-14, one can see that particles go directly from Structure #22, through Structure #20 and arrive in Structure #21 where the pumping well is located. Although the fastest flow path here is slower than the fastest flow path in the previous model, most flow paths are close to the fastest one, yielding more concentrated arrival times, i.e. the tracer explores a smaller part of the available network with less dispersion in the breakthrough as a result.

For Test 2 (B-2c), first arrivals are around 18 000 hours ; the peak breakthrough is quite late like in the March 2000 model, around 32 000 hours. The particles, injected in Structure #19, travel through Structure #13 before arriving into Structure # 21 (Figure 3-16). Again here, most of the travel time is spent in Structure 19 (Figure 3-17), with some tracer travelling "directly" (but also more slowly) through the background fractures.

In Test 3 (B-2b), one can observe like for the March 2000 model, the quickest first arrivals and peak breakthrough : 30 hours for the first arrivals (instead of 25 for the March 2000 model) and 150 hours for the peak breakthrough (instead of 100 hours for the March 2000 model). The transport paths in Test 3 involve Structure # 21 (Figure 3-18) almost exclusively.

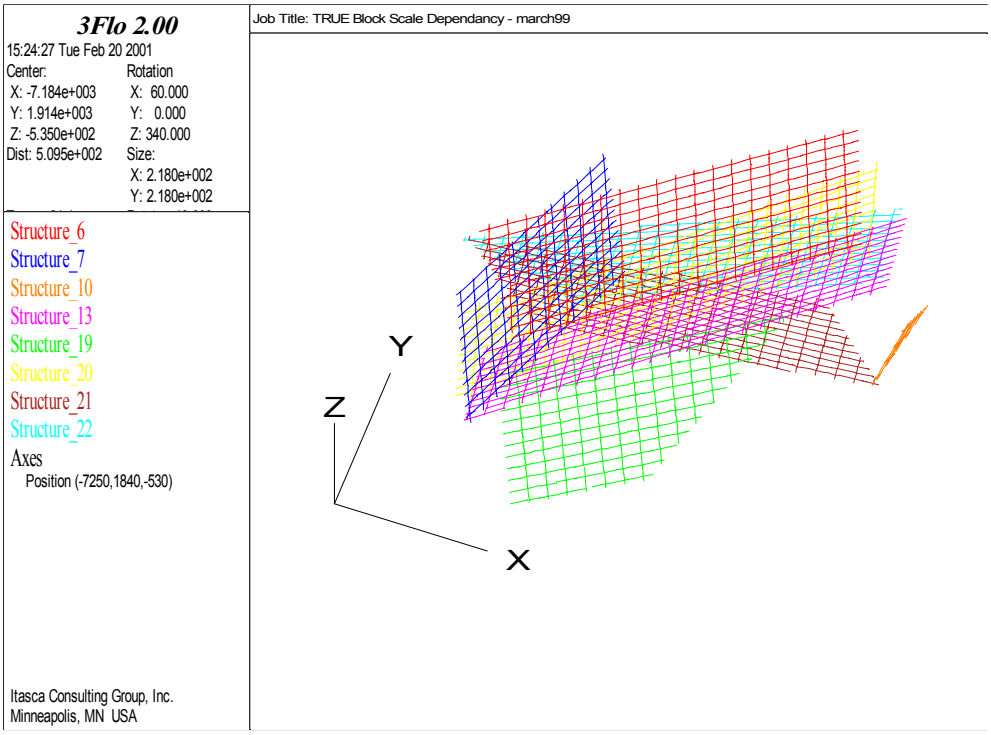

Figure 3-11 : *Detailed Characterisation stage model – Interrelation and shape of the structures (top view)*

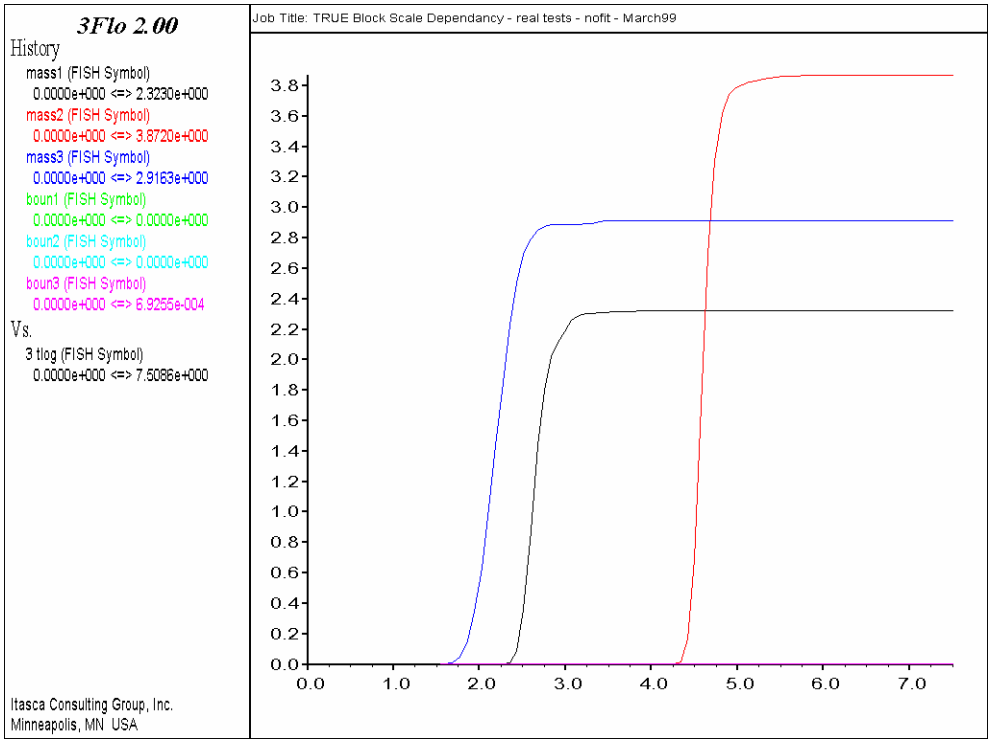

Figure 3-12 : *Detailed Characterisation stage model – Forward simulations Cumulative mass arrival (g) for the three tracer tests vs log (time in hours)*

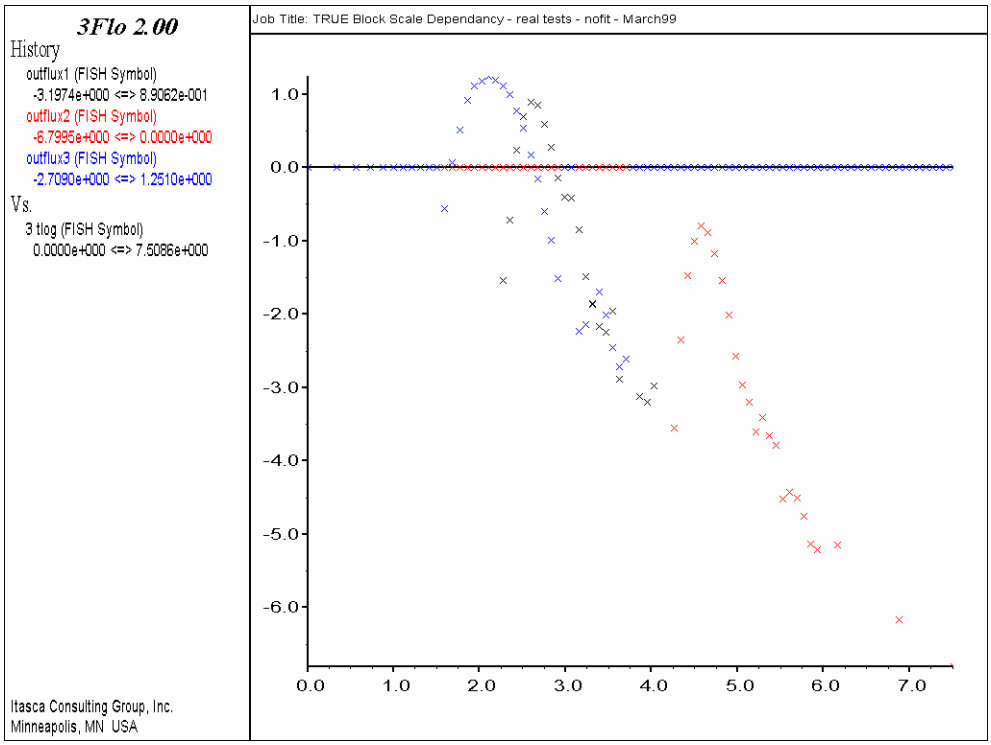

Figure 3-13 : *Detailed Characterisation stage model – Forward simulations Mass flux (mg/h) for the three tracer tests vs time in hours (log-log)*

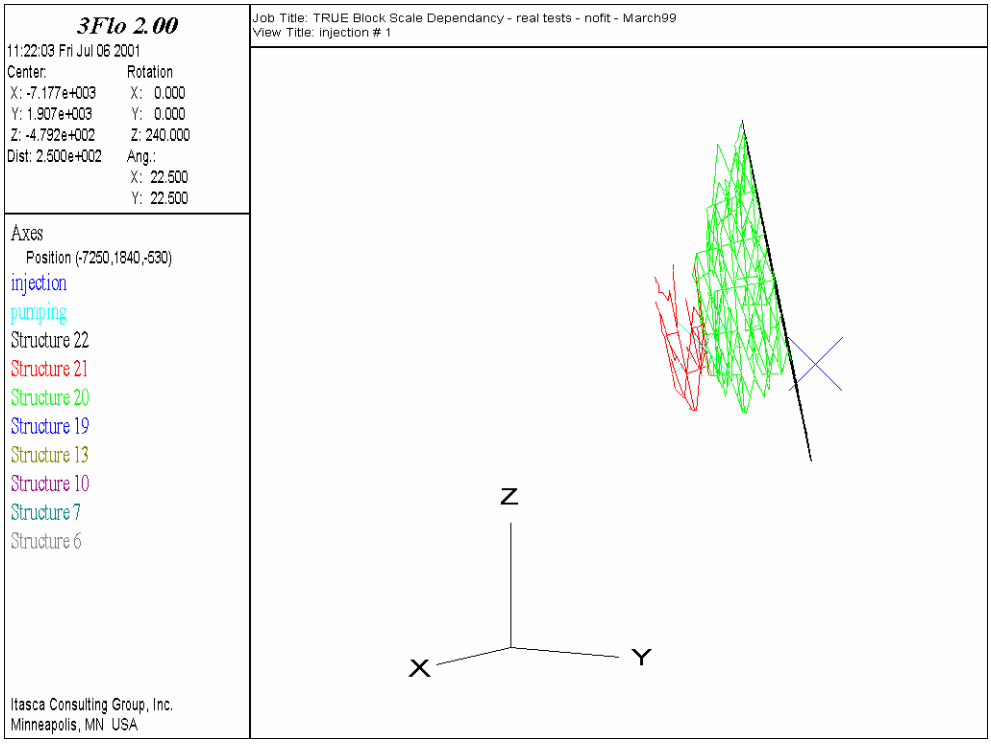

Figure 3-14 : *Detailed Characterisation stage model – Forward simulations Flow path for the simulated tracer Test 1*

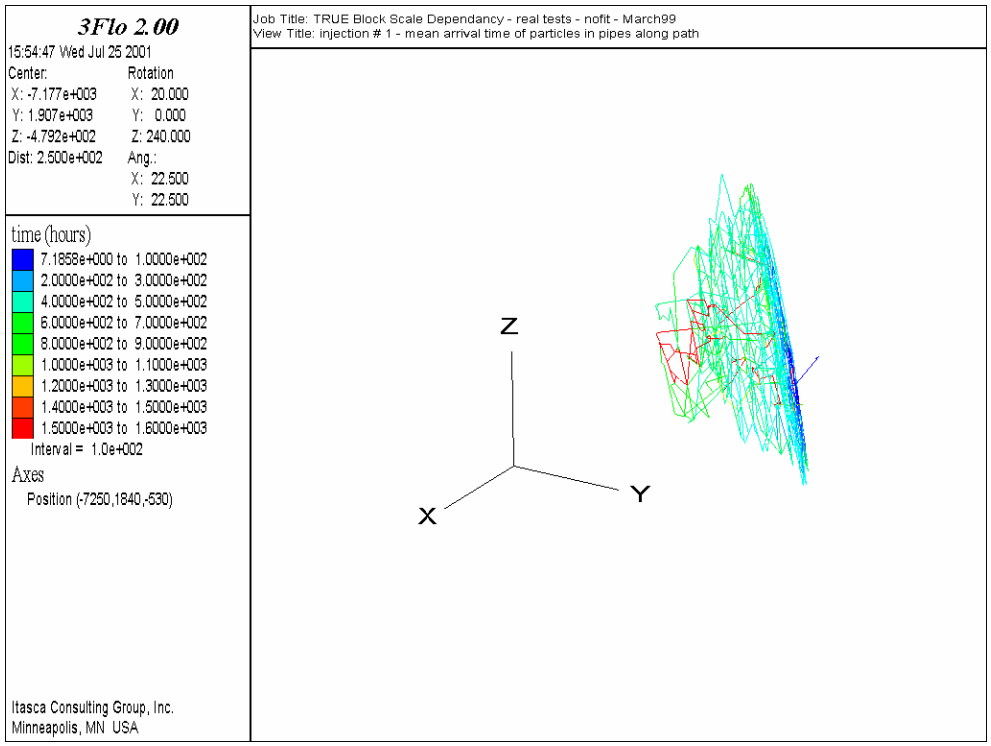

Figure 3-15 : *Detailed Characterisation stage model – Forward simulations Mean arrival time in hours of tracers in pipes along path for the simulated tracer Test 1*

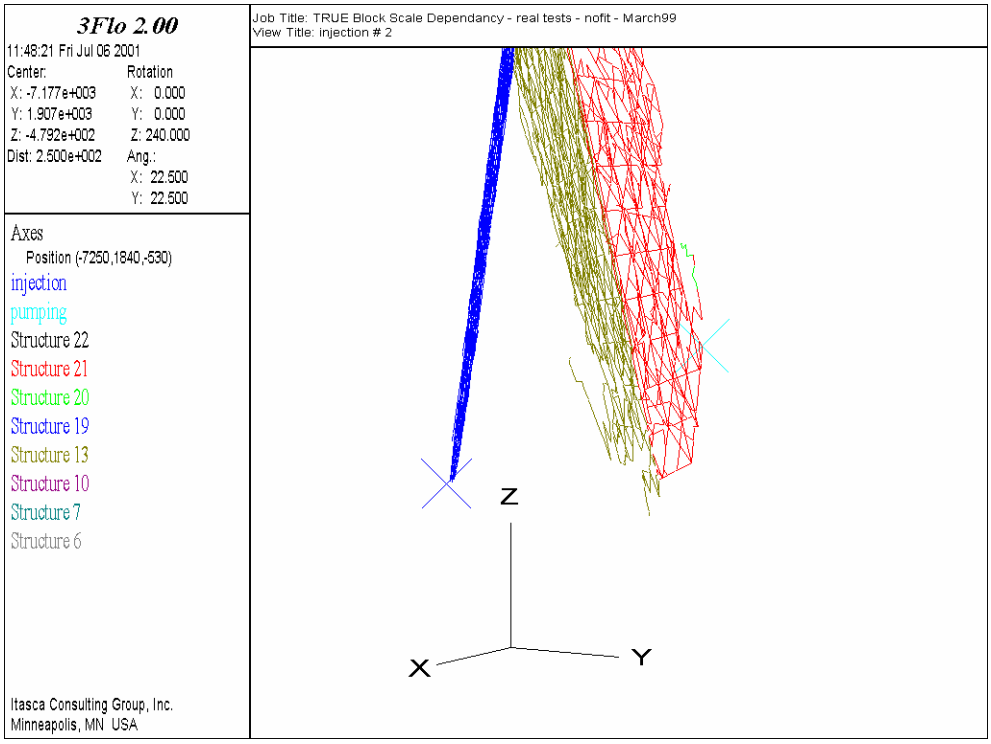

Figure 3-16 : *Detailed Characterisation stage model – Forward simulations*
Flow path for the simulated tracer Test 2

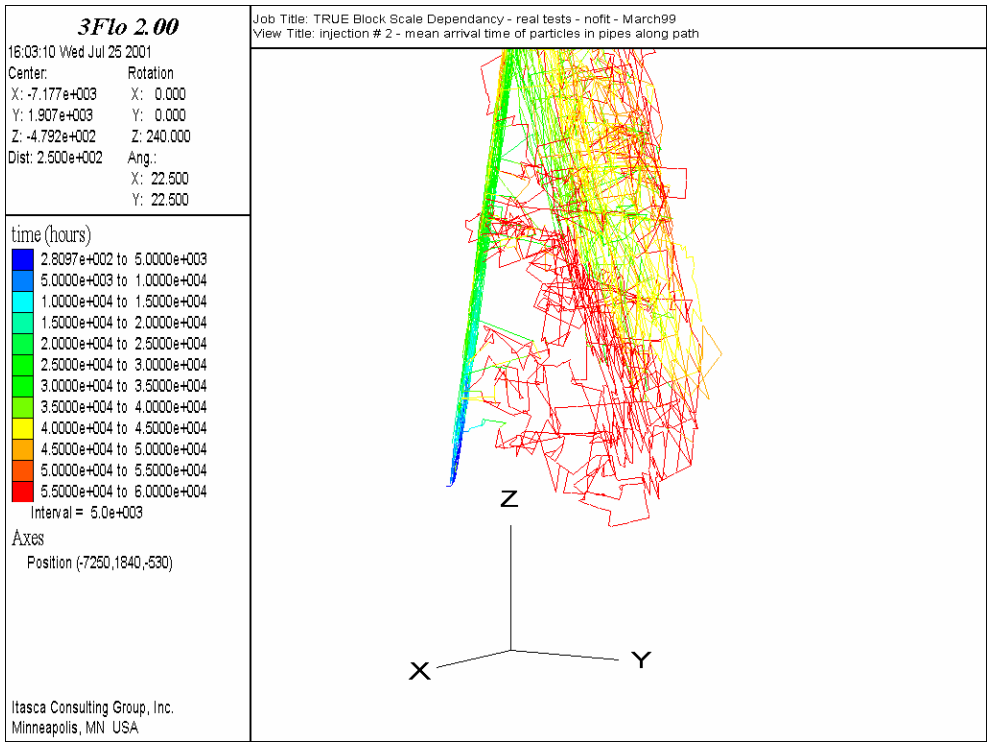

Figure 3-17 : *Detailed Characterisation stage model – Forward simulations*
Mean arrival time in hours of tracers in pipes along path for the simulated tracer Test 2

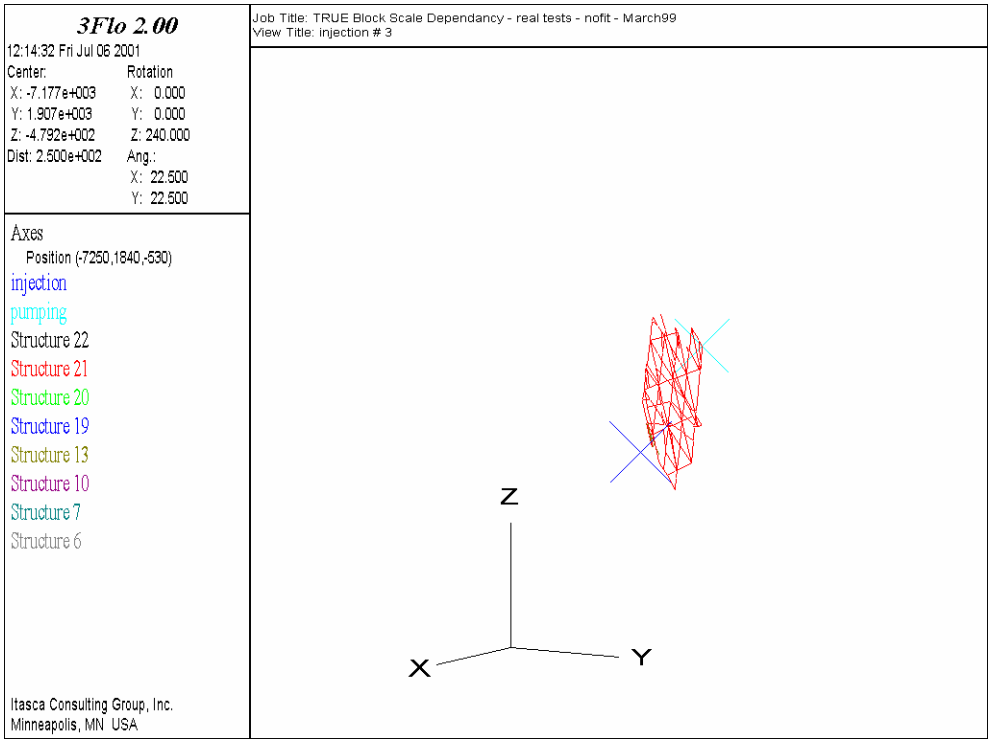

Figure 3-18 : *Detailed Characterisation stage model – Forward simulations*
Flow path for the simulated tracer Test 3

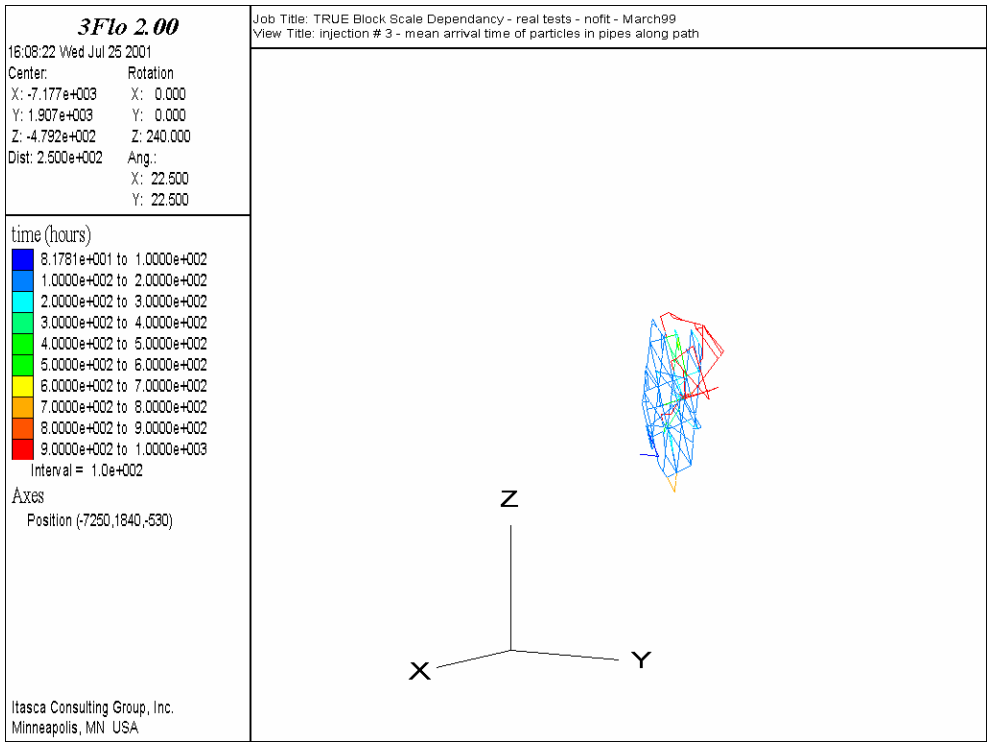

Figure 3-19 : *Detailed Characterisation stage model – Forward simulations*
Mean arrival time in hours of tracers in pipes along path for the simulated tracer Test 3

3.4 Preliminary Characterisation stage model

Figure 3-20 shows the shape in the *3FLO* model of the structures of the Preliminary Characterisation stage model. As Structures #23 and #21 do not exist in this model, the injection points and pumping point are somewhat modified. We then pump for the Preliminary Characterisation stage model in Structure #20 (see Table 3-4) and inject in Structure # 6 for Test 1 (B-2d), and in Structure 20 for test 3 (B-2b). Note that in this model, structure 9 provides a direct connection between the other structures, which is not the case in later models, since in the March 1999 and March 2000 models, where Structure #9 is omitted.

Table 3-4 : Points selected in the 3FLO Preliminary Characterisation stage model for simulation of three tracer tests

Test number	Test Name	Injection section	*Real Interval in borehole (m)*	*Real structures included*	*3FLO* Interval in borehole (m)	*3FLO* structures included
1	B-2d	KI0025F03:P7	*55.0-58.5*	*23*	50.0-53.5	6
2	B-2c	KA2563A:S1	*242-246*	*19*	224-228	19
3	B-2b	KI0025F02:P3	*93.4-99.25*	*13, 21*	93.4-99.25	13
Pumping well		KI0023B:P6	*70.95-71.95*	*21*	68.7-69.7	20

Mass recoveries and breakthrough curves, respectively, are plotted in Figure 3-21 and Figure 3-22. Figure 3-23 to Figure 3-28 also represent the flow paths along structures and the mean arrival time of tracer in pipes along paths for each of the three tracer tests.

There is a 100% recovery for the three tests. A comparison of Figure 3-21 with Figure 3-12 and Figure 3-3 shows that the response of the three models to the three tracer tests are still somewhat similar. Each of the three tracer tests respond in the same way for the three models analysed, although the arrival times are much closer in the Preliminary Characterisation stage mode than in the Detailed Characterisation stage model and in the Tracer test stage model.

For Test 1 (B-2d), first arrivals occur at about 300 hours, and the peak breakthrough is at 700 hours. Most tracer is recovered before 2 000 hours. This is in between the two previous models, with a behaviour close to the one in the March 1999 model: in Figure 3-23, one can see that three structures only are involved in the transport paths (structures 6, 9, and then 20), and arrivals are concentrated in time in the same manner.

For Test 2 (B-2c), the picture changes drastically from the previous to models: first arrivals are around 1600 hours ; the peak breakthrough is at around 1 500 hours, much shorter than 16 000 hours and 32 000 hours observed using the March 2000 and March 1999 models respectively. The particles, injected in Structure #19, travel through Structures #9 and #13 before arriving into the pump section in Structure # 20 (Figure 3-25). The connection through structure 9 is much more efficient than the connection through Structure 13 in the later models. Again, most of the transport occurs in the interpreted deterministic structures, with a few slow transport paths developed through background fractures (Figure 3-26).

In Test 3 (B-2b), first arrivals are about 200 hours and the peak breakthrough is around 500 hours, which is much slower than what is observed in the March 2000 model (25 and 100 hours respectively). Here the effect is inverse from before: because the structure in which we previously injected and pumped (i.e. # 21) does not exist here, we end up injecting in a structure (# 13) which is not directly connected to the structure being pumped. Hence the longer paths through Structures #13, #9 and #20 (Figure 3-27) and the later arrivals (Figure 3-28).

From the above, one can see that the step back in time from March 1999 to the Preliminary Characterisation model seriously degrades the response of the model, with flow paths becoming quite different from the more recent ones.

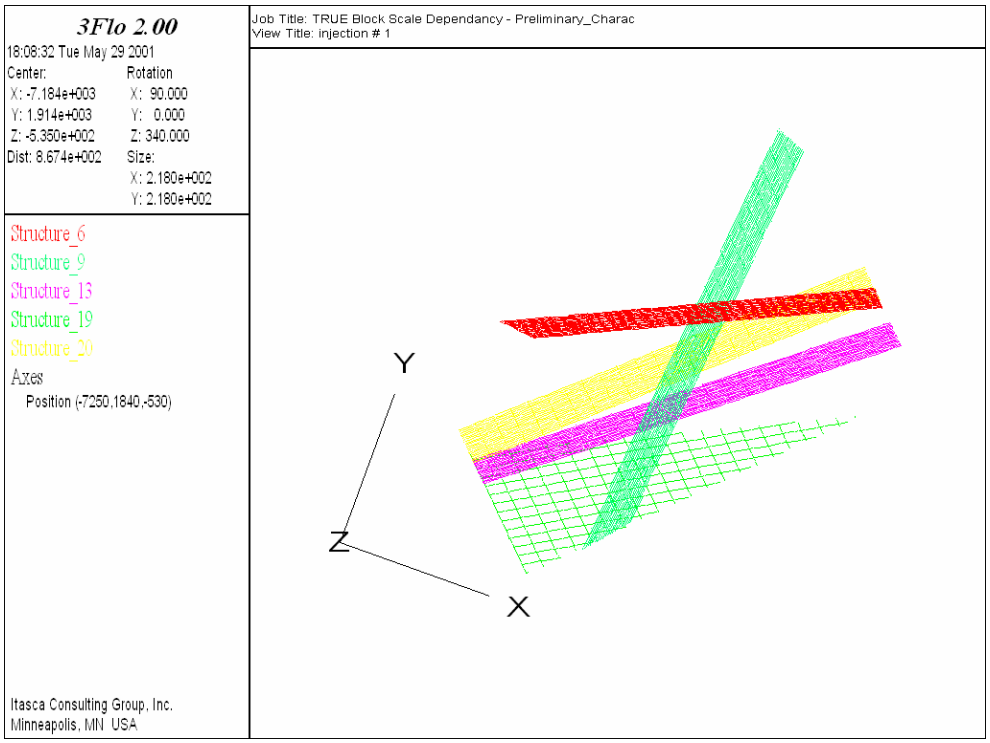

Figure 3-20 :*Preliminary Characterisation stage model – Interrelation and shape of the structures (top view)*

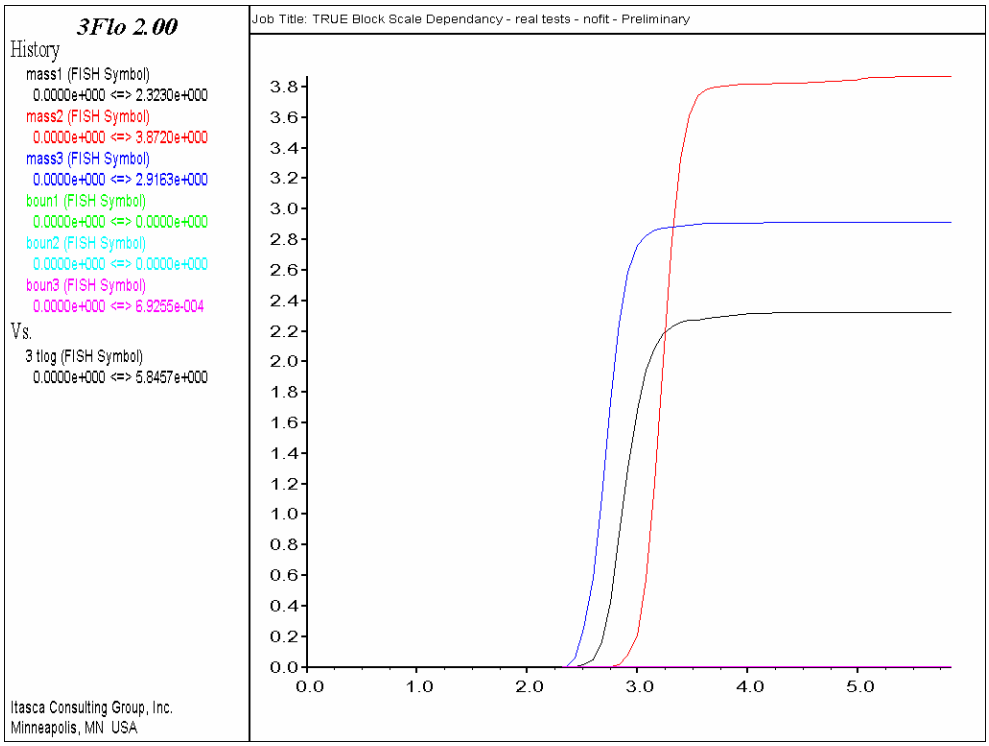

Figure 3-21 *: Preliminary Characterisation stage model – Forward simulations Mass recoveries (g) for the three tracer tests vs log (time in hours)*

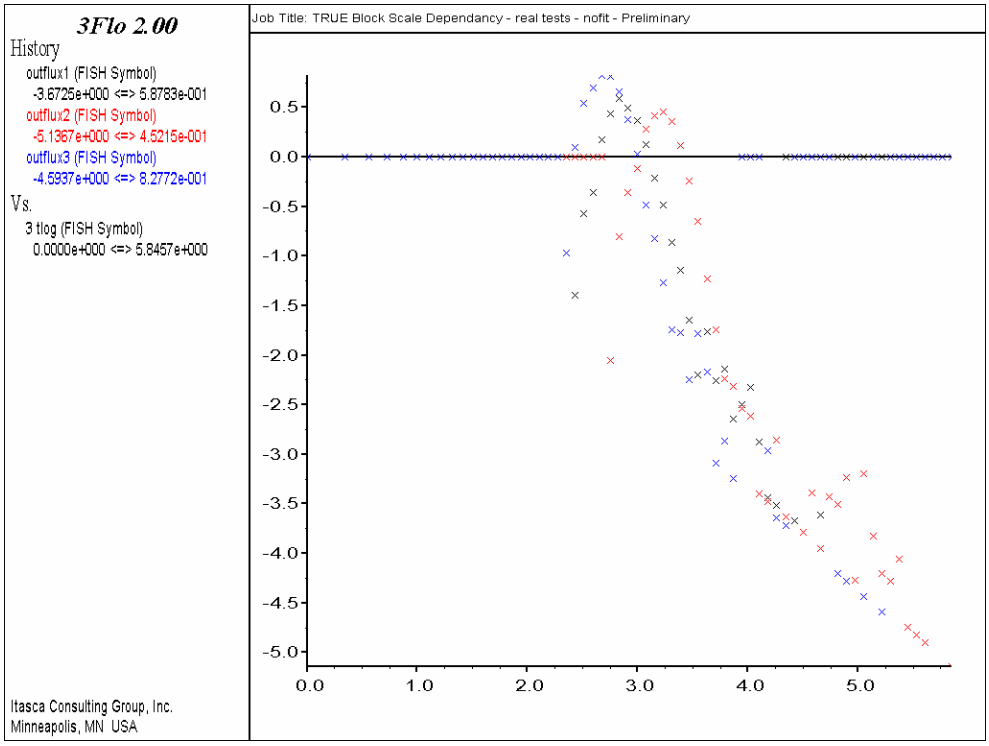

Figure 3-22 : *Preliminary Characterisation stage model – Forward simulations Mass flux (mg/h) for the three tracer tests vs time in hours (log-log)*

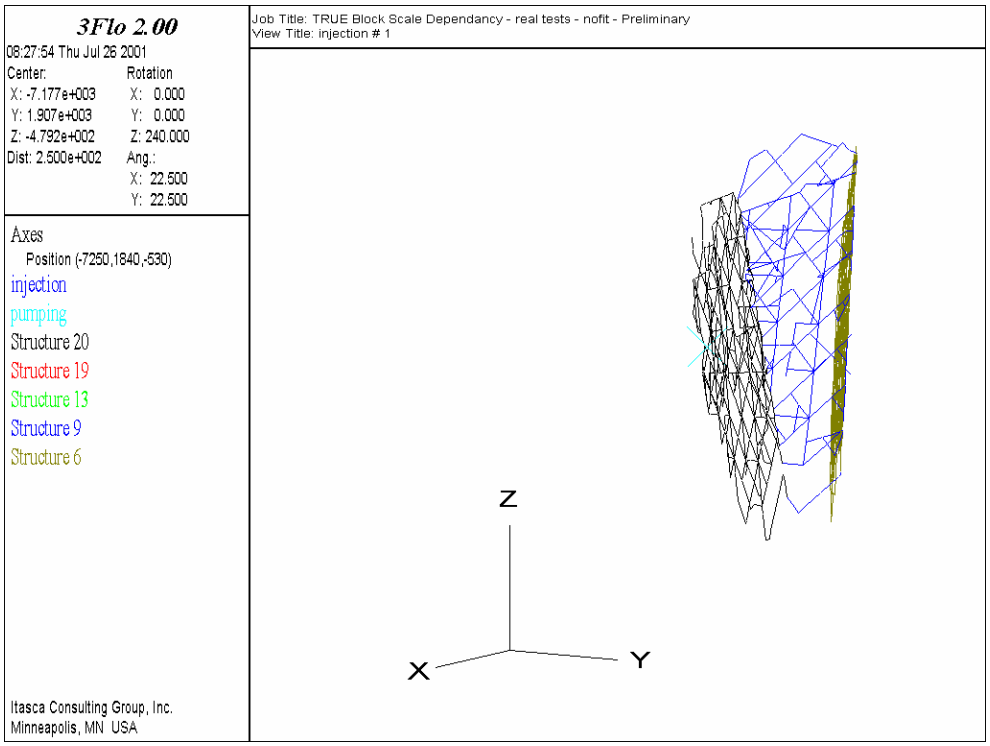

Figure 3-23 *: Preliminary Characterisation stage model – Forward simulations Flow path for the simulated tracer Test 1*

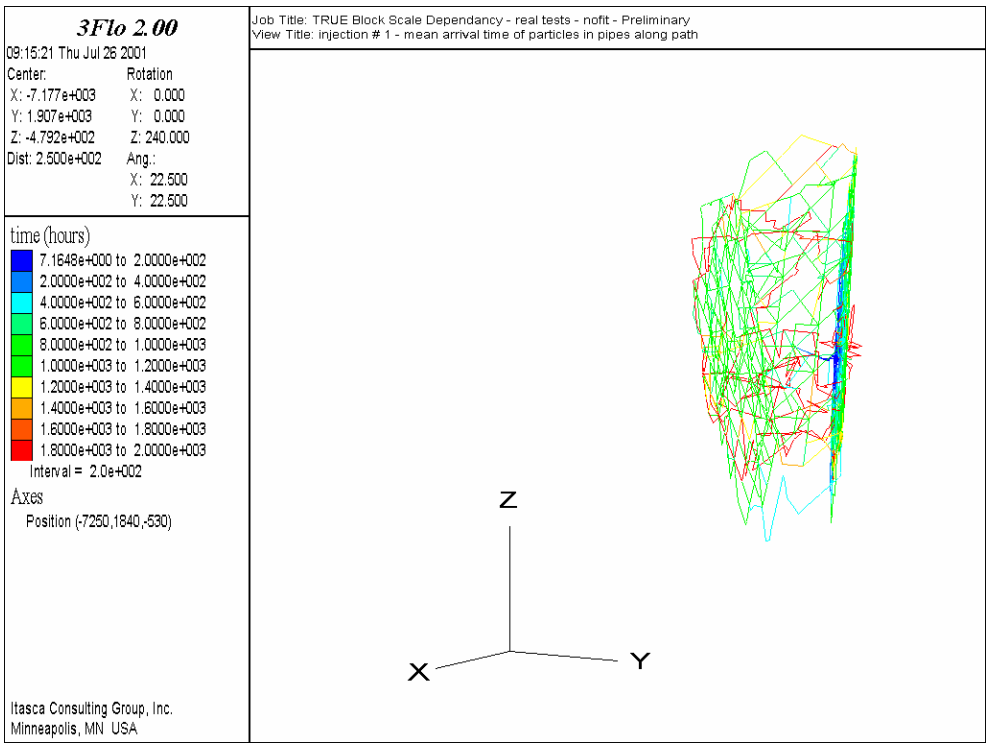

Figure 3-24 : *Preliminary Characterisation stage model – Forward simulations Mean arrival time in hours of tracers in pipes along path for the simulated tracer Test 1*

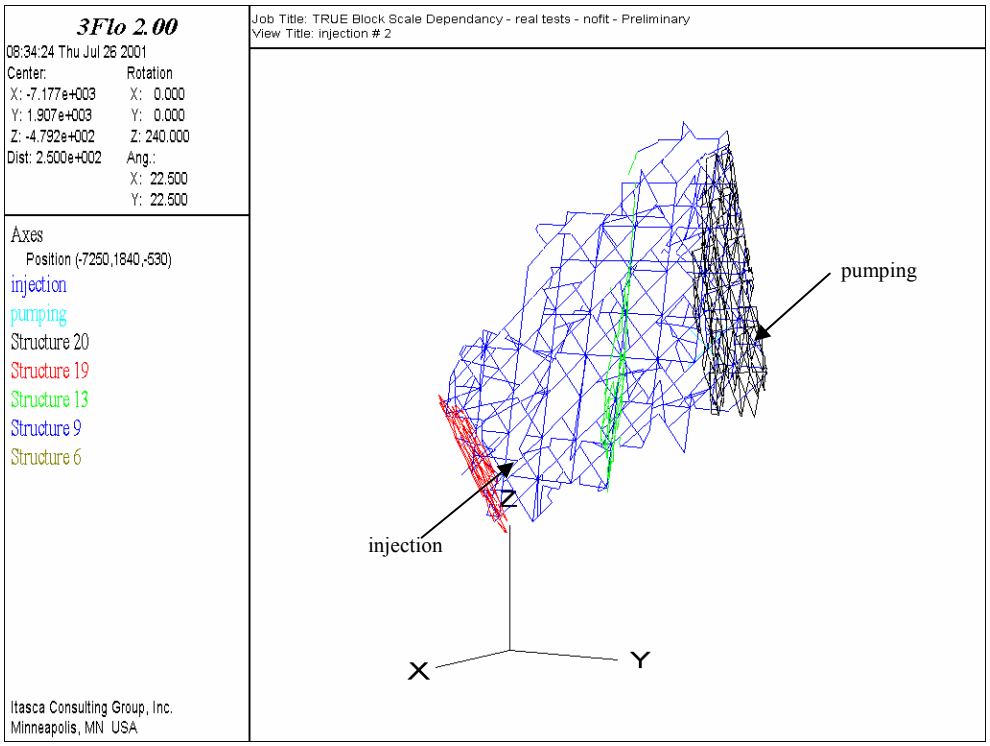

Figure 3-25 *: Preliminary Characterisation stage model – Forward simulations Flow path for the simulated tracer Test 2*

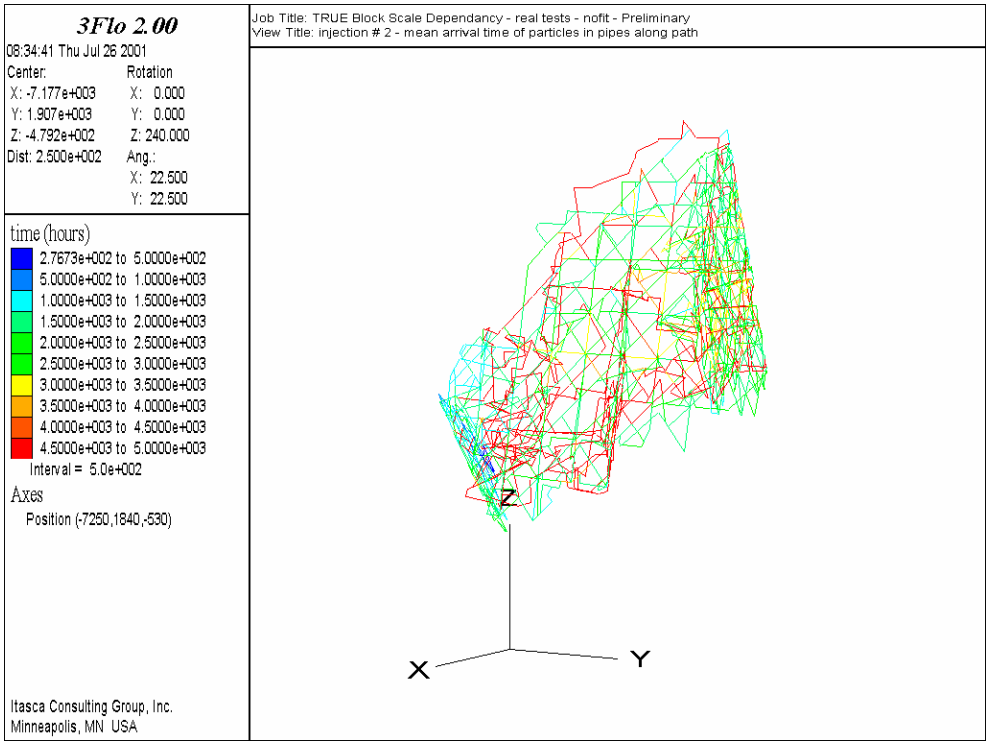

Figure 3-26 : *Preliminary Characterisation stage model – Forward simulations Mean arrival time in hours of tracers in pipes along path for the simulated tracer Test 2*

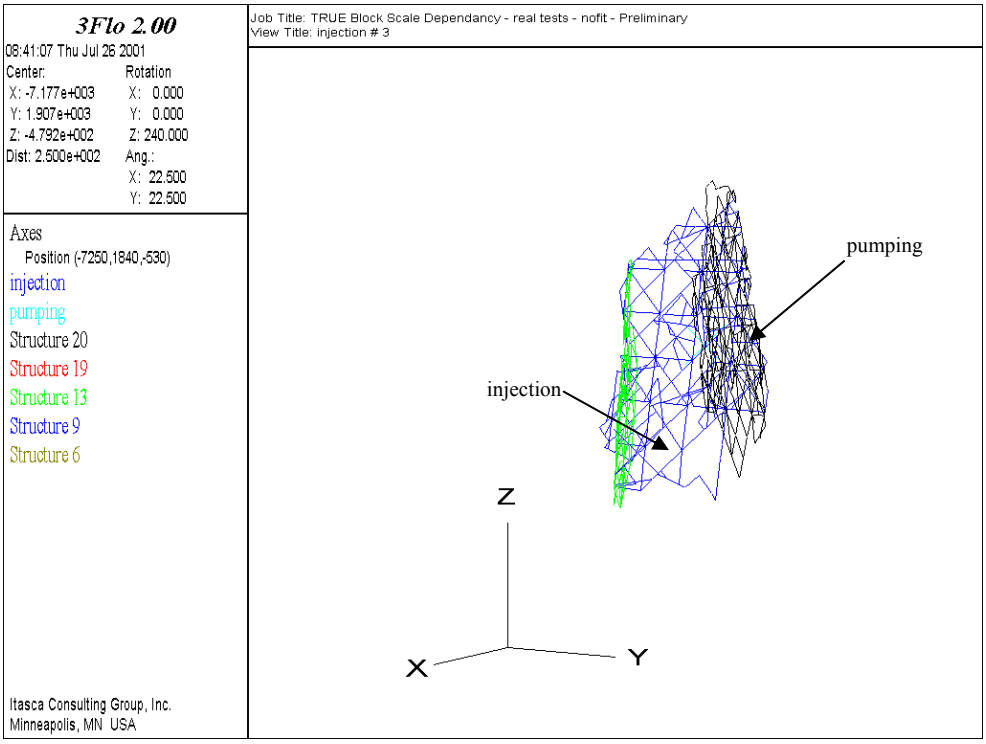

Figure 3-27 : *Preliminary Characterisation stage model – Forward simulations*
Flow path for the simulated tracer Test 3

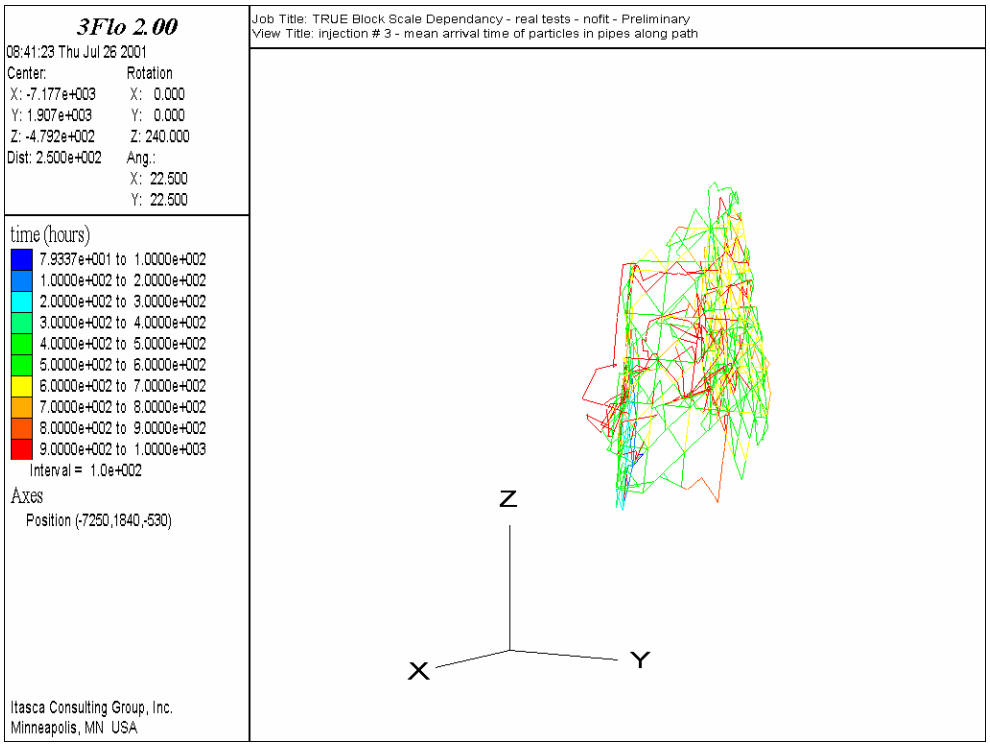

Figure 3-28 : *Preliminary Characterisation stage model – Forward simulations*
Mean arrival time in hours of tracers in pipes along path for the simulated tracer Test 3

3.5 Scoping Characterisation stage model

Figure 3-29 shows the interrelation and shape in the *3FLO* model of the selected fractures for the Scoping Characterisation stage model.

Table 3-5 gives the injection points and the pumping point chosen in the Scoping Characterisation stage model. For Test 1, as Structure #23 does not exist the interval along borehole KI0025F03 is slightly modified in order to cut a structure instead of cutting only the background fractures; the Structure #6 is chosen for Test 1 (B-2d). The same is done for Test 2 (B-2c) and choose Structure #8. For Test 3 (B-2b) and the pumping well, Structures #13 and #21 do not exist. Furthermore, the corresponding sections along the two boreholes KI0025F02 and KI0023B do not cross any structures. In order not to change too much the interval along the boreholes, it is decided to inject in the background fractures instead of trying to select a structure which would be too far from the real positions along boreholes of Structures #13 and #21.

Table 3-5 : Points selected in the 3FLO Scoping Characterisation stage model for simulation of three tracer tests

Test number	Test Name	Injection section	*Real Interval in borehole (m)*	*Real structures included*	*3FLO* Interval in borehole (m)	*3FLO* structures included
1	B-2d	KI0025F03:P7	*55.0-58.5*	*23*	45.0-48.5	6
2	B-2c	KA2563A:S1	*242-246*	*19*	208-212	8
3	B-2b	KI0025F02:P3	*93.4-99.25*	*13, 21*	94.0-99.85	one BF*
Pumping well		KI0023B:P6	*70.95-71.95*	*21*	70.0-71.0	3 BF*

* BF : back-ground fracture

Mass recoveries and breakthrough curves, respectively, are plotted in Figure 3-30 and Figure 3-31. Figure 3-32 to Figure 3-37 also represent the flow paths and the mean arrival time of tracer in pipes along paths for each of the three tracer tests.

There is a 100% recovery for the three tests. Adding Figure 3-30 to the comparison of model responses that has been made before (with Figure 3-21, Figure 3-12 and Figure 3-3) shows that the response to the three tracer tests is not further observed in the Scoping Characterisation stage model. than in the previous models: the three tests responses now have very little to do with the initial ones.

The first arrivals for Test 1 (B-2d) are around 60 hours and the peak breakthrough is around 110 hours, instead of 100 and 250 hours for the March 2000 model. Most of the tracers from Test 1 arrive before 1 000 hours. From the flow paths along structures plotted in Figure 3-32, one can see that particles go directly from Structure #6, through Structure #18 and arrive in the pumping well located in a background fracture. The mean arrival times in pipes along transport paths plotted in Figure 3-33 show that some tracer travels through background fractures, but that the paths developed in deterministic structures by far are the fastest.

For Test 2 (B-2c), first arrivals are around 40 hours; the peak breakthrough is very early compared to the ones observed for the previous models, at about 200 hours. The tracer, injected in Structure #8, travels through the background fractures and Structure #18 before arriving into the background fracture where we pump (Figure 3-34 and Figure 3-35).

In Test 3 (B-2b), the first arrivals and peak breakthrough are around 320 and 1 400 hours, instead of 25 and 100 which were the quickest arrivals out of the three tests. The reason is that in the Scoping Characterisation stage model, we inject and pump in the background fractures, instead of in structures like in the March 2000 model. The particles do not cross any structures and are only transported through the background fractures. That is why there isn't any path plotted in Figure 3-36, since we plot only the structures visited by the tracer there and not the background fractures.

From the above, we can obviously draw the same conclusions as for the Preliminary Characterisation stage: model response is quite far from the response in the two subsequent models. In fact, the response is also quite different from the Preliminary Characterisation model.

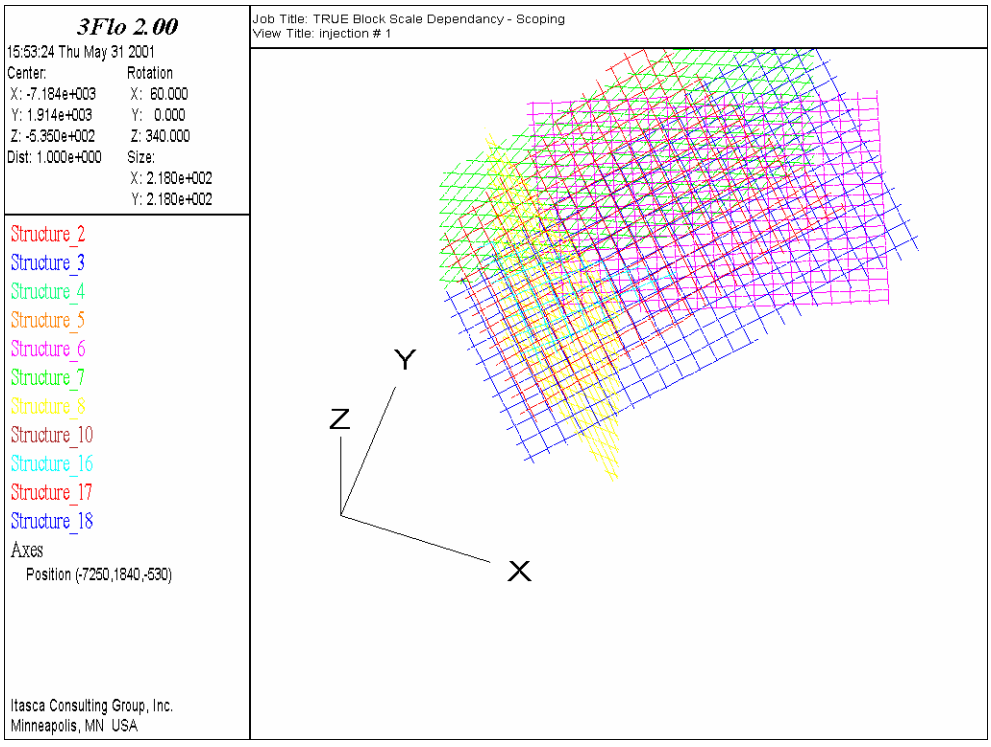

Figure 3-29 *: Scoping Characterisation stage model – Interrelation and shape of the structures (top view)*

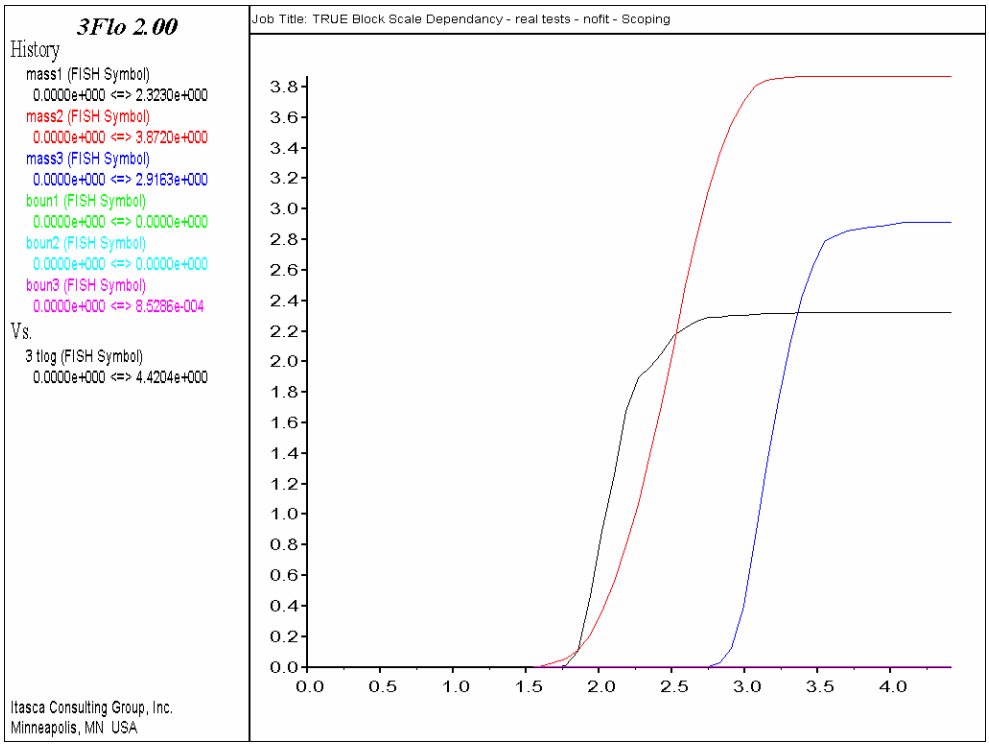

Figure 3-30 : *Scoping Characterisation stage model – Forward simulations Mass recoveries (g) for the three tracer tests vs log (time in hours)*

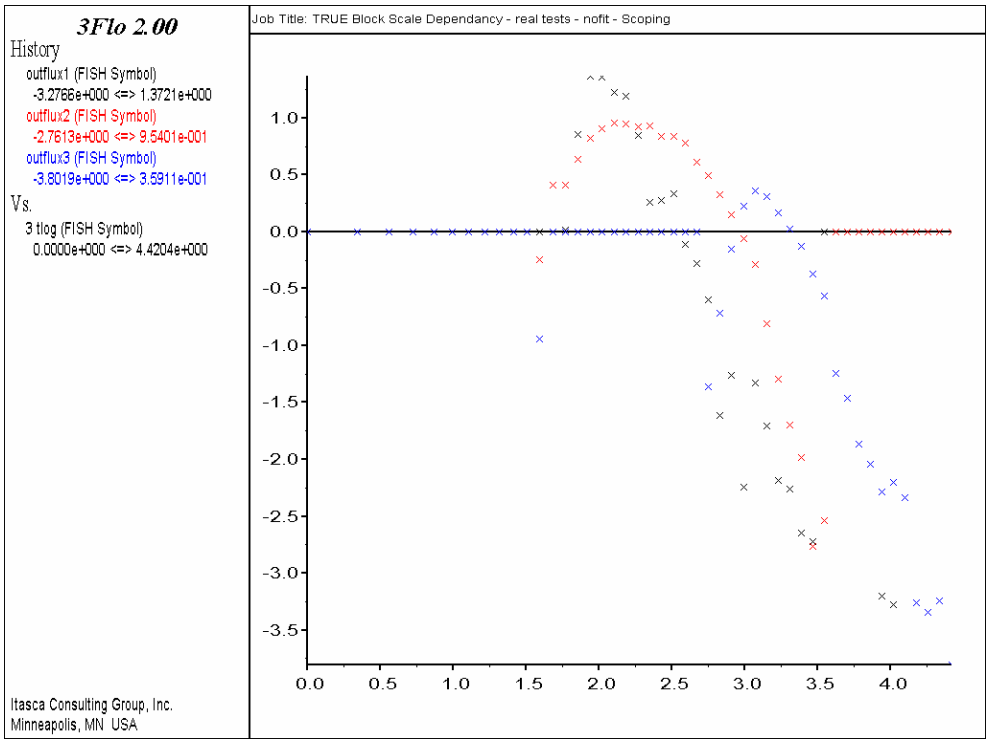

Figure 3-31 *: Scoping Characterisation stage model – Forward simulations Mass flux (mg/h) for the three tracer tests vs time in hours (log-log)*

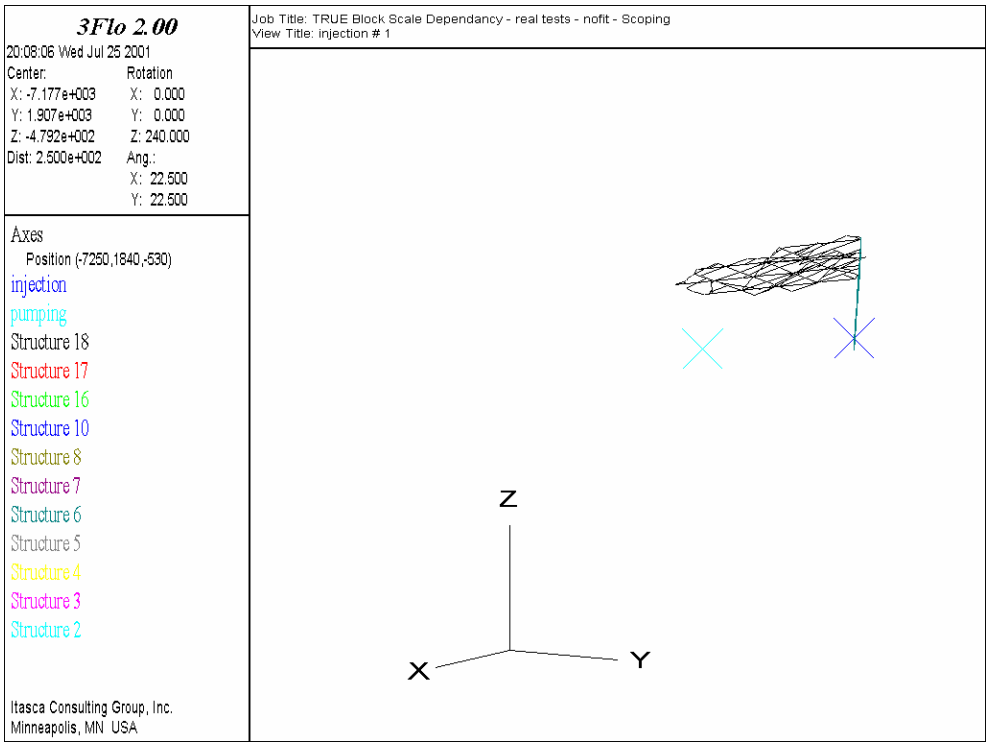

Figure 3-32 *: Scoping Characterisation stage model – Forward simulations Flow path for the simulated tracer Test 1*

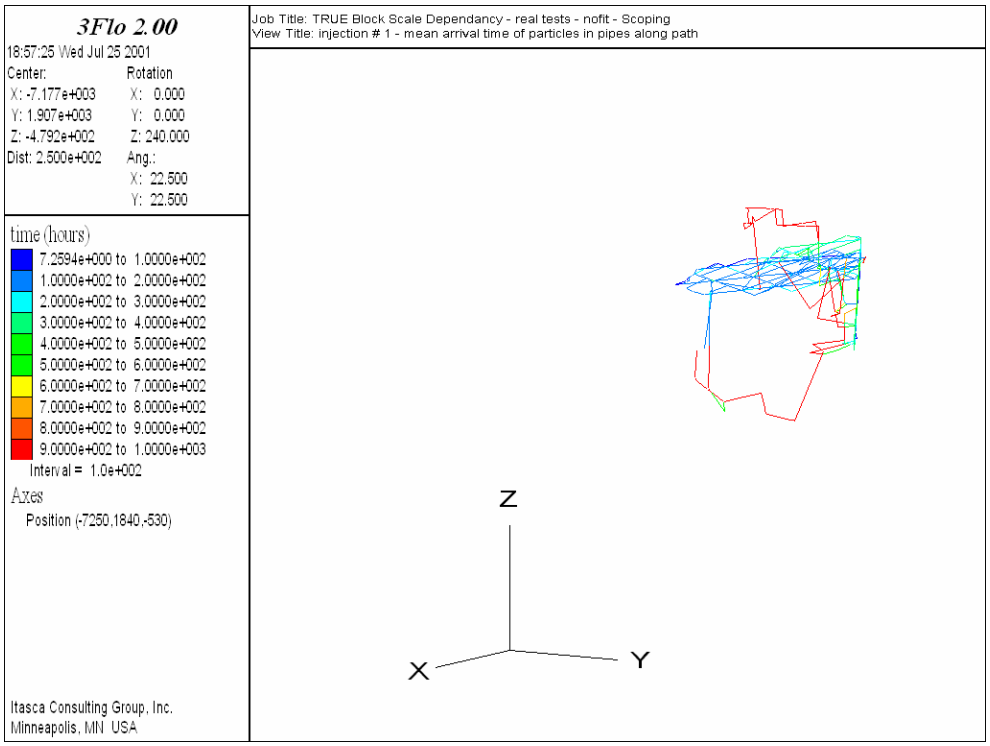

Figure 3-33 *: Scoping Characterisation stage model – Forward simulations Mean arrival time in hours of tracers in pipes along path for the simulated tracer Test 1*

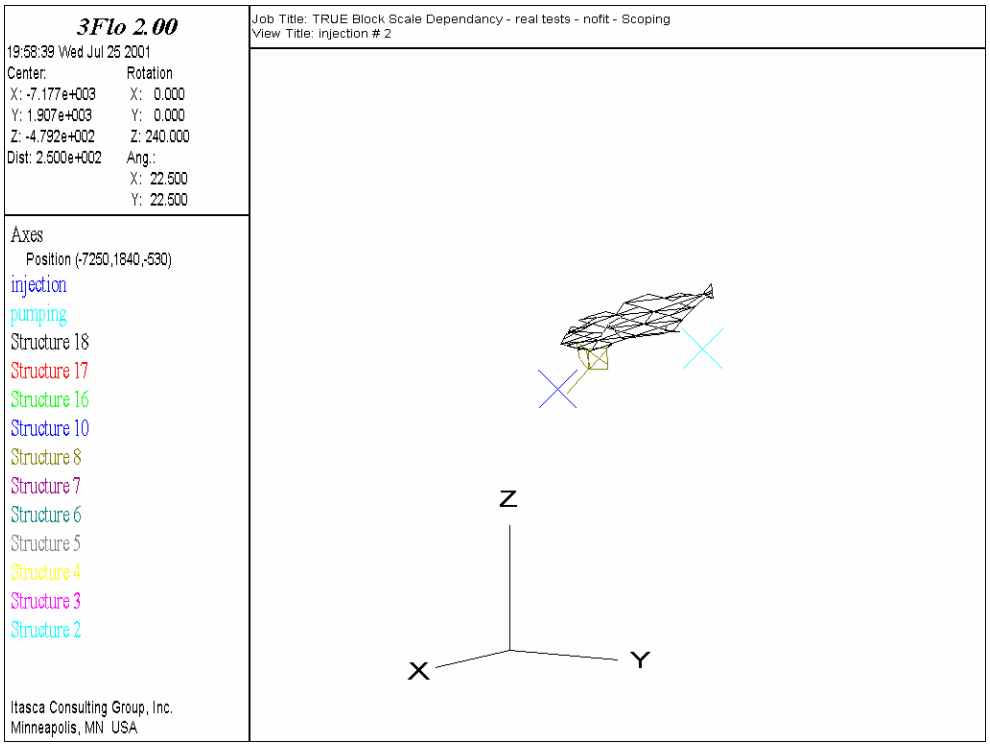

Figure 3-34 : *Scoping Characterisation stage model – Forward simulations Flow path for the simulated tracer Test 2*

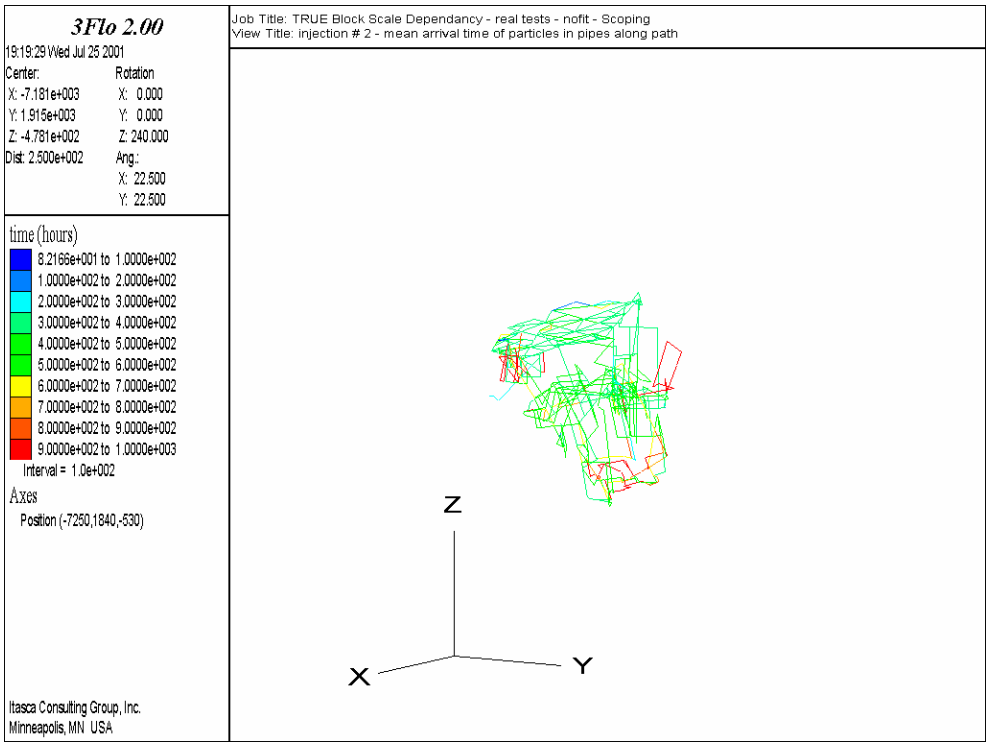

Figure 3-35 : *Scoping Characterisation stage model – Forward simulations Mean arrival time in hours of tracers in pipes along path for the simulated tracer Test 2*

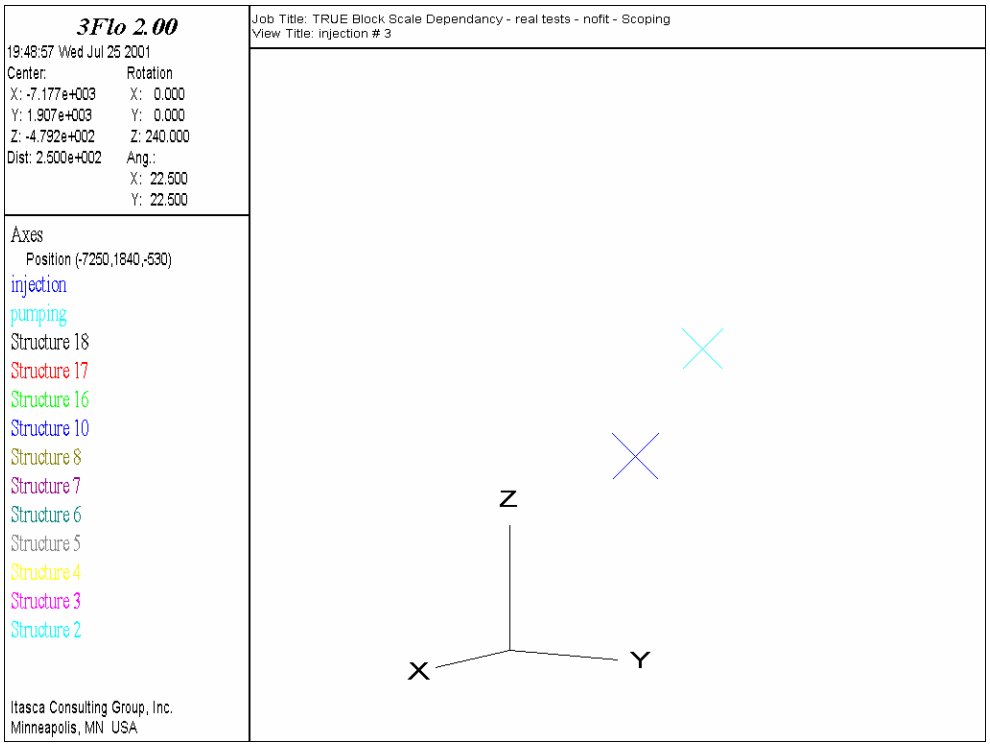

Figure 3-36 : *Scoping Characterisation stage model – Forward simulations Flow path for the simulated tracer Test 3*

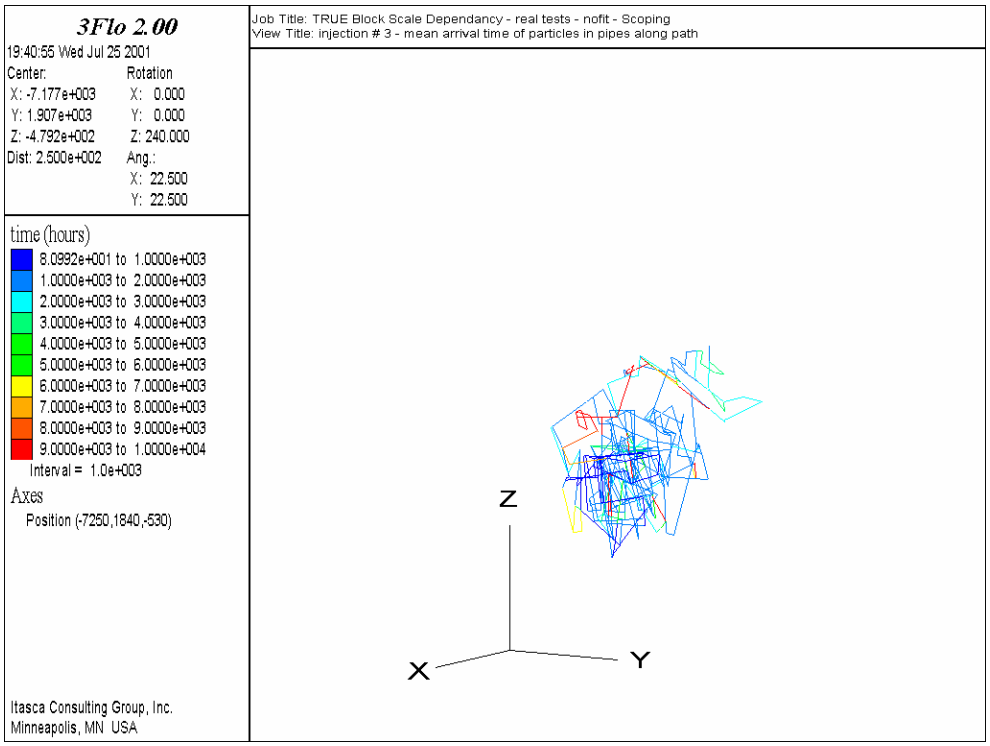

Figure 3-37 : *Scoping Characterisation stage model – Forward simulations Mean arrival time in hours of tracers in pipes along path for the simulated tracer Test 3*

4 Results from calibrated simulations

4.1 Calibration and results from Tracer test stage model

The available in situ experimental data from the three real tracer tests consist of breakthrough curves (Figure 4-1 to Figure 4-3) plotted as mass flux versus time in hours, in a log-log scale (from Andersson et al, 2000b).

The transport parameters of the "current" March 2000 structural model are simultaneously calibrated to the three tracer tests. We concentrate on reproducing first arrival times and peak arrival times.

The in situ first arrivals and peak arrivals for Test 1 (B2-d) are respectively around 30 and 100 hours, which are faster, by a factor of 2-3, than the arrivals observed by simulation using the "current" March 2000 structural model.

For Test 2 (B-2c), in situ first arrivals and peak arrivals are much faster (factor of 10-20) than the simulated ones : 300 and 1 800 hours respectively instead of 6 000 and 16 000 hours.

On the contrary, for Test 3 (B-2b), in situ first arrivals and peak arrivals are slower than the ones computed : 40 and 300 hours instead of 25 and 100 hours, respectively.

As seen in Chapter 3.2, for each tracer test, particles travel through the following structures :

- Test 1 : 23, 22, 20 and 13, 21
- Test 2 : 19, 13, 21
- Test 3 : 13, 21.

To accelerate the particles for Test 1 and Test 2, Structures #13, #19 and #23 are modified according to :

- Structure #19
  - reduce the porosity by a factor of 10,
  - keep the transmissivity unchanged (Structure #19 is already a very transmissive structure, with a mean transmissivity of 10^{-5} m²/s),
- Structure #13
  - reduce the porosity by a factor of 10,
  - increase the mean transmissivity by a factor of 10 (10^{-6} instead of 10^{-5} m²/s), and increase by a factor of 100 the minimum used in the transmissivity distribution (10^{-7} m²/s instead of 10^{-9} m²/s),
- Structure #23
  - increase by a factor of 10 the three parameters used in the transmissivity distribution (mean = 6 10^{-8} m²/s instead of 6 10^{-9} m²/s, sd = 3 10^{-8} m²/s instead of 3 10^{-9} m²/s and min = 3 10^{-8} m²/s instead of 3 10^{-9} m²/s).

This calibration accelerates a little bit arrivals from tracer Test 3, since this test involves mainly Structure #13.

Results for the Calibrated March 2000 structural model are presented in Figure 4-4 to Figure 4-11.

Table 4-1 compiles the first arrival and peak arrival times, as well as the peak mass fluxes, obtained for the March 2000 Structural model (real tests and numerical tests before and after calibration). One clearly sees that the calibration helps reducing the first and peak arrival times for Test 1 and Test 2. After calibration, the *3FLO* March 2000 structural model gives first and peak arrival times in a range of 1.5-2 greater than the one measured in situ. The mass flux computed at the peak breakthrough is also in the range of what has been measured in reality.

For Test 3, first and peak arrival times computed with the calibrated model are shortened a little bit compared to the times computed with the non-calibrated model, since Structure #13, the single structure involved in Test 3, is changed in order to accelerate particle in the two other tests. However, first and peak arrival times are still in the range of what has been measured in situ.

Transport paths, as seen in Figure 4-6 to Figure 4-11, are not affected a lot in test 1 (B-2d), where only the fastest paths from the unfitted model are kept; they are not affected in test 2 (B-2c); However, in test 3 (B-2b), a new group of paths is explored by the tracer, going from Structure # 13 to Structure # 22 and then Structure # 20.

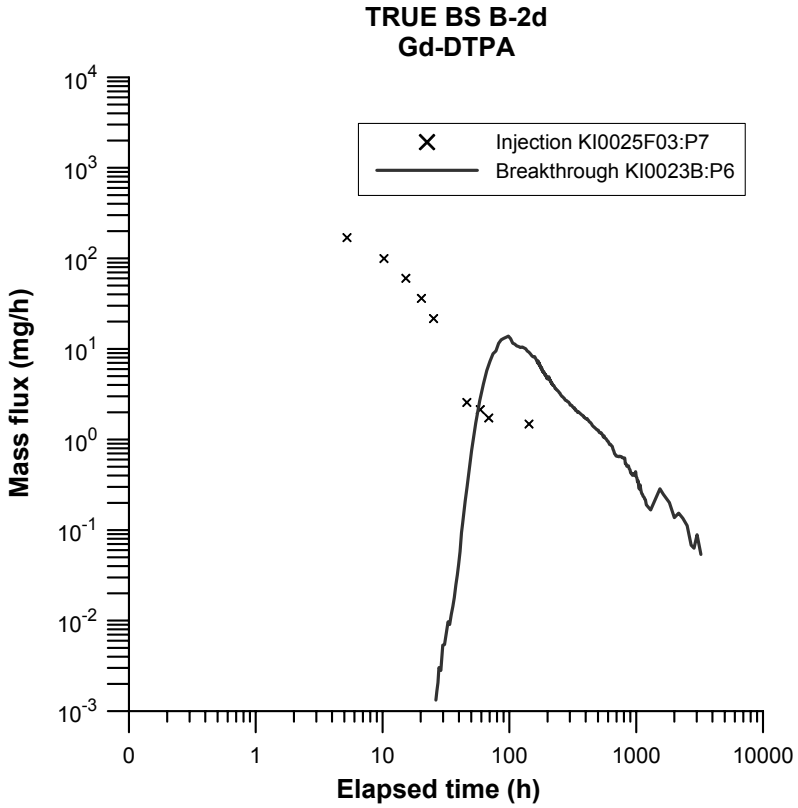

Figure 4-1 : *Breakthrough curve in a log-log scale for real first tracer test (B-2d) (from Andersson et al, 2000b)*

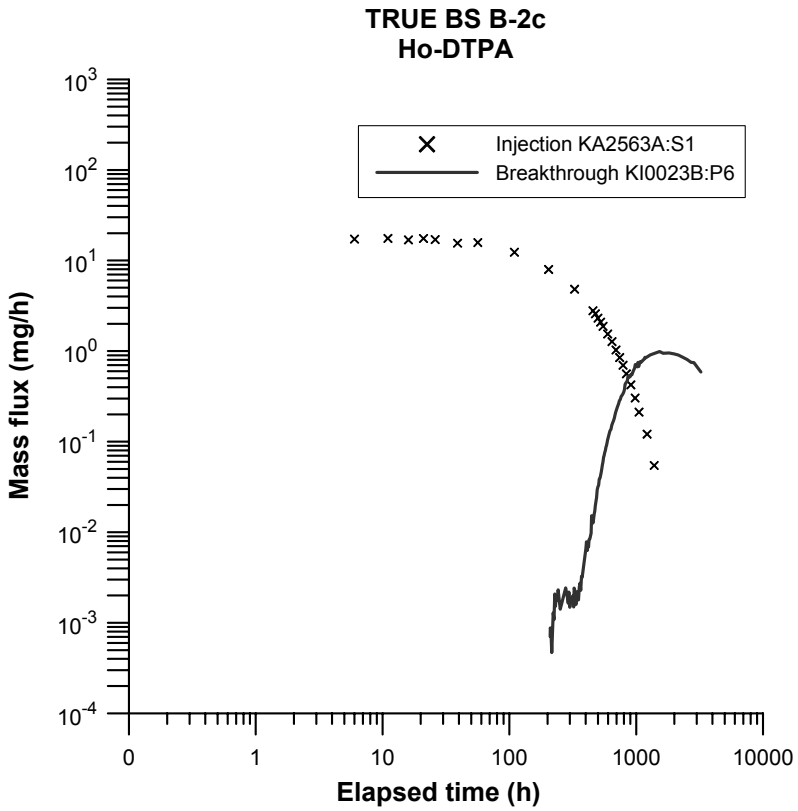

Figure 4-2 : *Breakthrough curve in a log-log scale for real second tracer test (B-2c) (from Andersson et al, 2000b)*

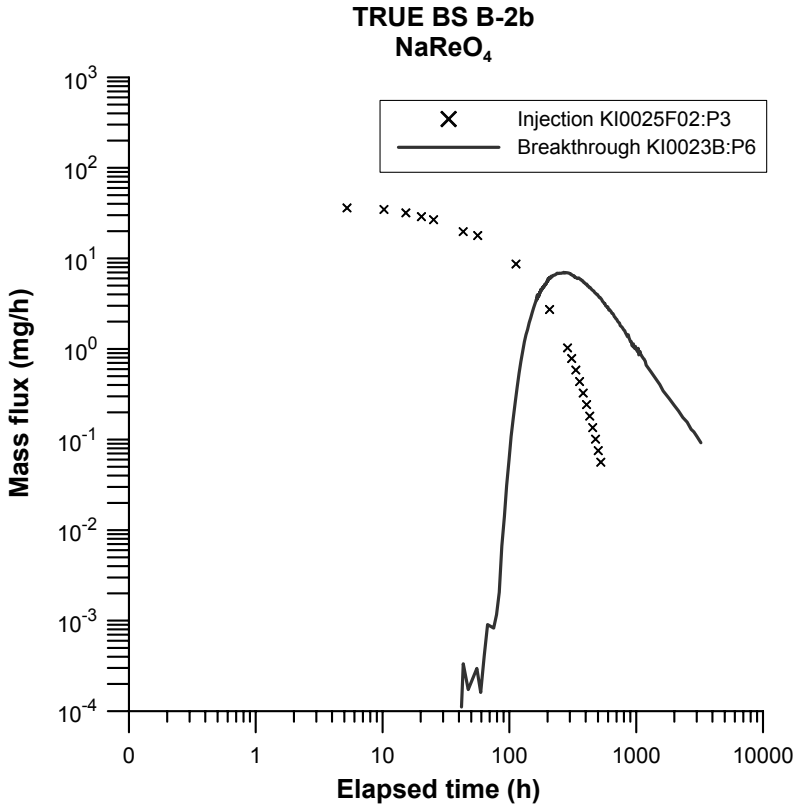

Figure 4-3 : *Breakthrough curve in a log-log scale for real third tracer test (B-2b) (from Andersson et al, 2000b)*

Table 4-1 : First arrival and peak breakthrough times for in situ tracer tests and for simulations based on Tracer Test stage model before calibration and after calibration										
Test number	**Test Name**	**First arrivals (time in hours)**			**Peak breakthrough time (in hours)**			**Mass flux at peak (mg/h)**		
		Real	***3FLO***		***Real***	***3FLO***		***Real***	***3FLO***	
			Non calib.	**Calib.**		**Non calib.**	**Calib.**		**Non calib.**	**Calib.**
1	B-2d	*30*	100	70	*100*	250	150	*14*	10	10
2	B-2c	*300*	6000	600	*1800*	16000	2500	*1*	0.4	1
3	B-2b	*40*	25	20	*300*	100	100	*18*	12	8

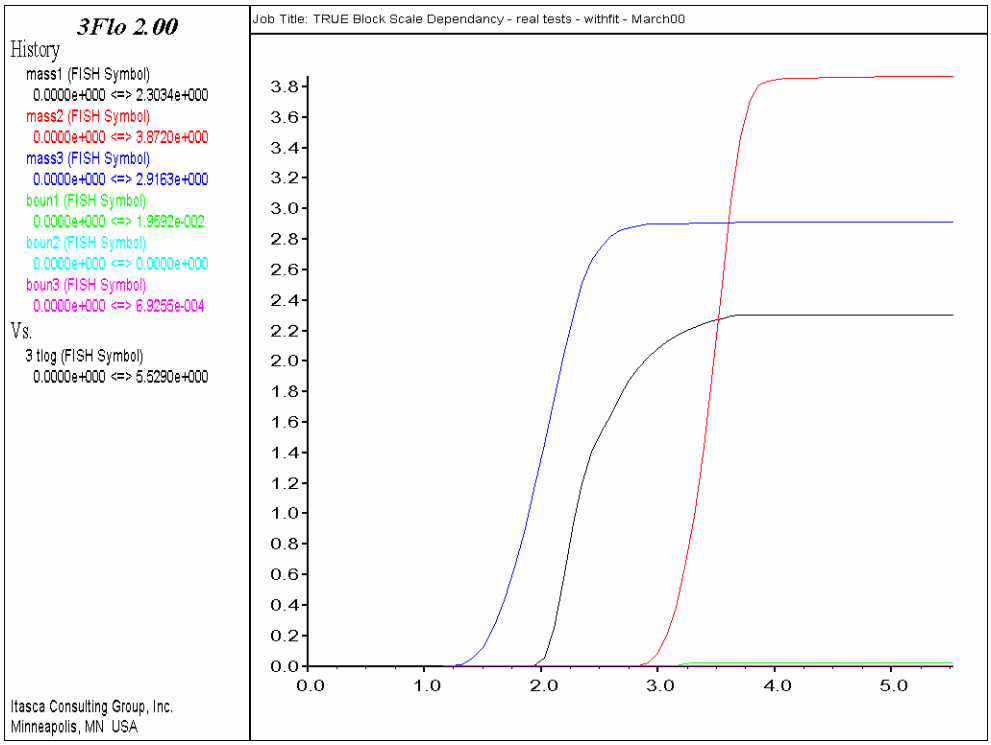

Figure 4-4 : *Tracer test stage model – Calibrated simulations*
Cumulative mass arrival (g) for the three tracer tests vs. log (time in hours)

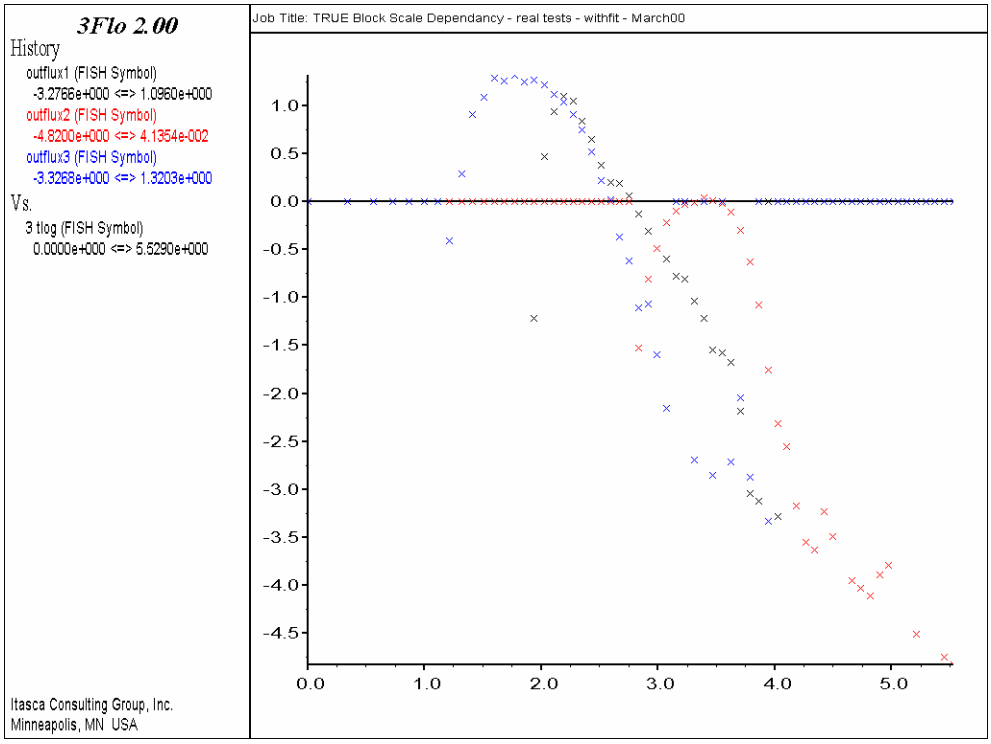

Figure 4-5 : *Tracer test stage model – Calibrated simulations*
Mass flux (mg/h) for the three tracer tests vs time in hours (log-log)

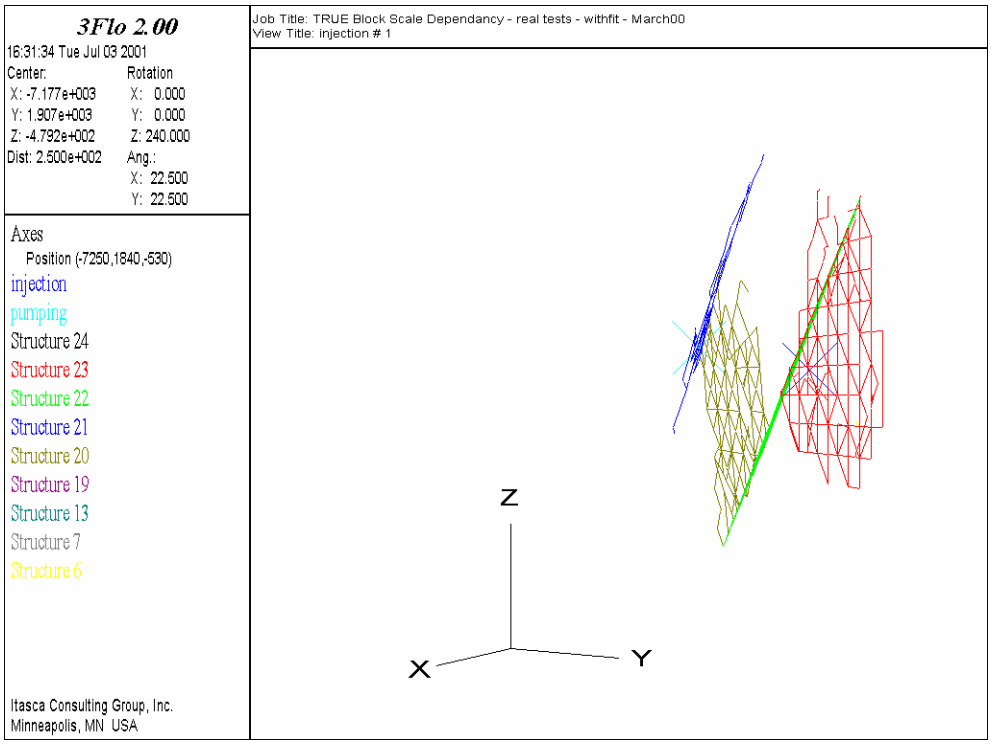

Figure 4-6 : *Tracer test stage model – Calibrated simulations*
Flow path for the simulated tracer Test 1

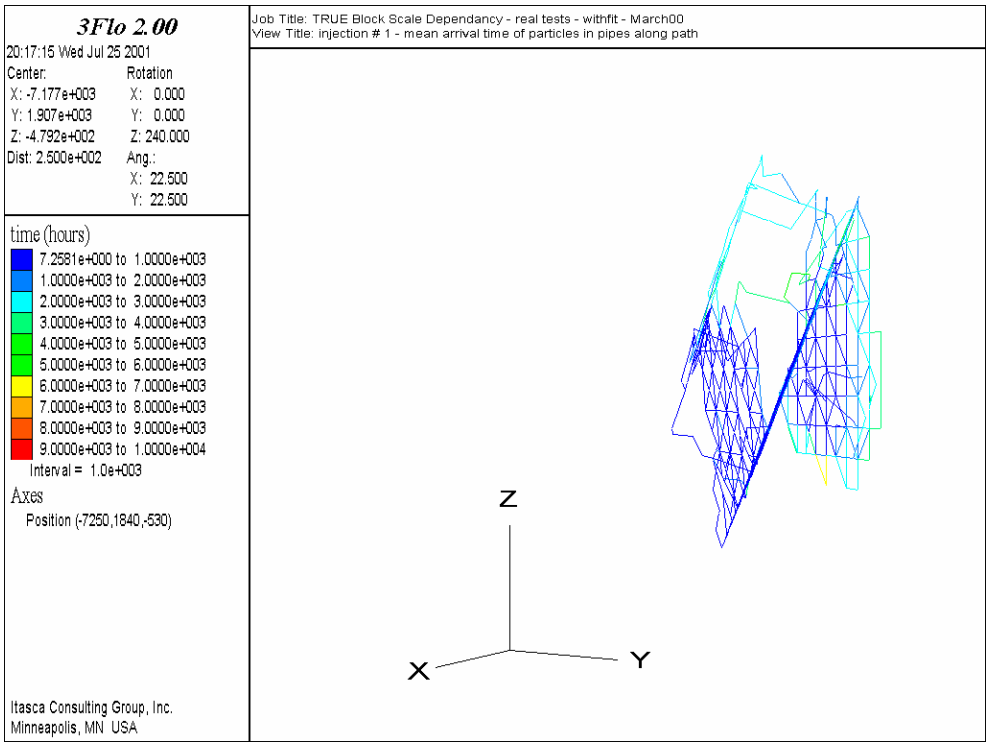

Figure 4-7 : *Tracer test stage model – Calibrated simulations*
Mean arrival time in hours of tracers in pipes along path for the simulated tracer Test 1

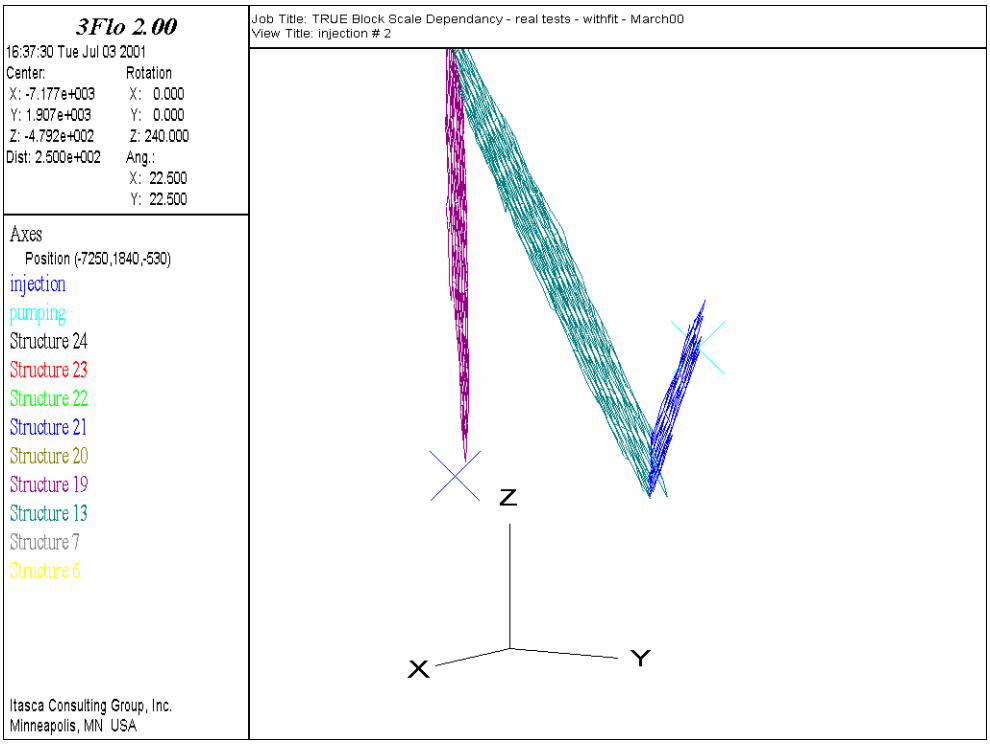

Figure 4-8 *: Tracer test stage model – Calibrated simulations*
Flow path for the simulated tracer Test 2

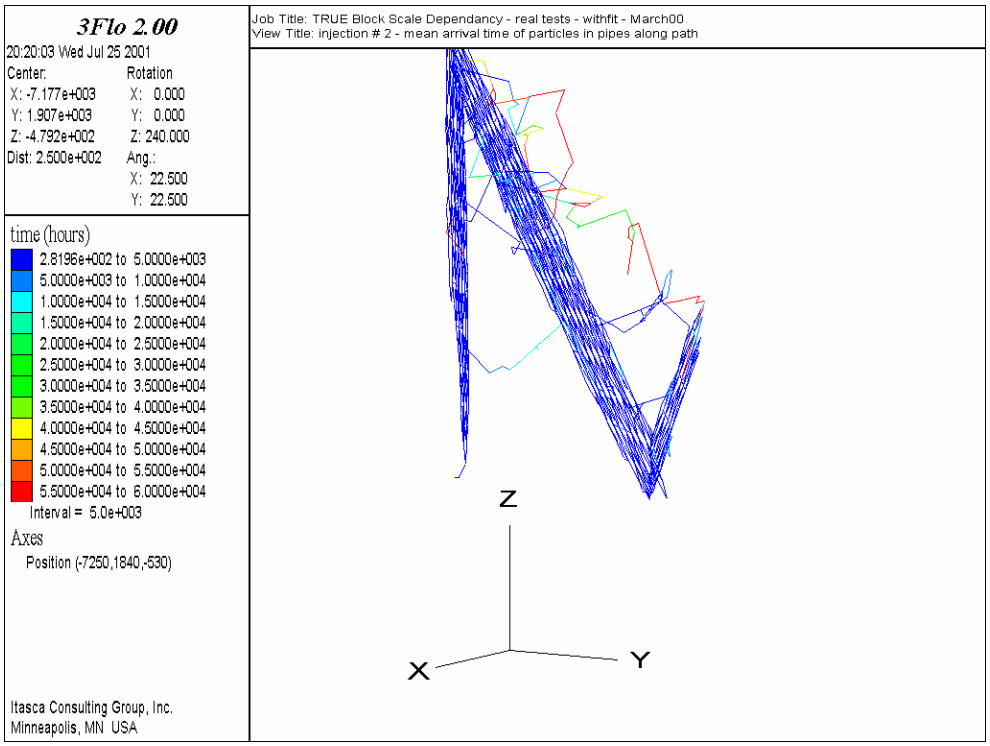

Figure 4-9 : *Tracer test stage model – Calibrated simulations*
Mean arrival time in hours of tracers in pipes along path for the simulated tracer Test 2

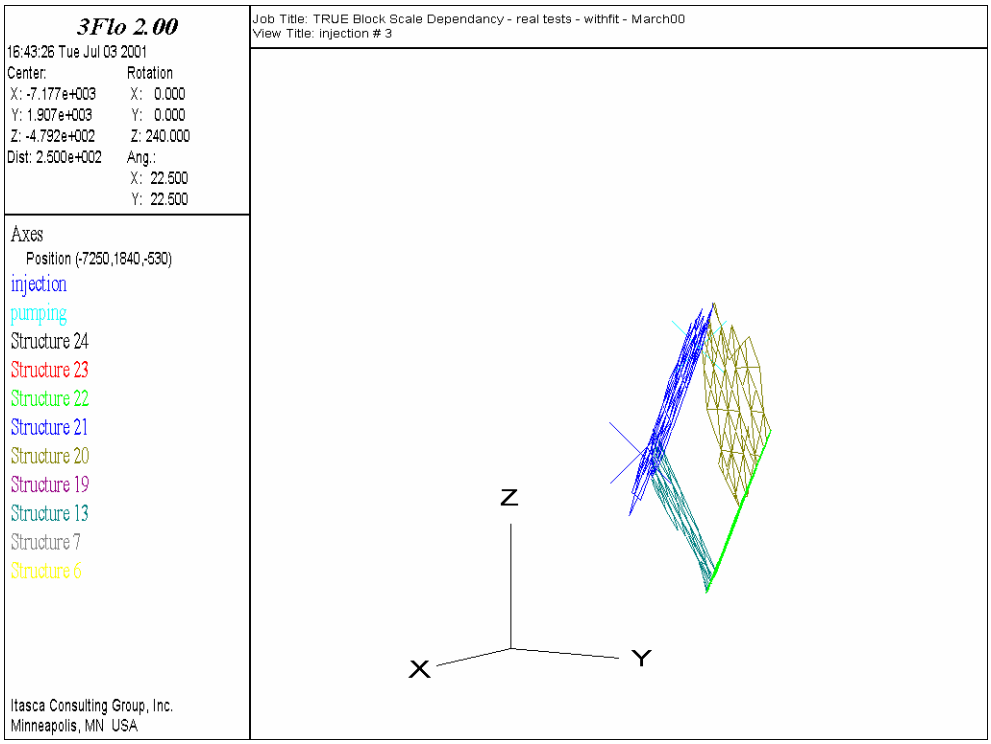

Figure 4-10 : *Tracer test stage model – Calibrated simulations*
Flow path for the simulated tracer Test 3

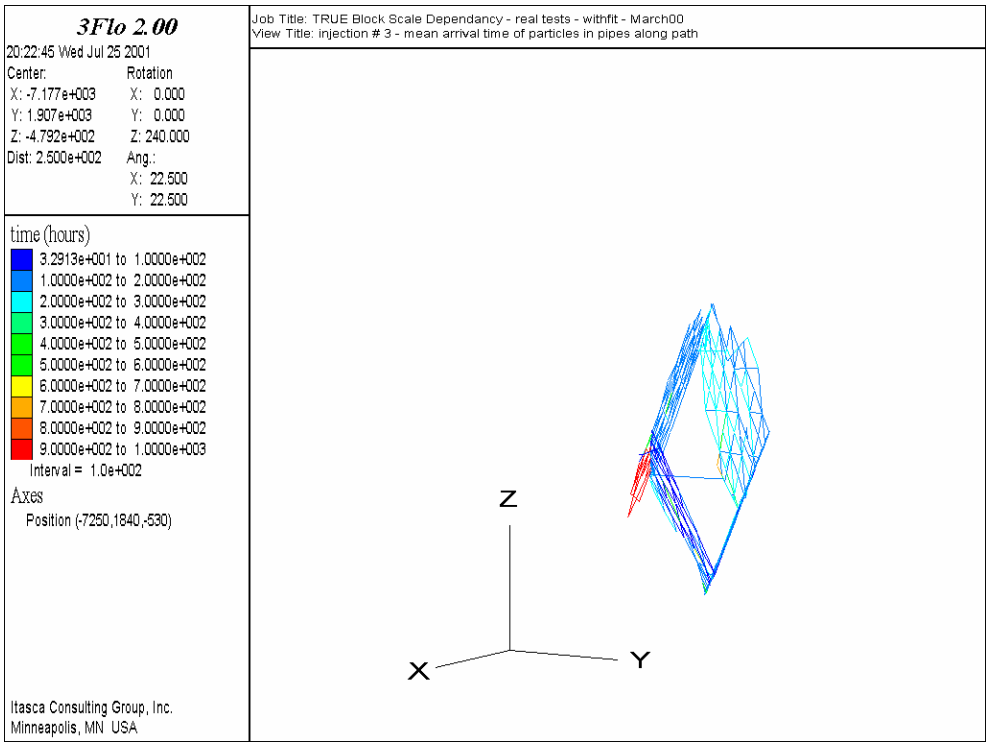

Figure 4-11 : *Tracer test stage model – Calibrated simulations*
Mean arrival time in hours of tracers in pipes along path for the simulated tracer Test 3

4.2 Detailed Characterisation stage model

In the March 1999 structural model, Structure #23 does not exist. So, only Structures #13 and #19 are modified. The resulting parameters used for the calibrated March 1999 structural model are given Table 4-2. Note that by simplification this model is called the "Calibrated March 1999 model". In fact, this model has NOT been calibrated. We simply use the results from the calibration performed on the March 2000 model.

Results for the Calibrated March 1999 structural model are presented Figure 4-12 to Figure 4-19.

Table 4-3 compiles the first arrival and peak arrival times, as well as the peak mass fluxes, obtained for the March 1999 Structural model (in situ tests and numerical tests before and after calibration).

The calibration barely modifies results for Test 1. For Test 2, the first arrival and peak arrival times are greatly reduced, but the reduction is less than in the March 2000 model. They are still overestimated by a factor of 7-10 compared to the measured travel times. For Test 3, the calibration slightly modifies the first arrival and peak arrival times in the wrong way : particles accelerate, increasing the gap compared to the real times measured.

Comparing the results between the calibrated March 1999 and March 2000 structural models shows that adding Structures #23 & #24 and removing Structure #10 changes greatly the response to the three tracer tests. By comparing the responses of this model before and after calibration (Figure 3-12 and Figure 4-12), we can conclude that the variations in the parameter from calibration have a small effect compared to the modifications of geometry implemented from one model to the other. If we now look at flow paths, they are essentially unchanged.

Table 4-2 : CALIBRATED Detailed Characterisation stage model Truncated normal distributions of the structures transmissivity and □ coefficient determining the pipes cross section

Structure #	Transmissivity (m^2/s)			α
	mean	sd	Min	
6	$2.0\ 10^{-7}$	$1.0\ 10^{-7}$	$1\ 10^{-8}$	0.05
7	$2.0\ 10^{-5}$	$1.0\ 10^{-5}$	$1\ 10^{-6}$	0.05
10	$5.0\ 10^{-7}$	$2.5\ 10^{-7}$	$5\ 10^{-8}$	0.05
13	**$1.0\ 10^{-6}$**	$1.0\ 10^{-7}$	**$1\ 10^{-7}$**	**0.005**
19	$1.5\ 10^{-5}$	$1.0\ 10^{-5}$	$1\ 10^{-7}$	**0.005**
20	$8.0\ 10^{-7}$	$2.0\ 10^{-8}$	$5\ 10^{-7}$	0.05
21	$1.0\ 10^{-8}$	$1.0\ 10^{-8}$	$1\ 10^{-9}$	0.05
22	$4.0\ 10^{-7}$	$2.0\ 10^{-7}$	$1\ 10^{-7}$	0.05

Note : **bold black** show the data changed by the calibration

Table 4-3 : First arrival and peak breakthrough times for in situ tracer tests and for simulations based on the Detailed Characterisation stage model before calibration and after calibration

Test number	Test Name	First arrivals (time in hours)			Peak breakthrough time (in hours)			Mass flux at peak (mg/h)		
		Real	*3FLO*		*Real*	*3FLO*		*Real*	*3FLO*	
			Non calib.	Calib.		Non calib.	Calib.		Non calib.	Calib.
1	B-2d	*30*	200	200	*100*	550	450	*14*	8	6
2	B-2c	*300*	18000	4200	*1800*	32000	20000	*1*	0.2	0.2
3	B-2b	*40*	30	20	*300*	150	110	*18*	15	15

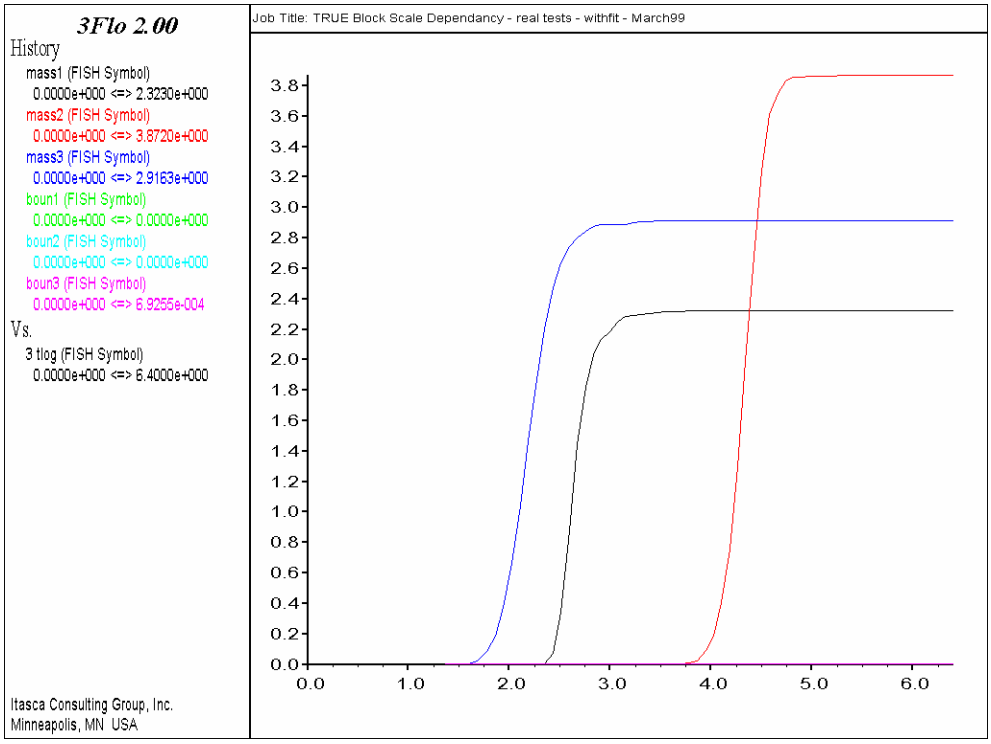

Figure 4-12 : *Detailed Characterisation stage model – Calibrated simulations Cumulative mass arrival (g) for the three tracer tests vs log (time in hours)*

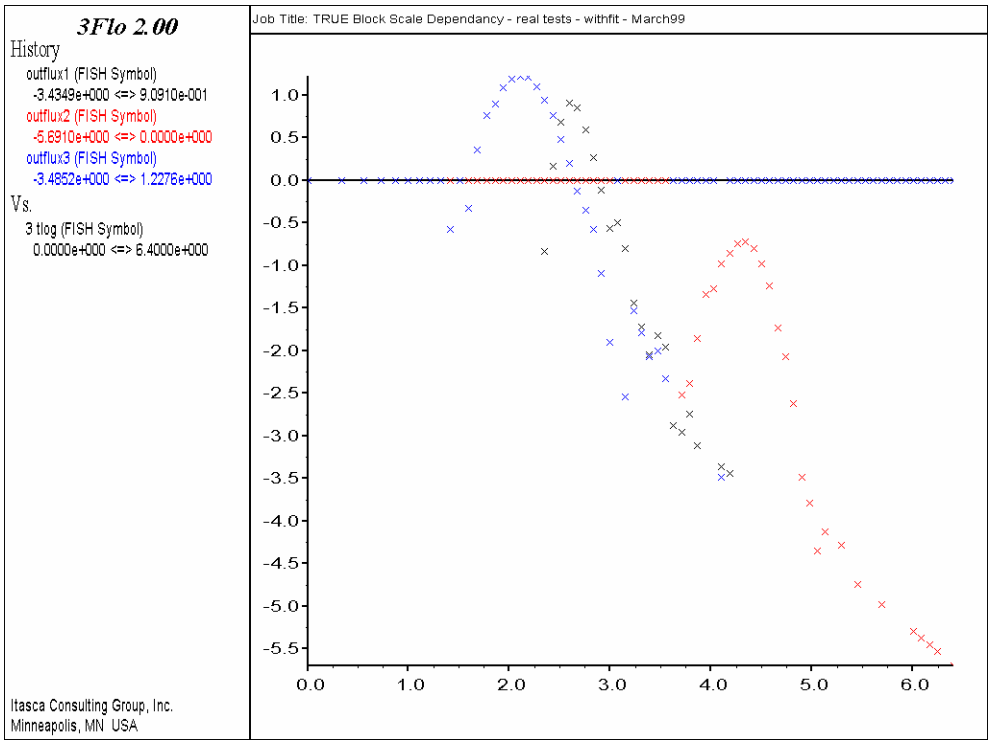

Figure 4-13 : *Detailed Characterisation stage model – Calibrated simulations Mass flux (mg/h) for the three tracer tests vs time in hours (log-log)*

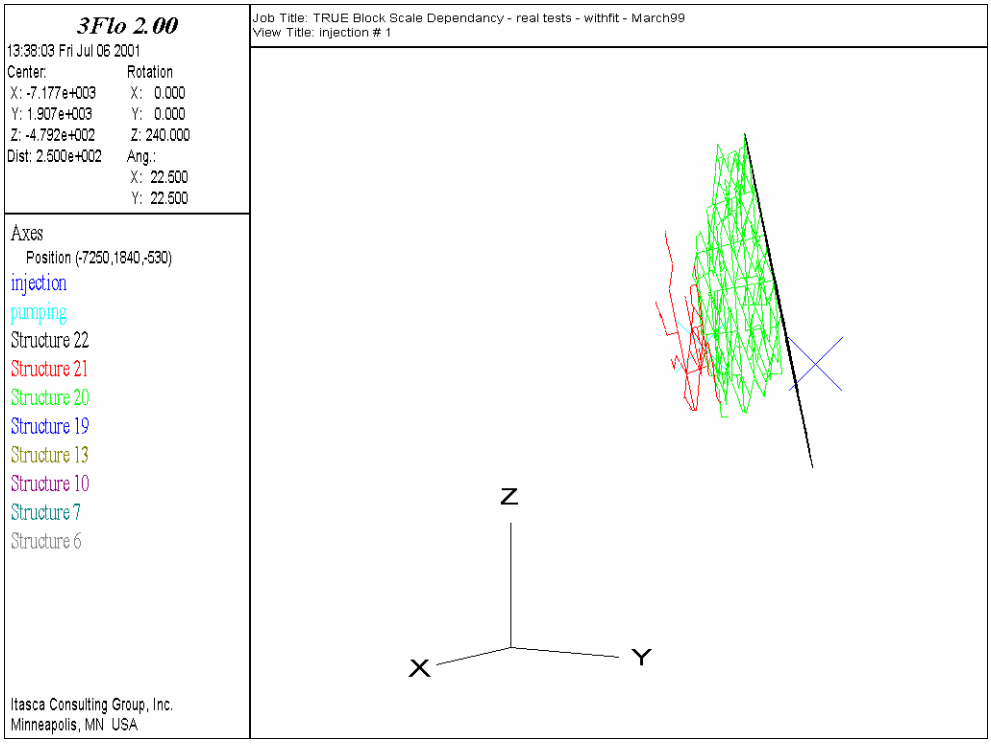

Figure 4-14 : *Detailed Characterisation stage model – Calibrated simulations*
Flow path for the simulated tracer Test 1

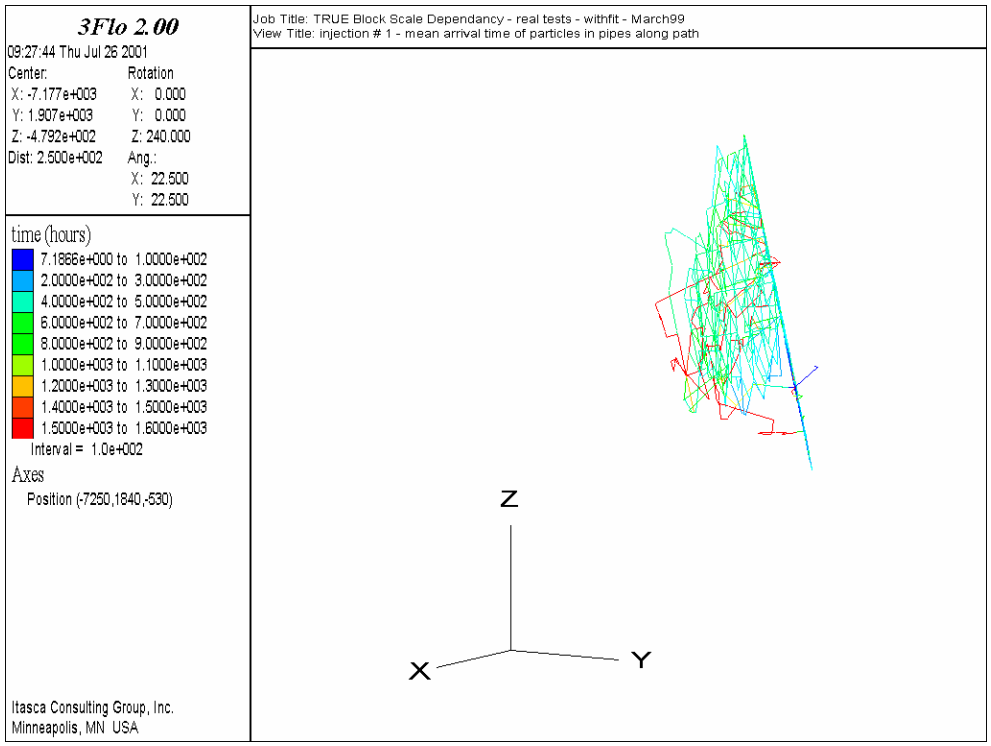

Figure 4-15 : *Detailed Characterisation stage model – Calibrated simulations*
Mean arrival time in hours of tracers in pipes along path for the simulated tracer Test 1

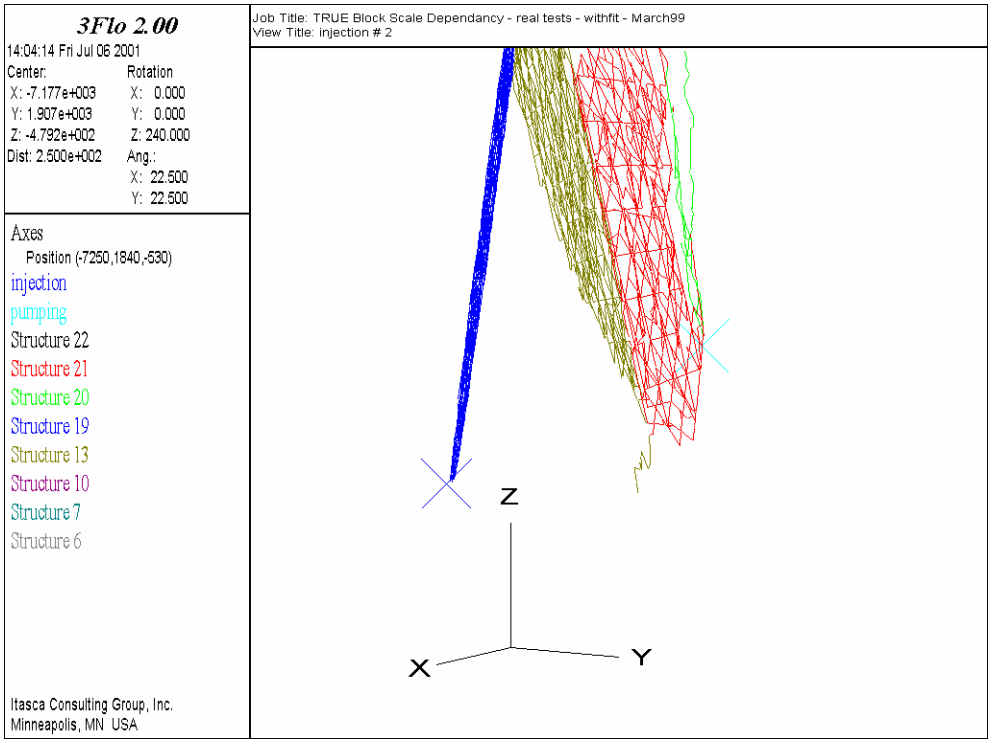

Figure 4-16 *: Detailed Characterisation stage model – Calibrated simulations Flow path for the simulated tracer Test 2*

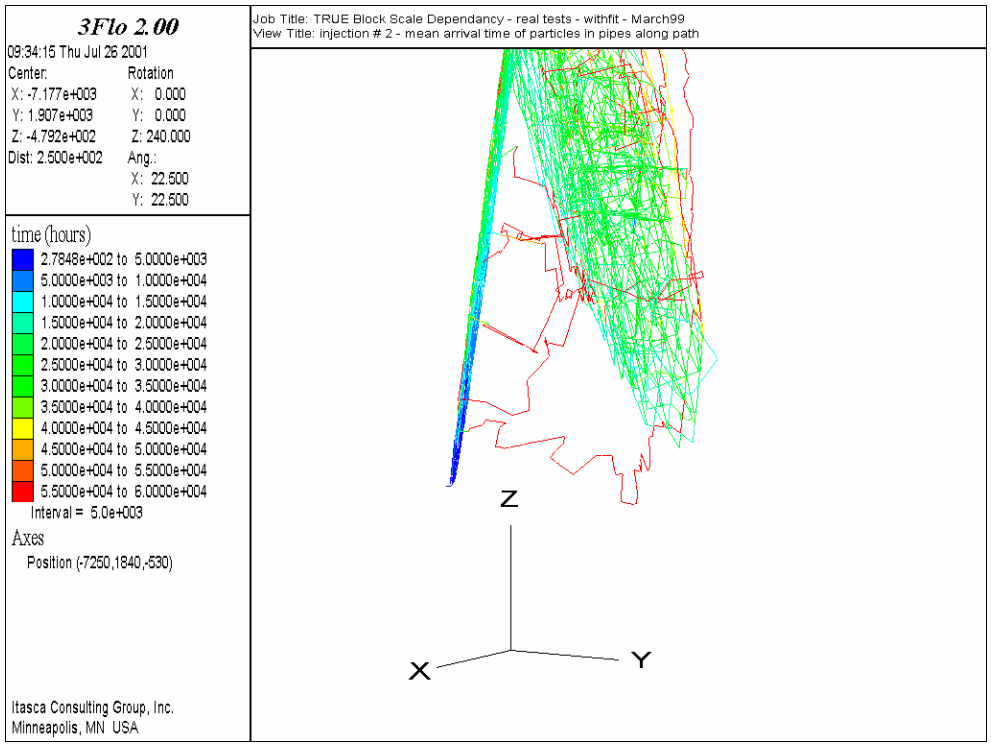

Figure 4-17 : *Detailed Characterisation stage model – Calibrated simulations Mean arrival time in hours of tracers in pipes along path for the simulated tracer Test 2*

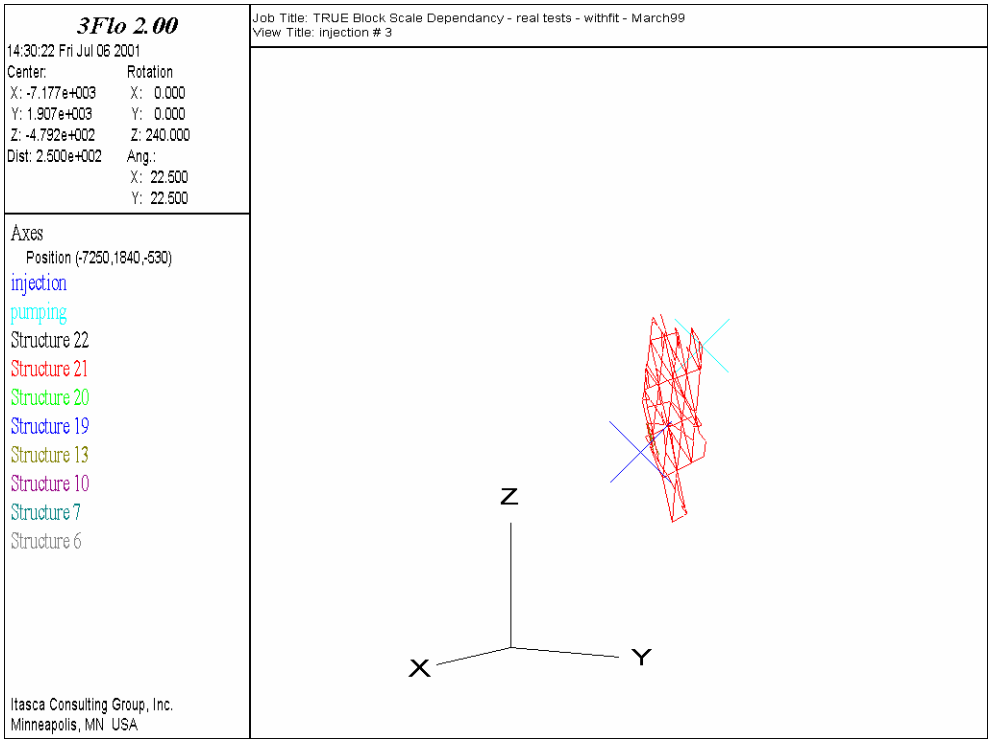

Figure 4-18 : *Detailed Characterisation stage model – Calibrated simulations*
Flow path for the simulated tracer Test 3

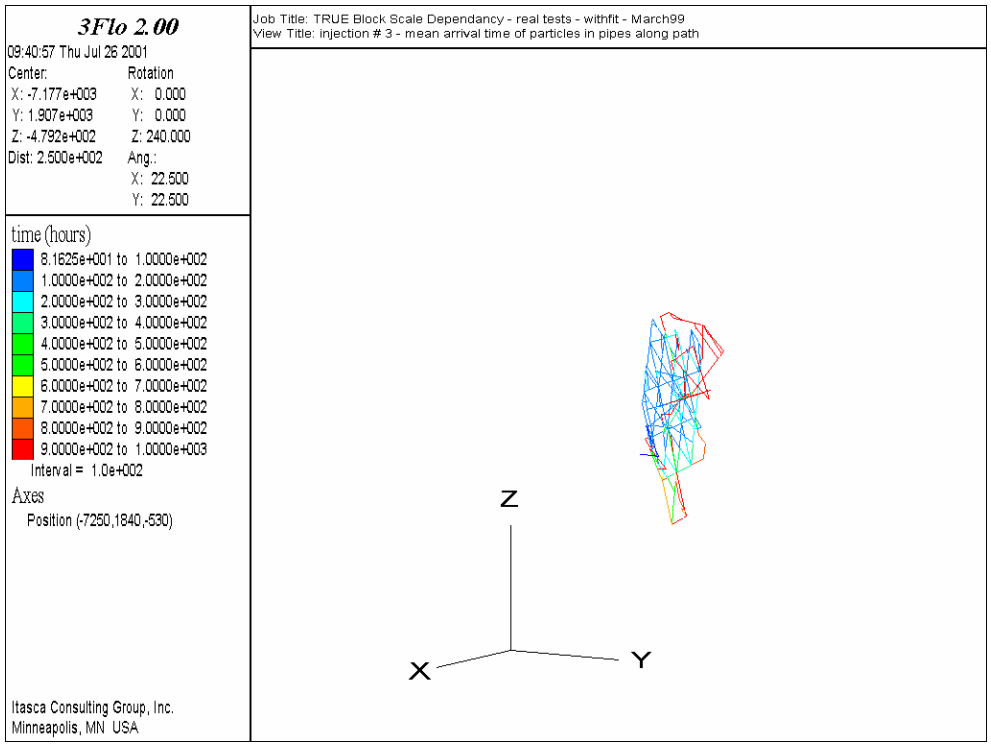

Figure 4-19 : *Detailed Characterisation stage model – Calibrated simulations*
Mean arrival time in hours of tracers in pipes along path for the simulated tracer Test 3

4.3 Preliminary Characterisation stage model

The Preliminary Characterisation stage model considers Structures #6, #9, #13, #19 and #20. As Structure #6 does not exist in the March 2000 structural model, data for Structure #6 remain unchanged, whereas the 4 other structures are modified such that their parameters correspond to the ones used for the calibrated March 2000 structural model. Again, this model is not calibrated, but simply uses the parameter values taken from the calibrated March 2000 model.

The resulting parameters for the "calibrated Preliminary Characterisation stage model" are given in Table 4-4.

Results for the Calibrated Preliminary Characterisation stage model are presented in Figure 4-20 to Figure 4-27.

Table 4-5 compiles the first arrival and peak arrival times, as well as the peak mass fluxes, obtained for the Preliminary Characterisation stage model (in situ tests and numerical tests before and after calibration).

The calibration does not globally improve the results. Transport paths are essentially identical to the ones in the non calibrated Preliminary Characterisation stage model; arrival times are much longer than the ones observed in situ, and arrival time contrasts between the three tests are larger than the ones obtained with the non calibrated run.

Table 4-4 : CALIBRATED Preliminary Characterisation Stage Model Truncated normal distributions of the structures transmissivity and α coefficient determining the pipes cross section

Structure #	Transmissivity (m^2/s)			α
	mean	sd	Min	
6	**$2.0\ 10^{-7}$**	**$1.0\ 10^{-7}$**	**$1\ 10^{-8}$**	0.05
9	$5.0\ 10^{-7}$	$2.5\ 10^{-7}$	$6.25\ 10^{-8}$	0.05
13	**$1.0\ 10^{-6}$**	**$1.0\ 10^{-7}$**	**$1\ 10^{-7}$**	**0.005**
19	**$1.5\ 10^{-5}$**	**$1.0\ 10^{-5}$**	**$1\ 10^{-7}$**	**0.005**
20	**$8.0\ 10^{-7}$**	**$2.0\ 10^{-8}$**	**$5\ 10^{-7}$**	0.05

Note : **bold black** show the data changed by the calibration

Table 4-5 : First arrival and peak breakthrough times for in situ tracer tests and for simulations based on the Preliminary Characterisation stage model before calibration and after calibration										
Test number	**Test Name**	**First arrivals (time in hours)**			**Peak breakthrough time (in hours)**			**Mass flux at peak (mg/h)**		
		Real	***3FLO***		***Real***	***3FLO***		***Real***	***3FLO***	
			Non calib.	**Calib.**		**Non calib.**	**Calib.**		**Non calib.**	**Calib.**
1	B-2d	*30*	270	500	*100*	700	1200	*14*	3	2
2	B-2c	*300*	570	700	*1800*	1500	3500	*1*	2	0.6
3	B-2b	*40*	225	100	*300*	500	400	*18*	7	8

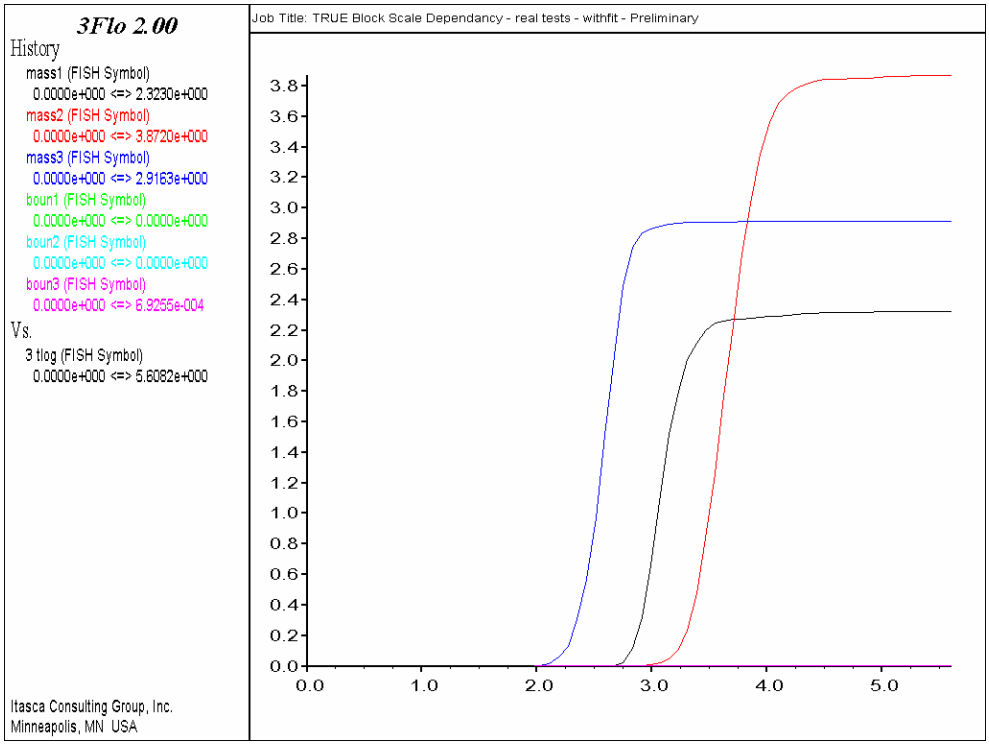

Figure 4-20 : *Preliminary Characterisation stage model – Calibrated simulations Cumulative mass arrival (g) for the three tracer tests vs log (time in hours)*

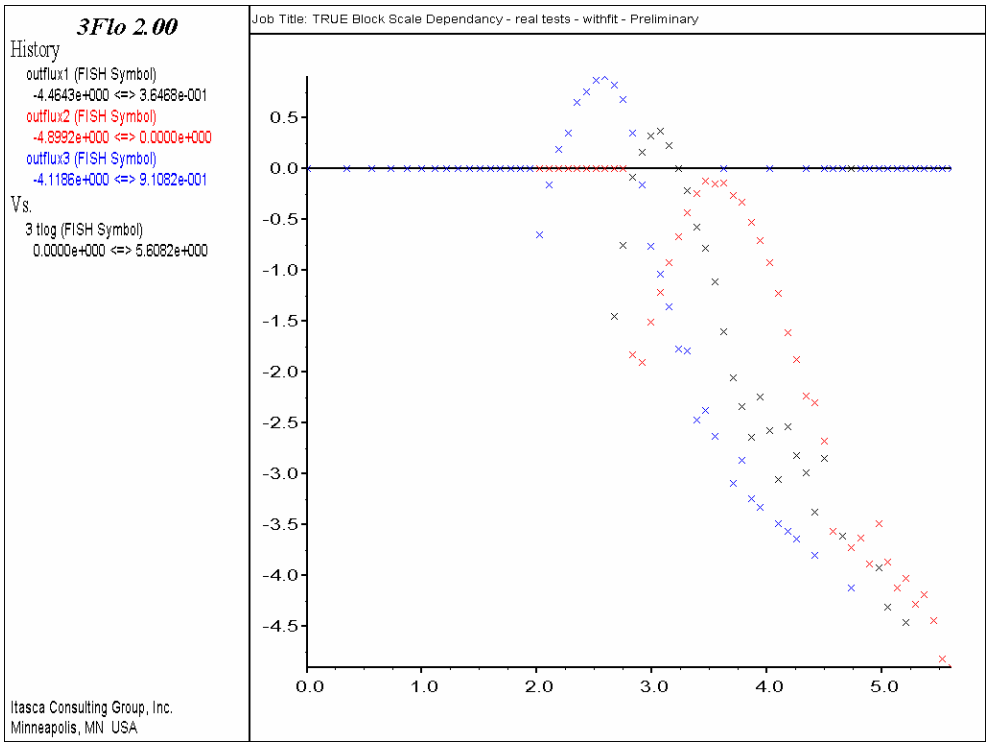

Figure 4-21 : *Preliminary Characterisation stage model – Calibrated simulations Mass flux (mg/h) for the three tracer tests vs time in hours (log-log)*

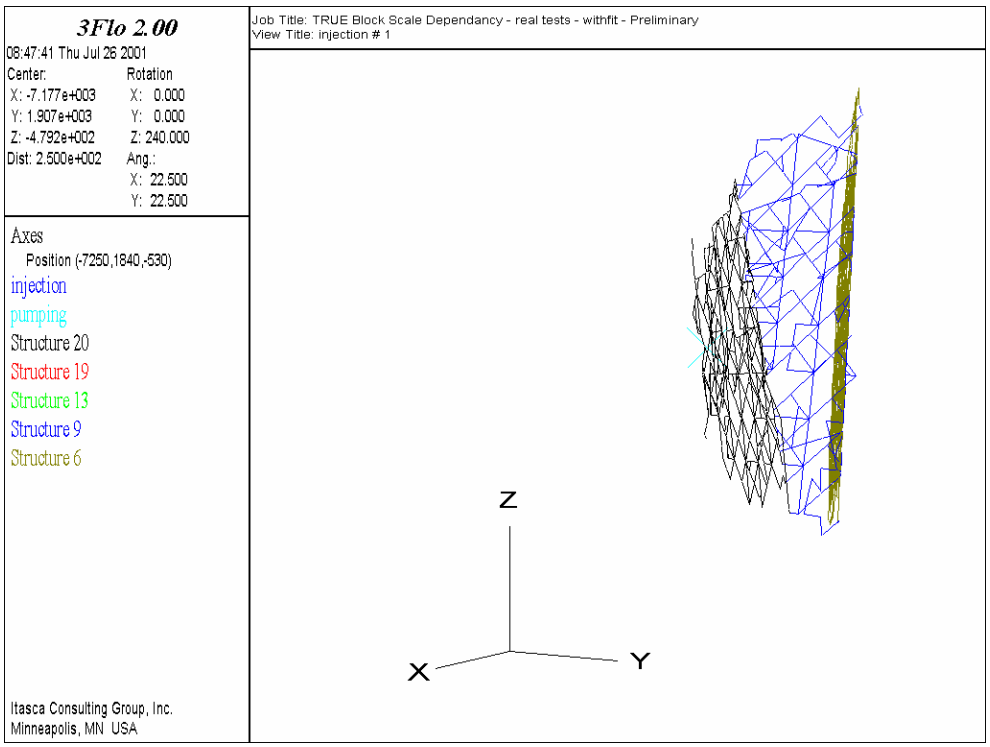

Figure 4-22 : *Preliminary Characterisation stage model – Calibrated simulations Flow path for the simulated tracer Test 1*

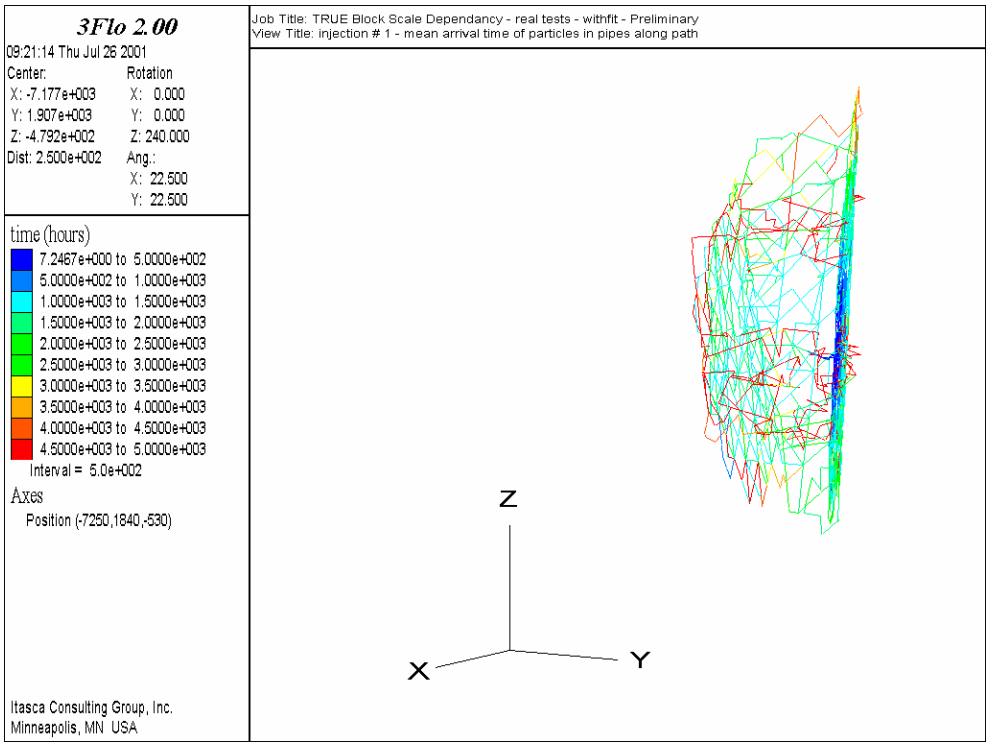

Figure 4-23 *: Preliminary Characterisation stage model – Calibrated simulations Mean arrival time in hours of tracers in pipes along path for the simulated tracer Test 1*

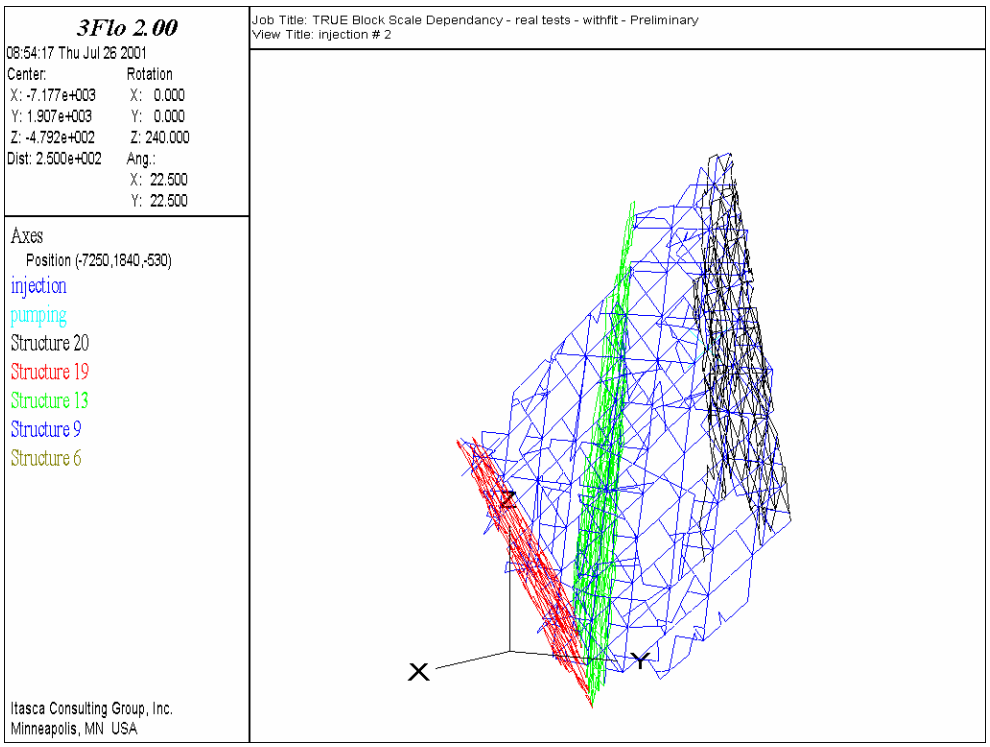

Figure 4-24 : *Preliminary Characterisation stage model – Calibrated simulations Flow path for the simulated tracer Test 2*

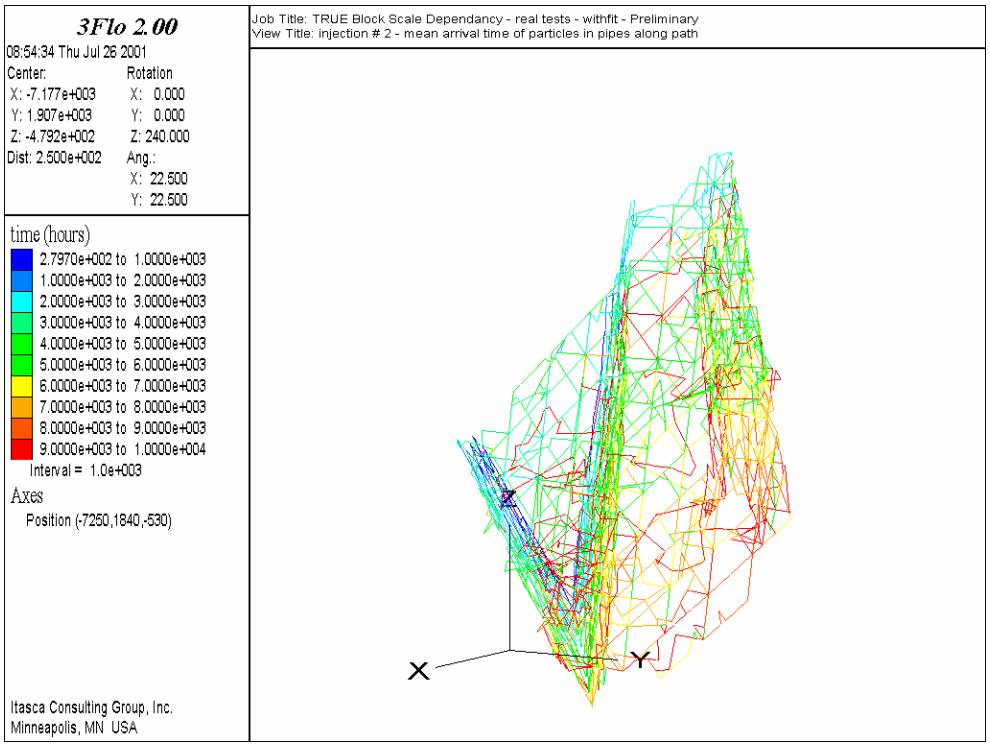

Figure 4-25 : *Preliminary Characterisation stage model – Calibrated simulations Mean arrival time in hours of tracers in pipes along path for the simulated tracer Test 2*

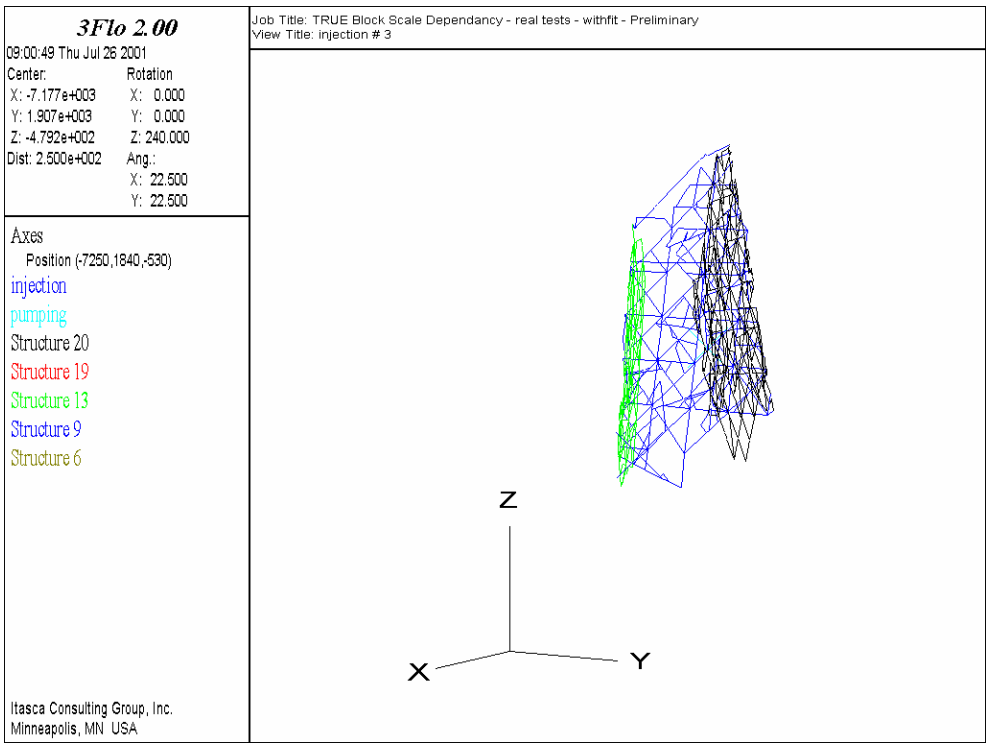

Figure 4-26 : *Preliminary Characterisation stage model – Calibrated simulations Flow path for the simulated tracer Test 3*

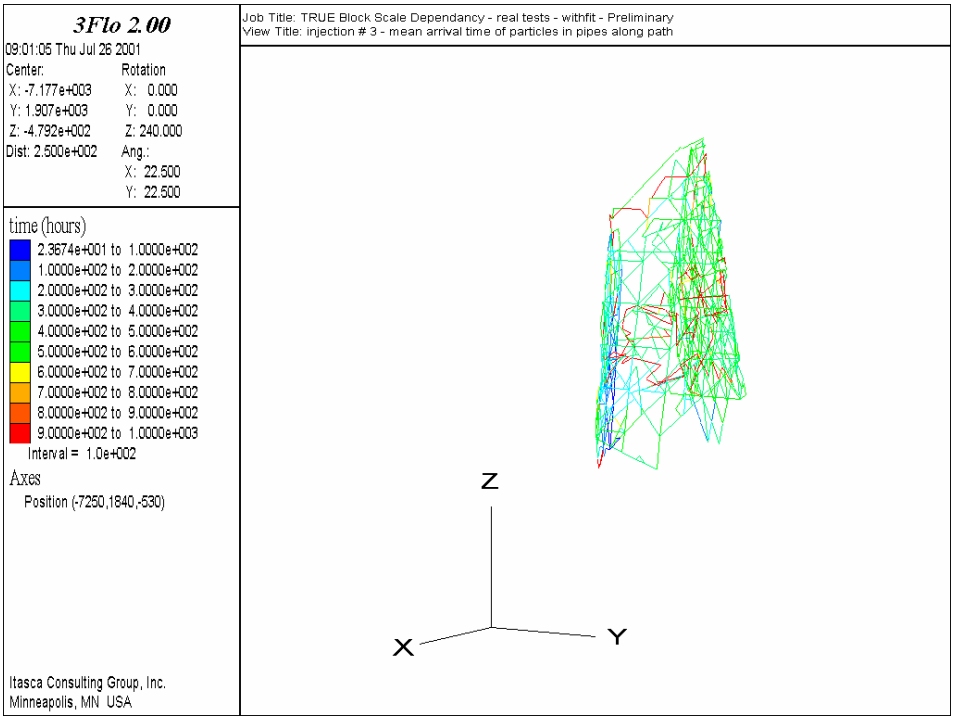

Figure 4-27 : *Preliminary Characterisation stage model – Calibrated simulations Mean arrival time in hours of tracers in pipes along path for the simulated tracer Test 3*

4.4 Scoping Characterisation stage model

The structures common to the Scoping Characterisation stage model and the March 2000 structural model are Structures #6, #7, and between the Scoping Characterisation stage model and the March 1999 structural model is Structure #10.

These 3 structures are modified such that their parameters correspond to the ones used for the calibrated March 2000 and March 1999 structural models whereas the other structures simulated in the Scoping Characterisation stage model remain unchanged.

The resulting parameters for the calibrated Scoping Characterisation stage model are given in Table 4-6.

Results for the Scoping Characterisation stage model are presented in Figure 4-28 to Figure 4-35. Table 4-7 compiles the first arrival and peak arrival times, as well as the peak mass fluxes, obtained for the Scoping Characterisation stage model (in situ tests and numerical simulations before and after calibration).

The calibration does not improve the results at all. It does not change the first arrival and peak arrival times for Test 2, and modifies the response for the two other tests in the wrong direction. This is not surprising since our knowledge of the TRUE Block Scale site during the scoping characterisation stage was very limited and had no common features with the March 2000 structural model on which was performed the calibration.

Comparing the responses to the three tracer tests obtained with the four models (Figure 4-4, Figure 4-12, Figure 4-20 Figure 4-28) yields the same conclusion as the forward models: the response to the three tests is progressively degraded when going from the latest model to the earlier one, with essentially nothing of the overall response left in the Scoping Characterisation model.

Table 4-6 : CALIBRATED Scoping Characterisation Stage Model Truncated normal distributions of the structures transmissivity and coefficient determining the pipes cross section

Structure #	Transmissivity (m^2/s)			α
	mean	sd	Min	
2	$1.0\ 10^{-6}$	$1.3\ 10^{-6}$	0.0	0.05
3	$1.0\ 10^{-6}$	$1.3\ 10^{-6}$	0.0	0.05
4	$1.5\ 10^{-5}$	$1.95\ 10^{-5}$	0.0	0.05
5	$1.0\ 10^{-4}$	$1.3\ 10^{-4}$	0.0	0.05
6	**$2.0\ 10^{-7}$**	**$1.0\ 10^{-7}$**	**$1.0\ 10^{-8}$**	0.05
7	**$2.0\ 10^{-5}$**	**$1.0\ 10^{-5}$**	**$1.0\ 10^{-6}$**	0.05
8	$1.0\ 10^{-6}$	$1.3\ 10^{-6}$	0.0	0.05
10	**$5.0\ 10^{-7}$**	**$2.5\ 10^{-7}$**	**$5.0\ 10^{-8}$**	0.05
16	$1.0\ 10^{-6}$	$1.3\ 10^{-6}$	0.0	0.05
17	$1.0\ 10^{-6}$	$1.3\ 10^{-6}$	0.0	0.05
18	$1.0\ 10^{-6}$	$1.3\ 10^{-6}$	0.0	0.05

Note : **bold balck** show the data changed by the calibration

Table 4-7 : First arrival and peak breakthrough times for in situ tracer tests and for simulations based on the Scoping Characterisation stage model before calibration and after calibration

Test number	Test Name	First arrivals (time in hours)			Peak breakthrough time (in hours)			Mass flux at peak (mg/h)		
		Real	*3FLO*		*Real*	*3FLO*		*Real*	*3FLO*	
			Non calib.	Calib.		Non calib.	Calib.		Non calib.	Calib.
1	B-2d	*30*	60	125	*100*	110	300	*14*	50	4
2	B-2c	*300*	40	40	*1800*	200	180	*1*	10	10
3	B-2b	*40*	320	560	*300*	1400	1400	*18*	2.5	2.5

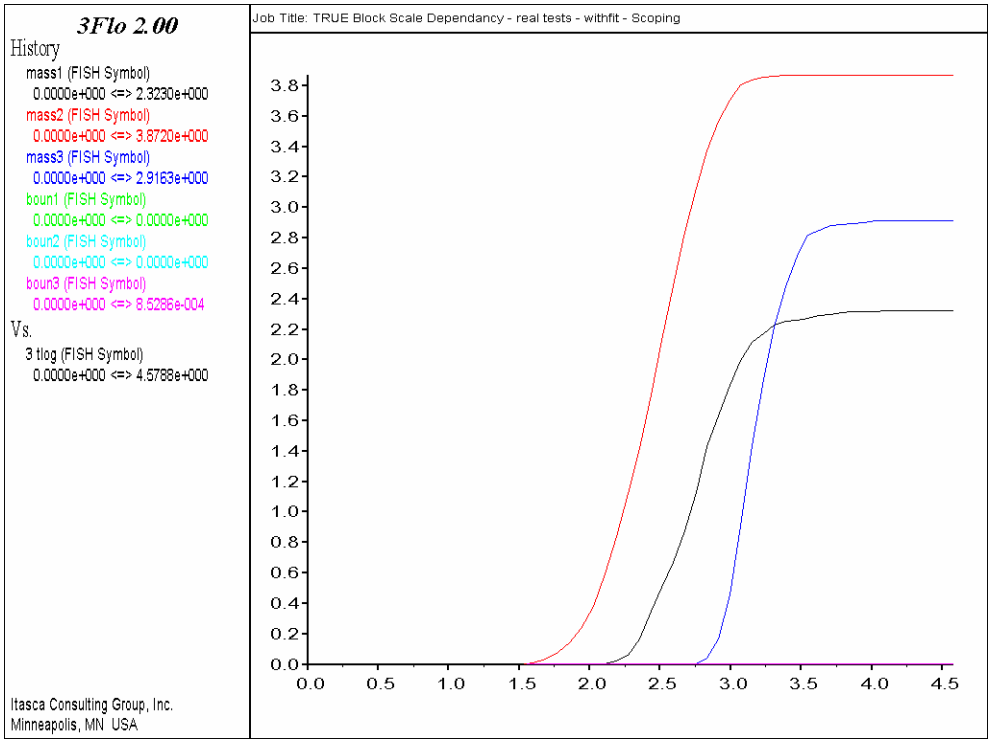

Figure 4-28 *: Scoping Characterisation stage model – Calibrated simulations Cumulative mass arrival (g) for the three tracer tests vs log (time in hours)*

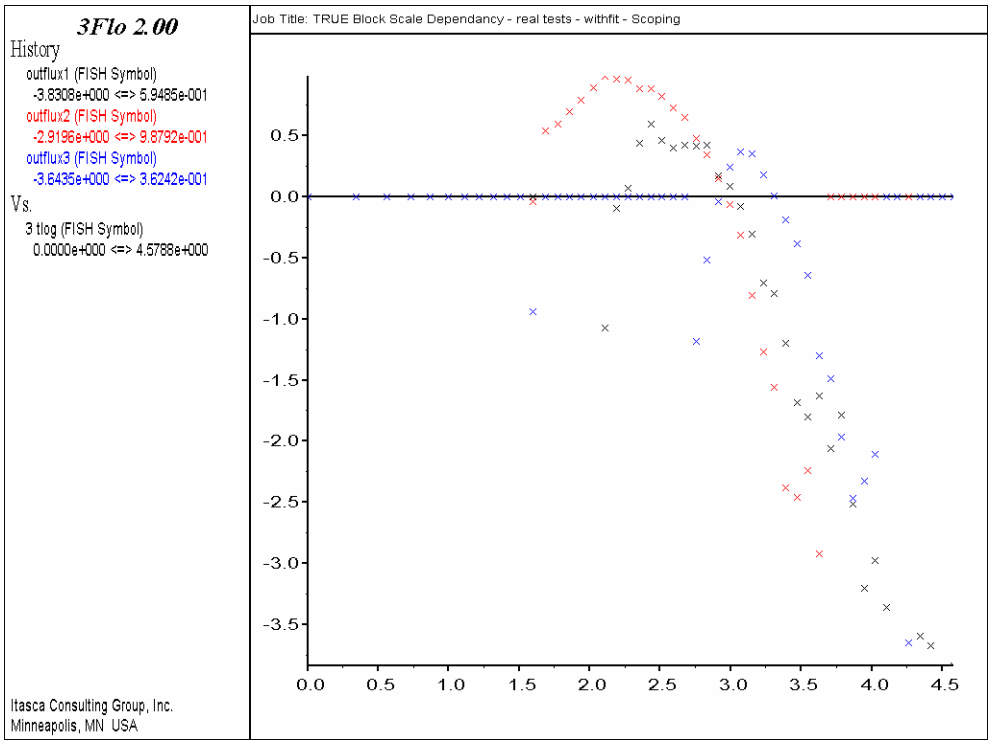

Figure 4-29 : *Scoping Characterisation stage model – Calibrated simulations Mass flux (mg/h) for the three tracer tests vs time in hours (log-log)*

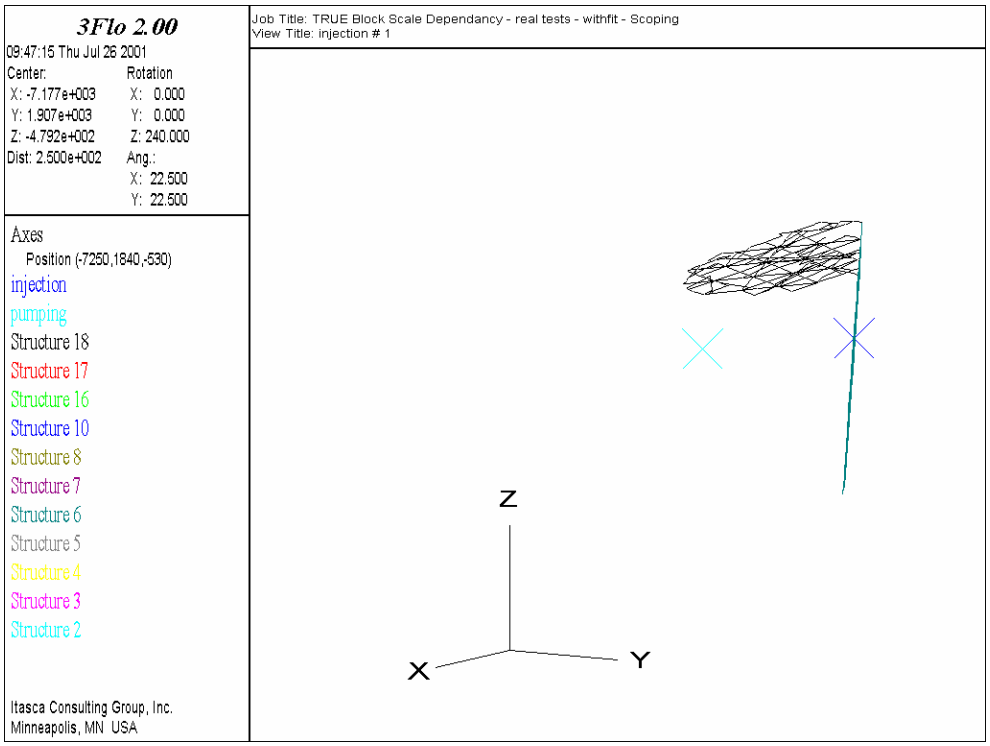

Figure 4-30 : *Scoping Characterisation stage model – Calibrated simulations*
Flow path for the simulated tracer Test 1

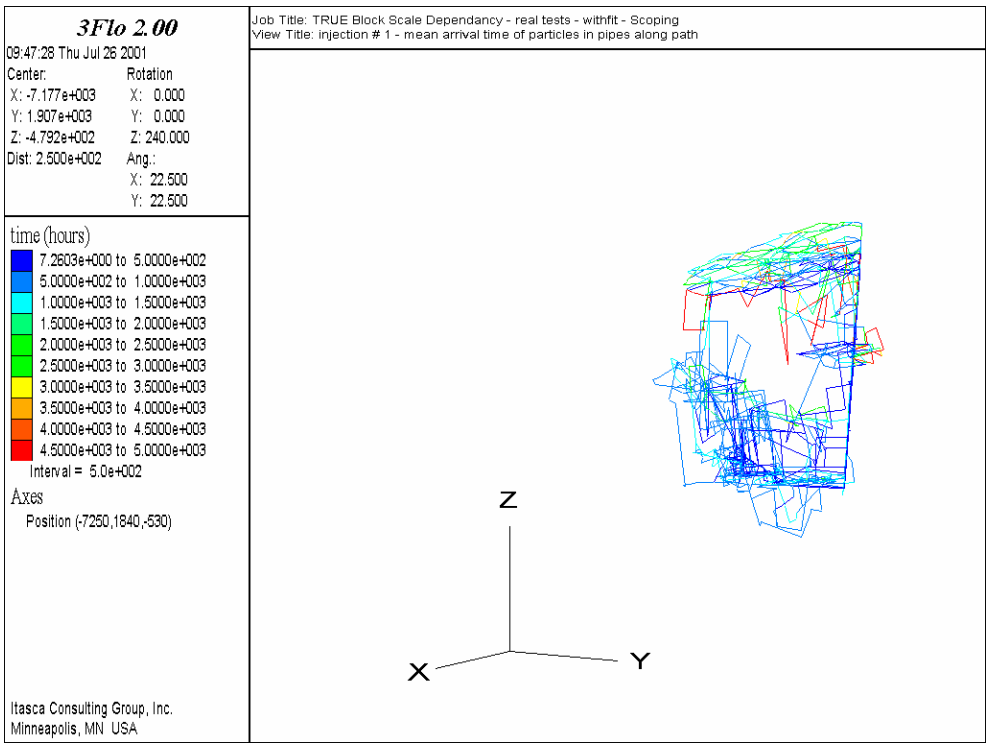

Figure 4-31 *: Scoping Characterisation stage model – Calibrated simulations*
Mean arrival time in hours of tracers in pipes along path for the simulated tracer Test 1

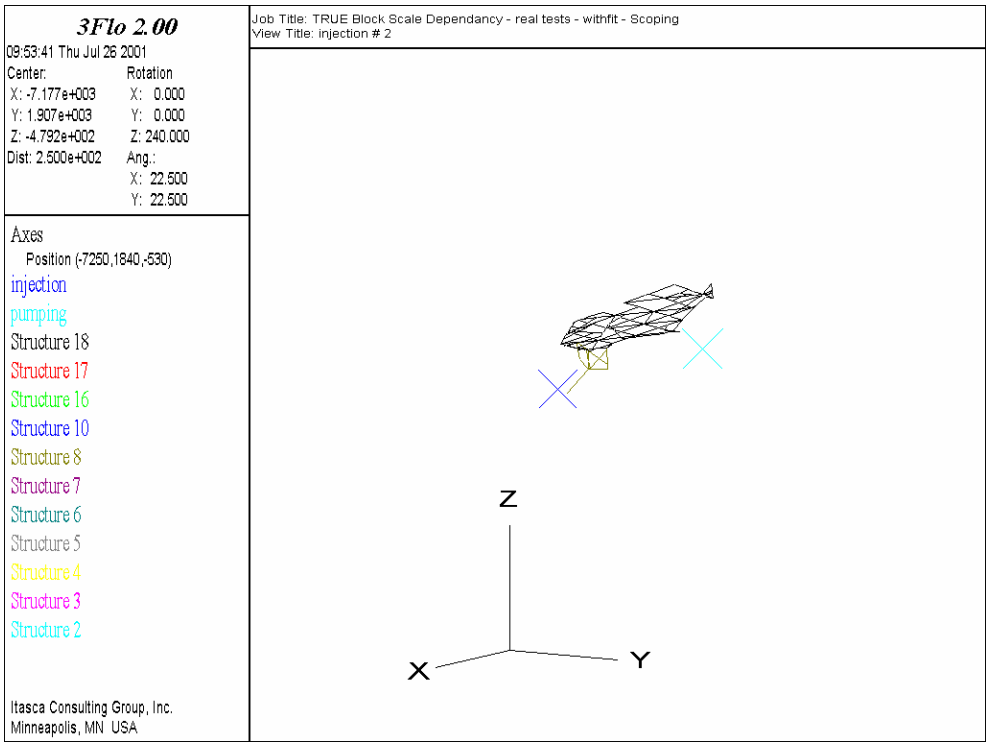

Figure 4-32 *: Scoping Characterisation stage model – Calibrated simulations Flow path for the simulated tracer Test 2*

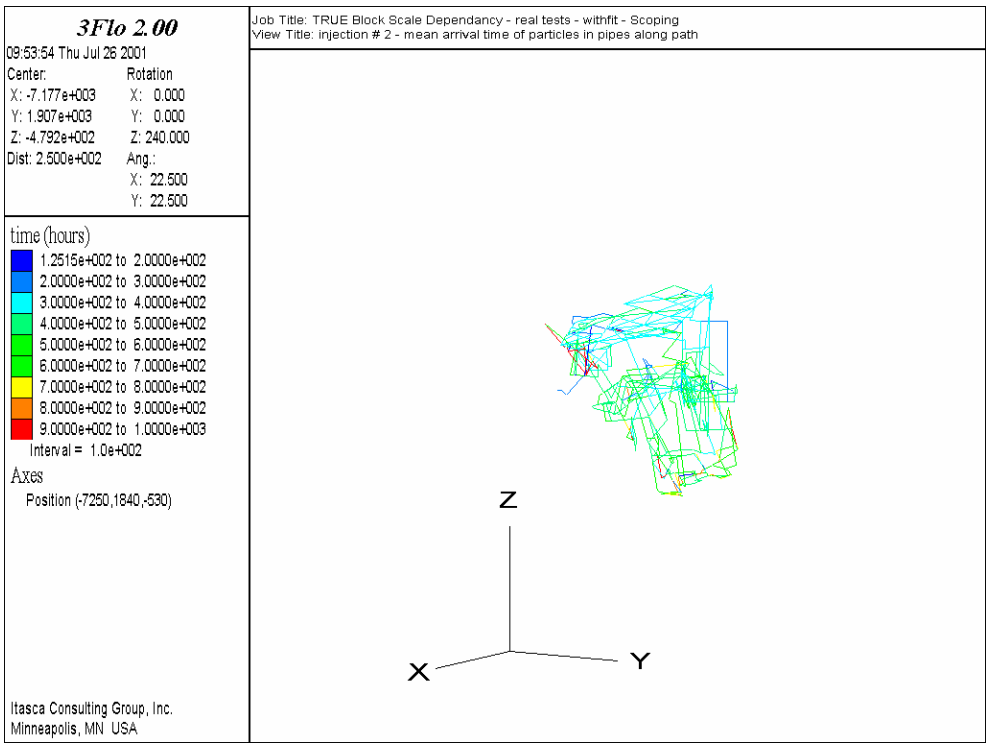

Figure 4-33 *: Scoping Characterisation stage model – Calibrated simulations Mean arrival time in hours of tracers in pipes along path for the simulated tracer Test 2*

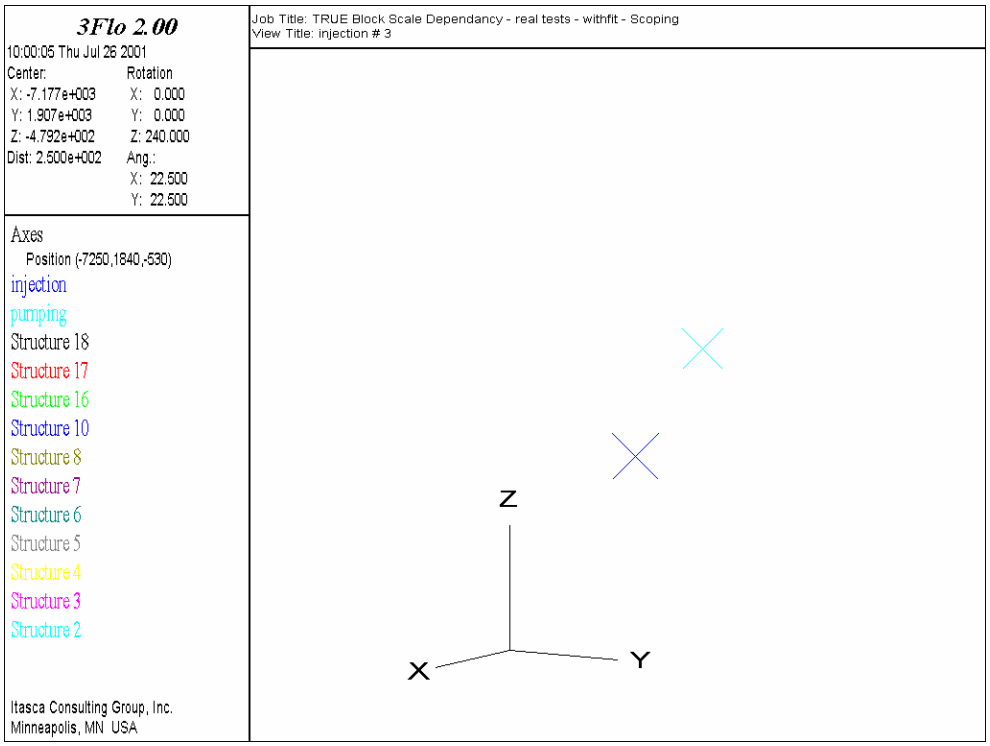

Figure 4-34 *: Scoping Characterisation stage model – Calibrated simulations Flow path for the simulated tracer Test 3*

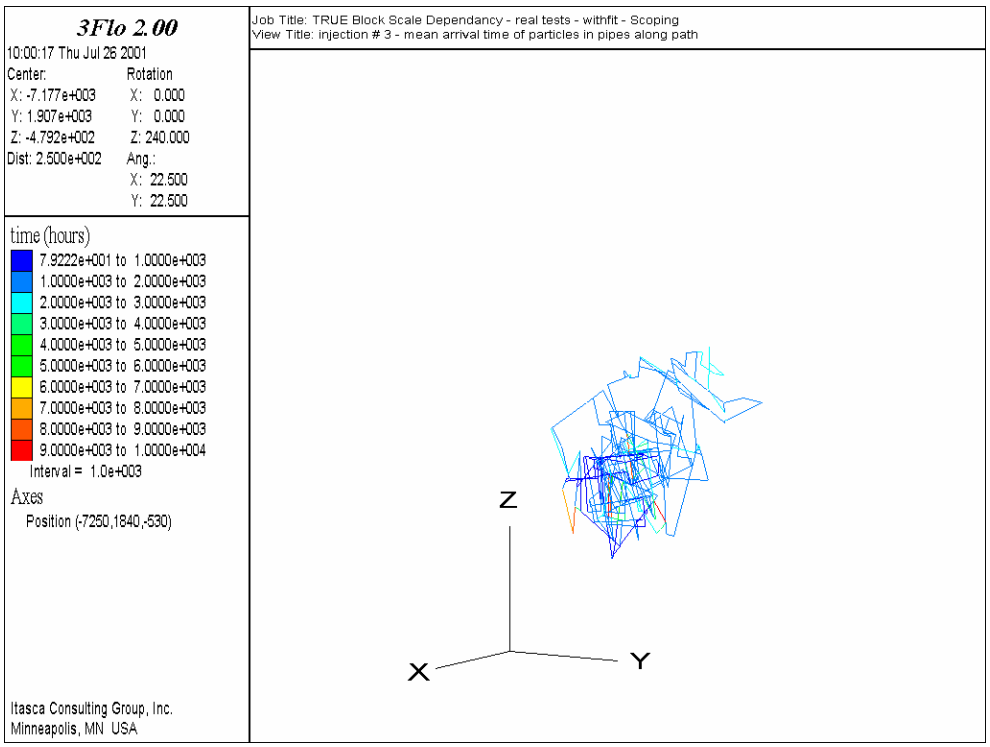

Figure 4-35 : *Scoping Characterisation stage model – Calibrated simulations Mean arrival time in hours of tracers in pipes along path for the simulated tracer Test 3*

5 Comparsion of the synthetic tracer test for each model

In this chapter, we consider the "March 2000 calibrated" response as our reference, and look at how the response in the other models deviates from this reference for the simulated synthetic tracer tests. For this purpose, we order the models in inverse chronological order as in Chapters 0 and 4, but we present first the calibrated runs, then the non-calibrated ones, so that the reference run is shown first.

Table 5-1 gives the test sections chosen in the March 2000 model to perform the 10 synthetic tracer tests. The same amount of tracer (3 g) is injected with the same injection flowrate (3 10^{-8} m^3/s) and pump with a flowrate of 2 10^{-5} m^3/s. In this way, radially converging tests are simulated.

Table 5-2 gives the test sections chosen in the March 1999 model to perform the 10 synthetic tracer tests, corresponding to the sections closest to the ones in the March 2000 structural model. The injection parameters (mass injected and flow rates) remain unchanged.

Table 5-3 gives the points chosen in the Preliminary Characterisation model to perform the 10 synthetic tracer tests, corresponding to the closest representative points chosen for the March 2000 structural model. If a point is too far away from an existing structure (test 9), then a background fracture is chosen. The injection parameters (mass injected and flow rates) remain unchanged.

Table 5-4 gives the points chosen in the Scoping Characterisation model to perform the 10 synthetic tracer tests, corresponding to the closest representative points chosen for the March 2000 structural model. If a point is too far away from an existing deterministic structure, then a background fracture is chosen (tests 3, 5, 9 and 10). The injection parameters (mass injected and flow rates remain unchanged.

Figure 5-1 to Figure 5-8 show the responses of the four "calibrated" models to the ten tracer tests, while Figure 5-9 to Figure 5-16 show the responses of the four "forward" models.

Looking at Figure 5-4 for example, one can notice that the mass fluxes on the right of the Figure all lay on a straight line with a slope of one. This is a direct result of the "discretization" of the random walk transport method, that represent the tracer by particles with equal finite masses. When the mass flux becomes very small, at any time step, either one or zero particle arrives at the pumping section. When no particle arrives, a flux of zero is computed and the log is arbitrarily set to zero, hence the numerous crosses on the zero line in the figure. When one particle arrives, the flux computed is the particle mass divided by the time step. Since a time step that increases linearly with time is used, a flux varying inversely with time is obtained, producing the negative unit slope. All curves in the mass-flux vs. time log-log plots should therefore be considered only until they reach this unit slope line.

If we compare the results for the March 2000 model, with both calibrated properties (Figure 5-1) and non-calibrated properties (Figure 5-9), we notice that a number of tests yield similar responses: tests 1, 4, 6, and 10. Among the tests that yield different responses are the four tests where injection is in a structure that has been modified by calibration (tests 2, 3, 5 and 9, injected in Structures # 13, 19, 13, and 23, respectively). The other two tests (7, 8) should be discarded as influenced by the boundaries. We clearly see how the calibration, by lowering porosities or increasing transmissivities, speeds up the mass arrival for the tracers that are injected in the modified structures, while it has little influence for tracers exploring other parts of the network.

If we now compare the responses for the calibrated March 2000 (Figure 5-1) and March 1999 (Figure 5-3) models, the differences are much more drastic: only test 1 yields a similar response, while all other test responses vary in time by at least one order of magnitude, although the geometries of the structures, if not identical, are quite similar (compare Figure 3-11 with Figure 3-1111). Indeed, the responses of the other two "calibrated" models (Figure 5-5 and Figure 5-7) show the same type of behaviour, while if we compare for any of the three earlier models its "calibrated" and "forward" response, we see quite similar responses (compare Figure 5-3 and Figure 5-11 for example).

From this we can state that the four successive hydro-structural models are clearly very different in their response to tracer tests performed in the area of interest, while the change in properties we effected during calibration has a small influence on the overall response.

Table 5-1 : Points selected in the *3FLO* Tracer test stage model to perform the 10 synthetic tracer tests

Test number	Injection section	*3FLO* Interval in borehole (m)	*3FLO* structures included
1	KA2563A:S4	185-188	20
2	KA2563A:S3	204-206	13
3	KA2563A:S2	209-214	19
4	KI0023B:P5	68.5-70.0	21
5	KI0023B:P4	84.75-86.2	13
6	KI0025F:R5	41.5-42.5	7
7	KI0025F:R4	68.5-70.5	20
8	KI0025F02:P7	51-54.4	6
9	KI0025F02:P7	56.1-63	23
10	KI0025F02:P6	60-68.3	22
Pumping well	KI0025F03:P5	70.0-77.5	20

Table 5-2 : Points selected in the *3FLO* Detailed characterisation stage model to perform the 10 synthetic tracer tests			
Test number	**Injection section**	***3FLO* Interval in borehole (m)**	***3FLO* structures included**
1	KA2563A:S4	187-190	20
2	KA2563A:S3	205-207	13
3	KA2563A:S2	230-235	19
4	KI0023B:P5	41.0-42.0	7
5	KI0023B:P4	84.75-86.2	13
6	KI0025F:R5	61.0-62.0	6
7	KI0025F:R4	86.0-88.0	20
8	KI0025F02:P7	51-54.4	6
9	KI0025F02:P7	70.0-76.9	20
10	KI0025F02:P6	60-68.3	22
Pumping well	KI0025F03:P5	70.0-77.5	20

Table 5-3 : Points selected in the *3FLO* Preliminary Characterisation stage model to perform the 10 synthetic tracer tests			
Test number	**Injection section**	***3FLO* Interval in borehole (m)**	***3FLO* structures included**
1	KA2563A:S4	187-190	20
2	KA2563A:S3	203-205	13
3	KA2563A:S2	223-228	19
4	KI0023B:P5	44.5-45.5	6
5	KI0023B:P4	84.75-86.2	13
6	KI0025F:R5	74.0-75.0	6
7	KI0025F:R4	86.0-88.0	20
8	KI0025F02:P7	55.5-56.5	6
9	KI0025F02:P7	69.0-70.0	one BF*
10	KI0025F02:P6	84.0-85.0	9
Pumping well	KI0025F03:P5	66.5-74.0	20

* BF : back-ground fracture

Table 5-4 : Points selected in the *3FLO* Scoping Characterisation stage model to perform the 10 synthetic tracer tests			
Test number	**Injection section**	***3FLO* Interval in borehole (m)**	***3FLO* structures included**
1	KA2563A:S4	198-199	18
2	KA2563A:S3	209-210	8
3	KA2563A:S2	213-214	one BF*
4	KI0023B:P5	42.0-43.0	18
5	KI0023B:P4	85.5-87.8	two BF*
6	KI0025F:R5	44.0-45.0	7
7	KI0025F:R4	72.0-73.0	6
8	KI0025F02:P7	52.0-52.4	6
9	KI0025F02:P7	52.5-59.4	two BF*
10	KI0025F02:P6	74.0-79.0	three BF*
Pumping well	KI0025F03:P5	47.0-48.0	6

* BF : back-ground fracture

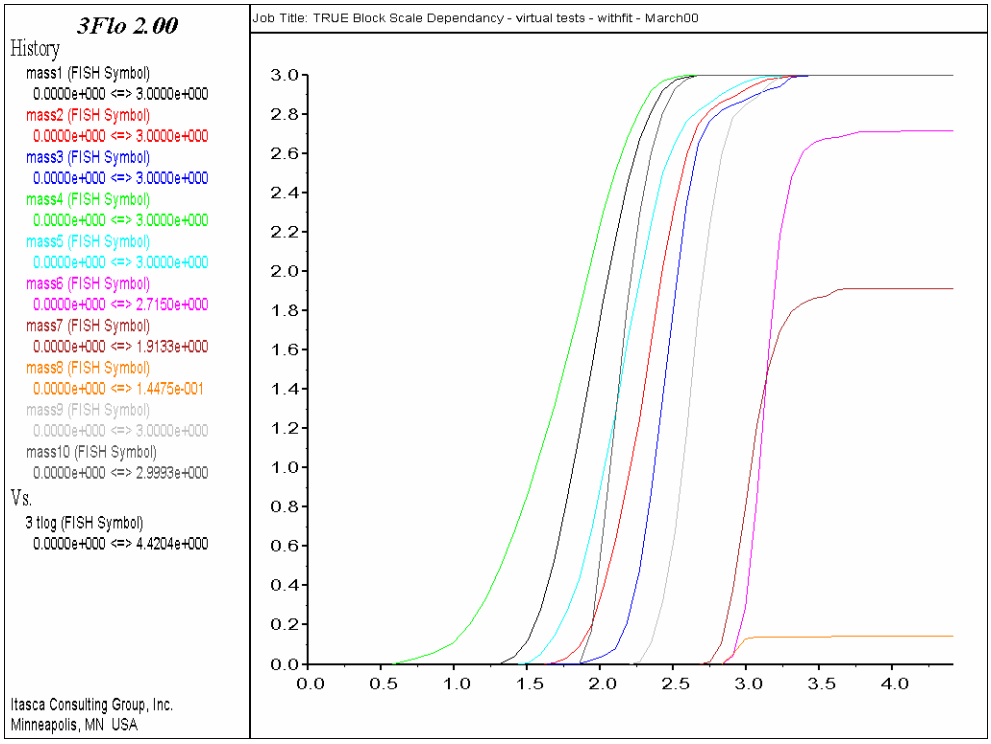

Figure 5-1 : *Tracer test stage model – Calibrated simulations*
Cumulative mass arrival in pumping well for the 10 synthetic tracer tests vs log (time in hours)

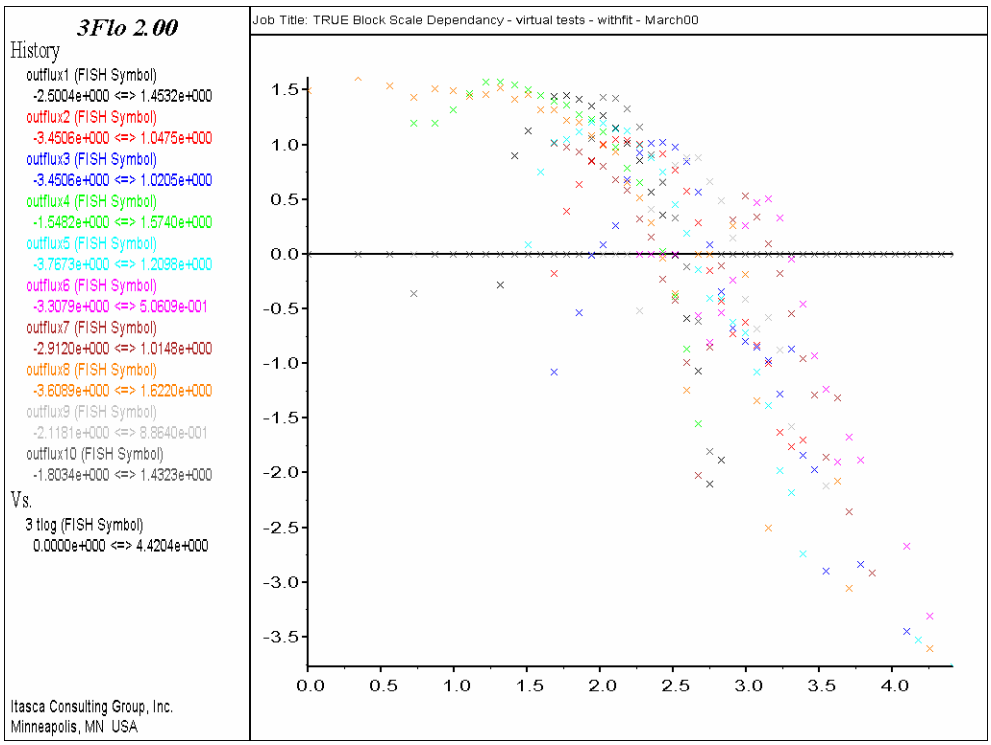

Figure 5-2 : *Tracer test stage model – Calibrated simulations*
Mass flux (mg/h) for the 10 synthetic tracer tests vs time in hours (log-log)

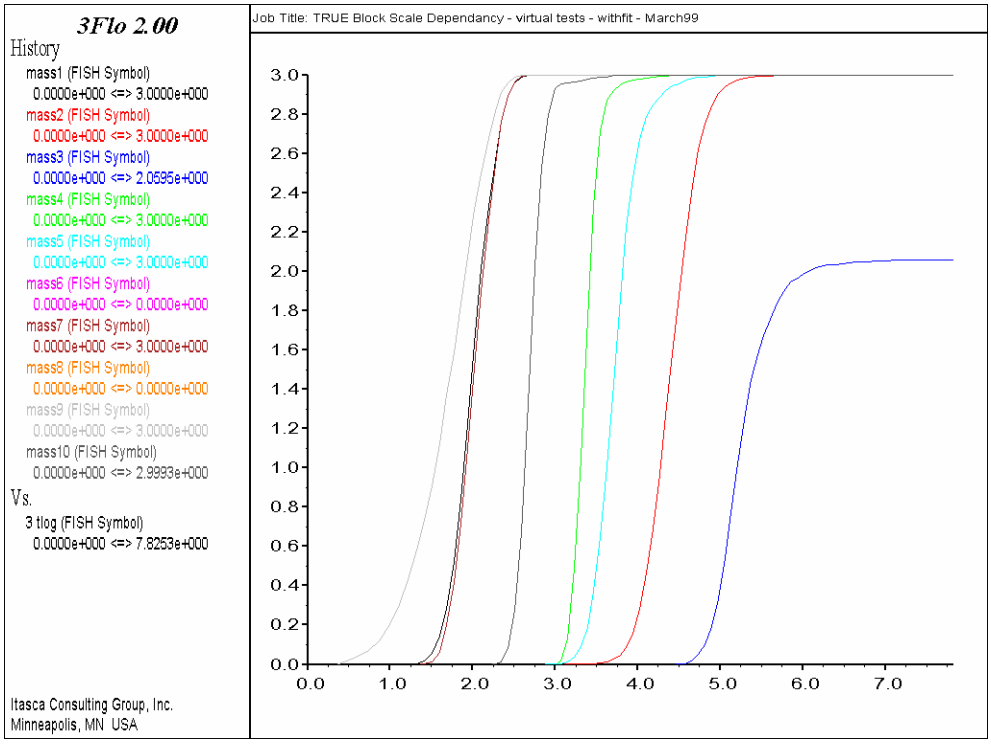

Figure 5-3 : *Detailed Characterisation stage model – Calibrated simulations Cumulative mass arrival in pumping well for the 10 synthetic tracer tests vs log (time in hours)*

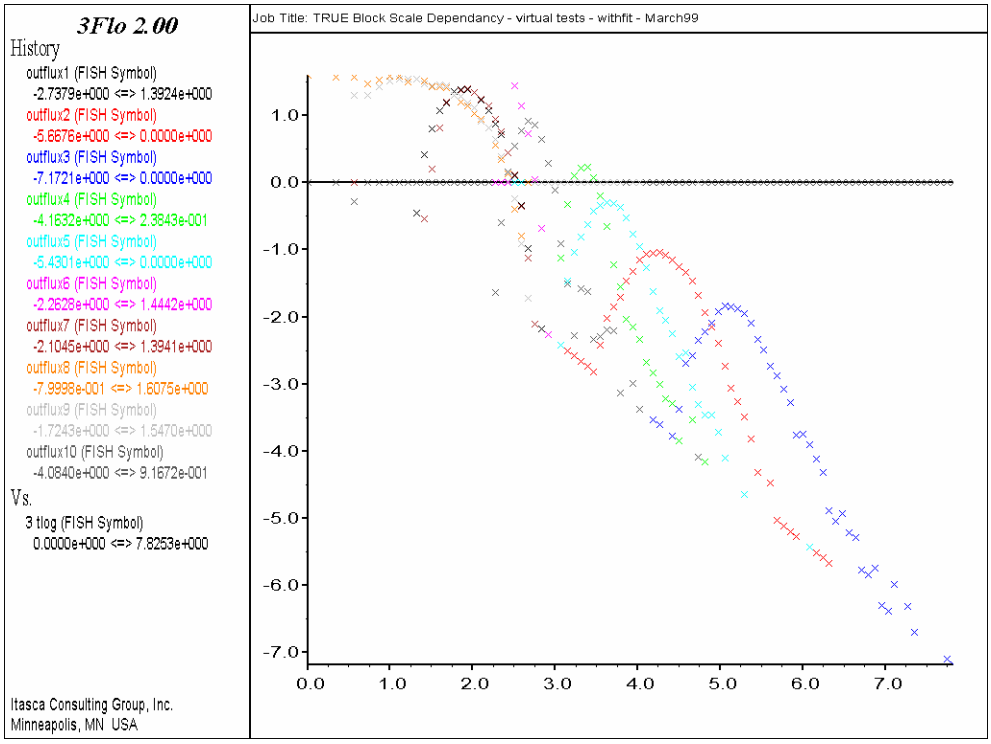

Figure 5-4 : *Detailed Characterisation stage model – Calibrated simulations Mass flux (mg/h) for the 10 synthetic tracer tests vs time in hours (log-log)*

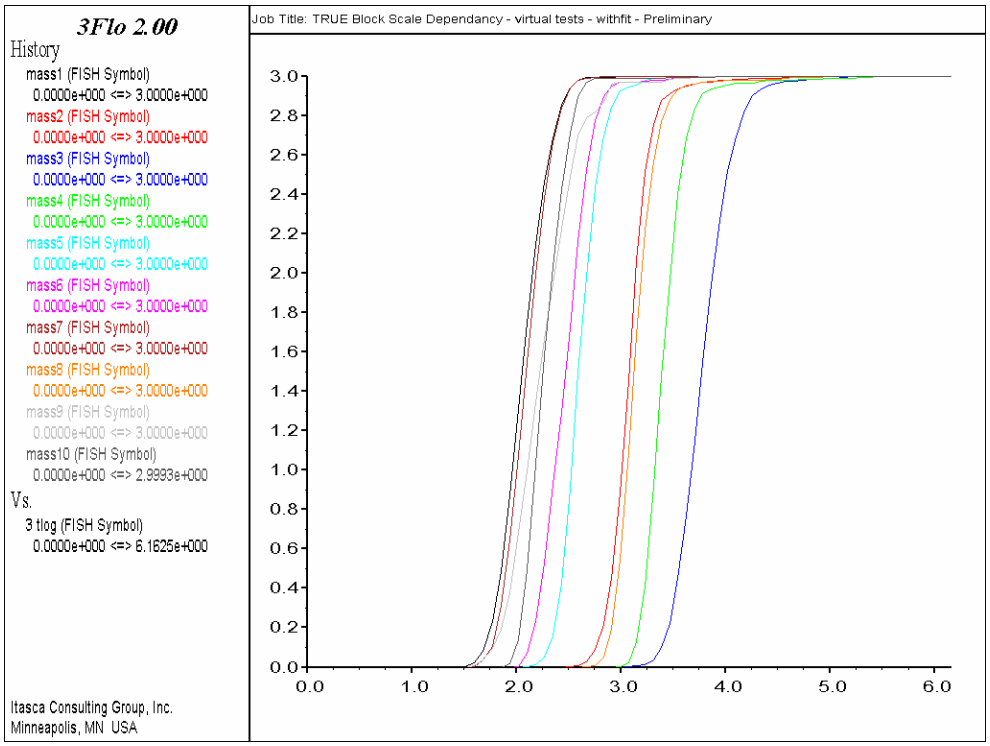

Figure 5-5 : *Preliminary Characterisation stage model – Calibrated simulations Cumulative mass arrival in pumping well for the 10 synthetic tracer tests vs log (time in hours)*

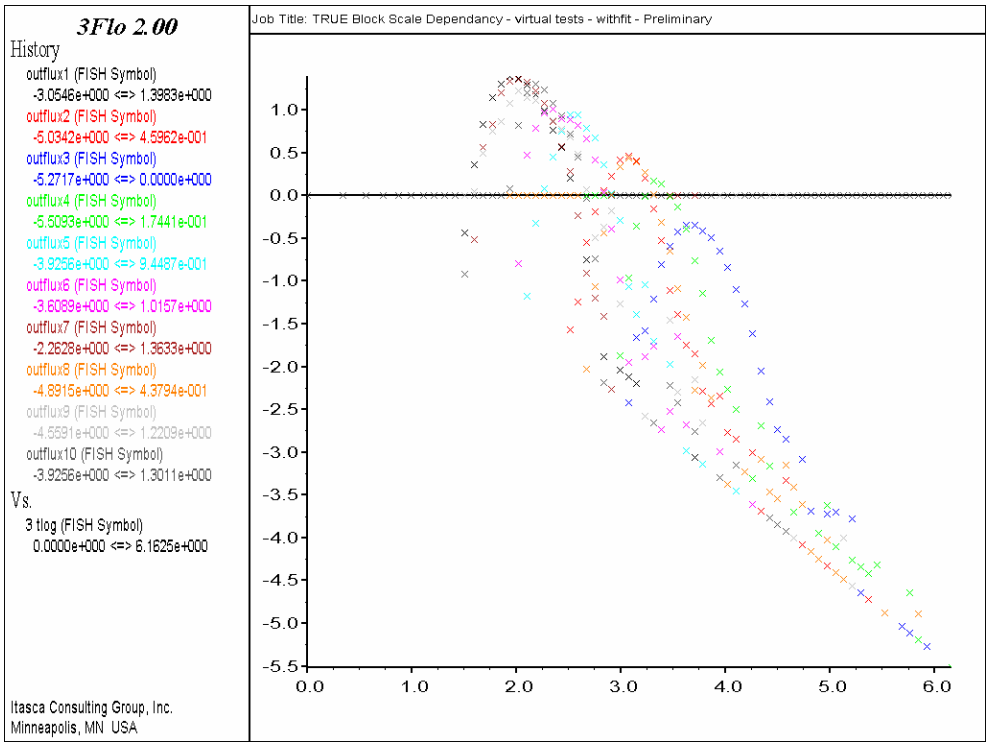

Figure 5-6 : *Preliminary Characterisation stage model – Calibrated simulations Mass flux (mg/h) for the 10 synthetic tracer tests vs time in hours (log-log)*

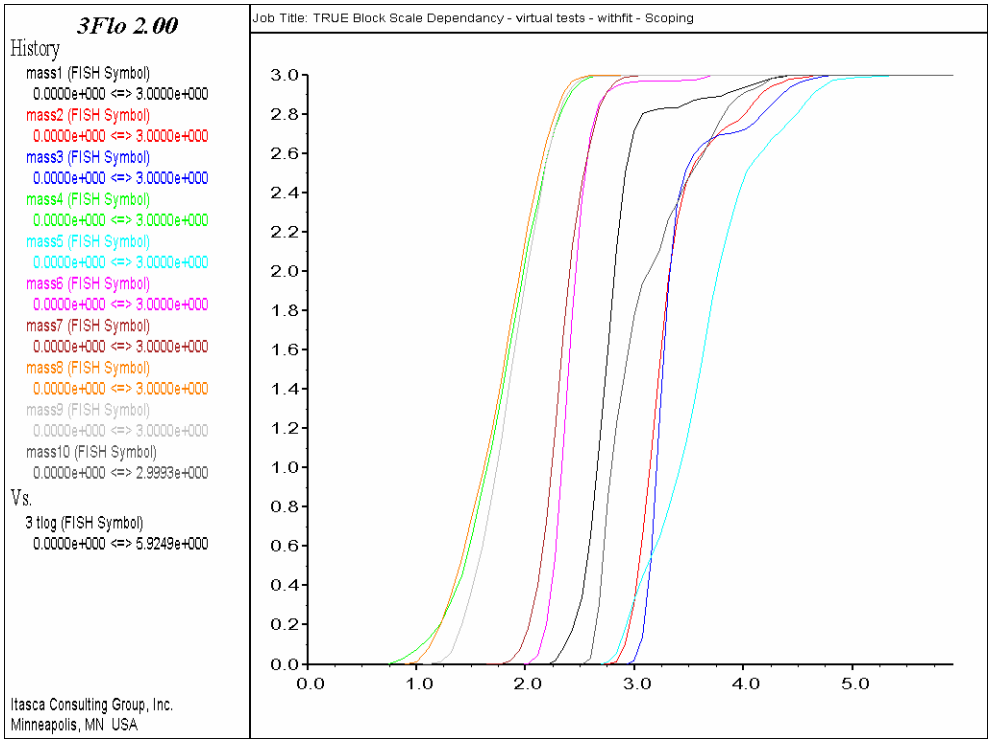

Figure 5-7 : *Scoping Characterisation stage model – Calibrated simulations Cumulative mass arrival in pumping well for the 10 synthetic tracer tests vs log (time in hours)*

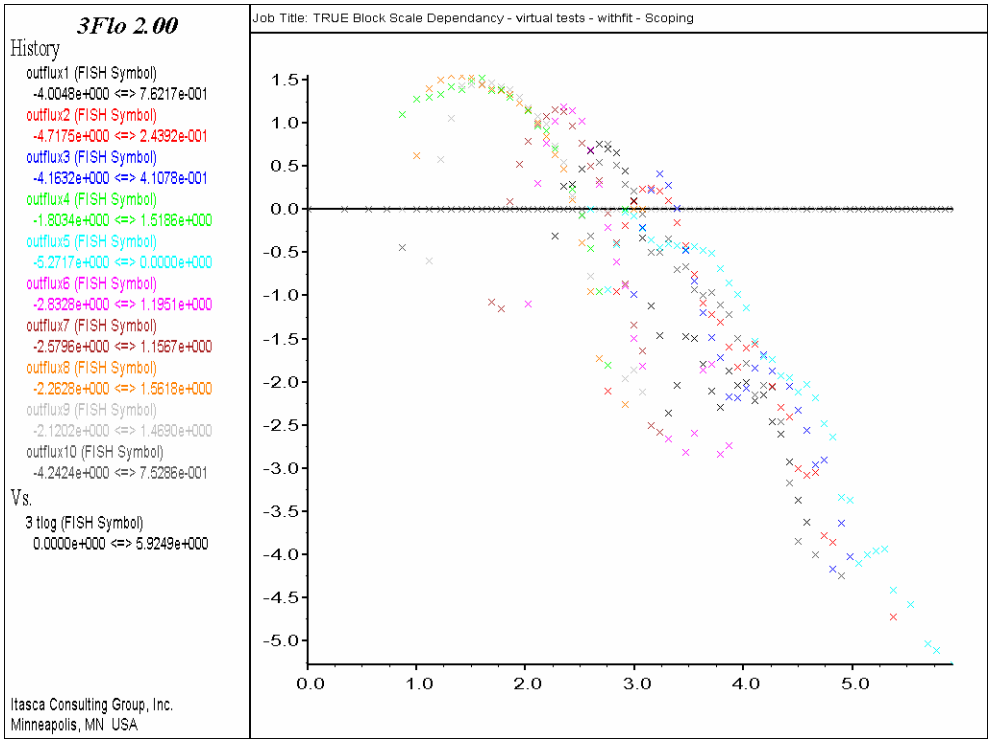

Figure 5-8 : *Scoping Characterisation stage model – Calibrated simulations Mass flux (mg/h) for the 10 synthetic tracer tests vs time in hours (log-log)*

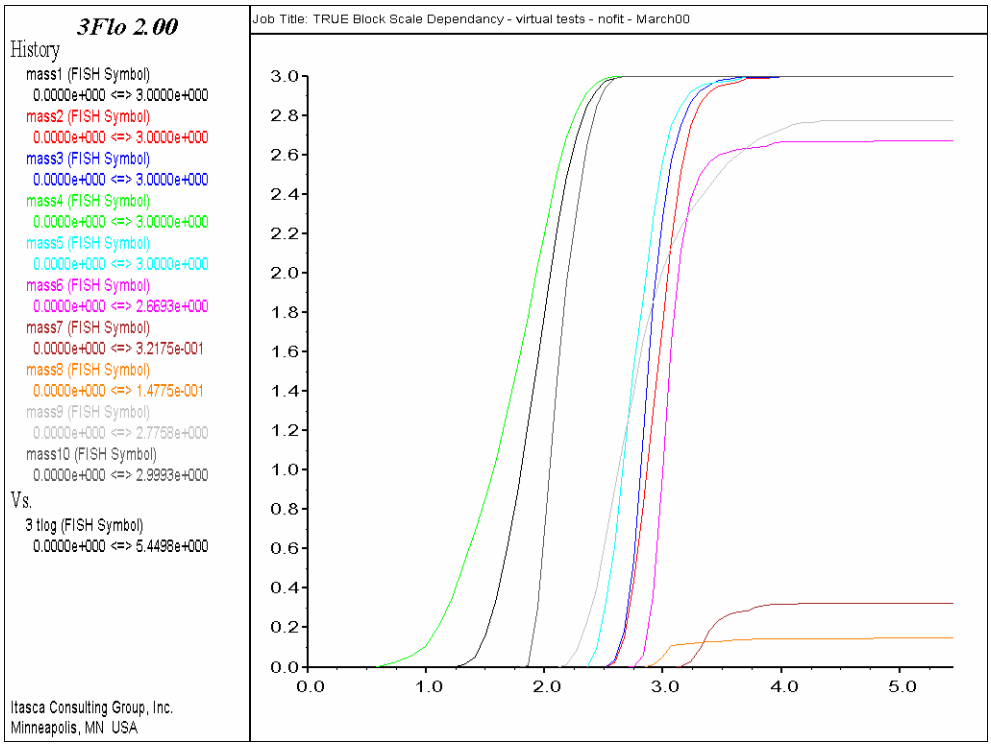

Figure 5-9 : *Tracer test stage model – Forward simulations*
Cumulative mass arrival in pumping well for the 10 synthetic tracer tests vs log (time in hours)

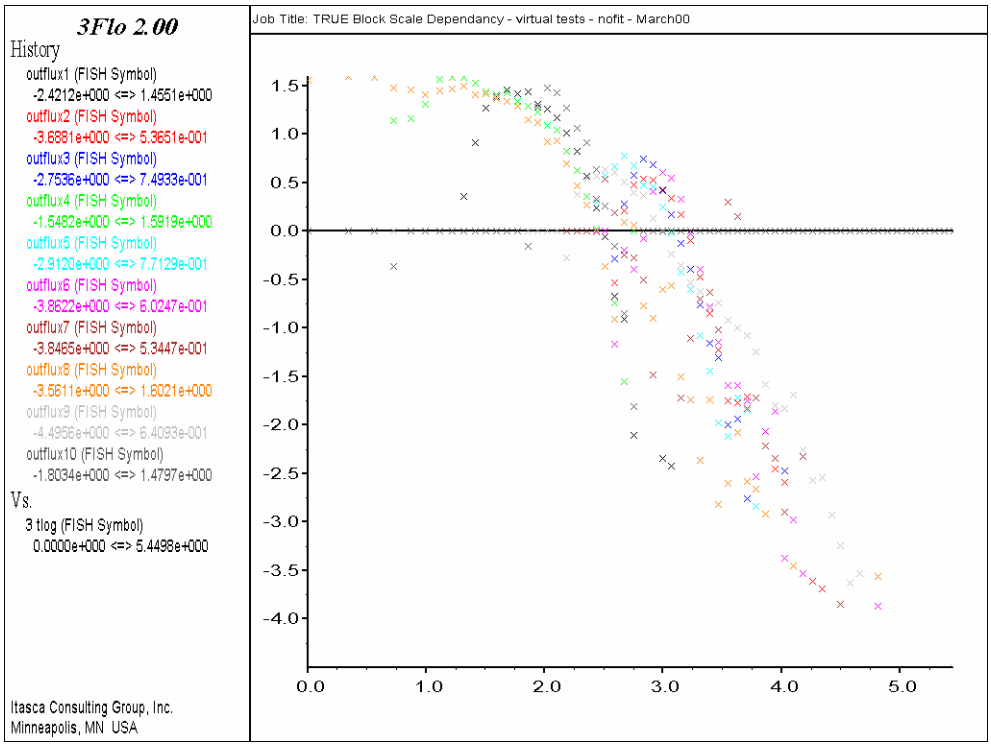

Figure 5-10 *: Tracer test stage model – Forward simulations*
Mass flux (mg/h) for the 10 synthetic tracer tests vs time in hours (log-log)

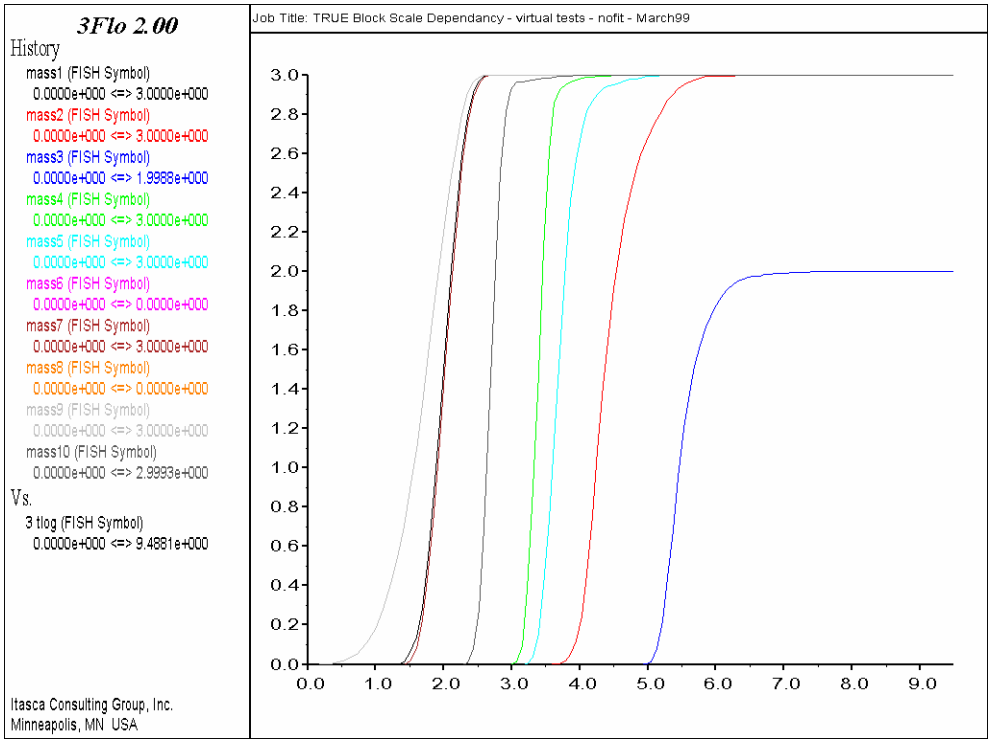

Figure 5-11 : *Detailed Characterisation stage model – Forward simulations Cumulative mass arrival in pumping well for the 10 synthetic tracer tests vs log (time in hours)*

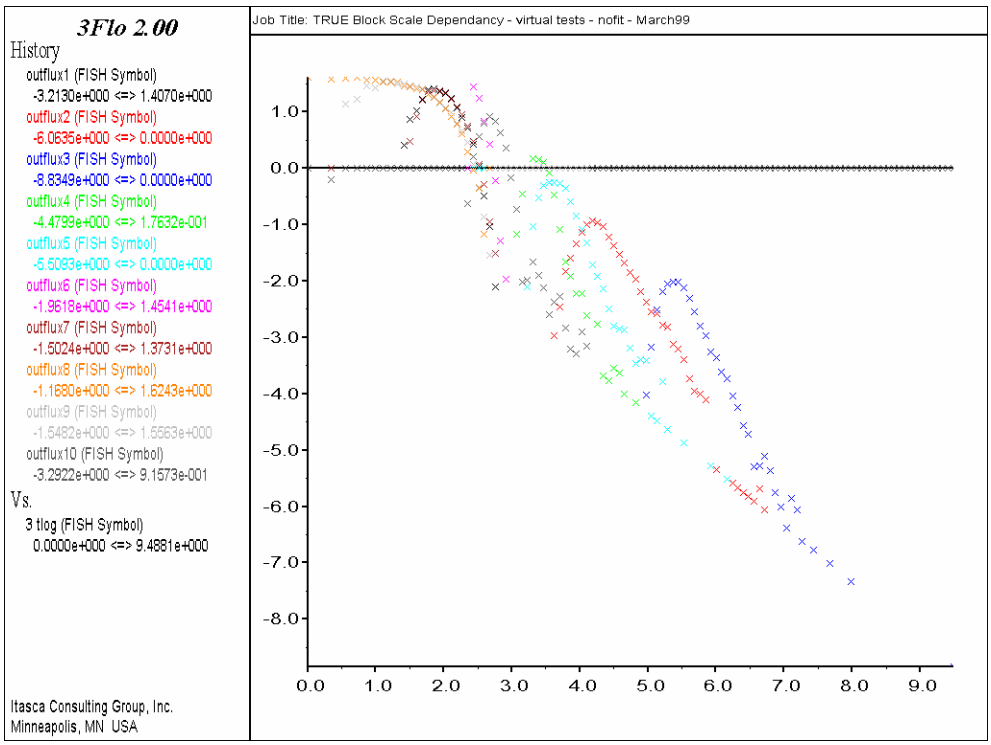

Figure 5-12 : *Detailed Characterisation stage model – Forward simulations Mass flux (mg/h) for the 10 synthetic tracer tests vs time in hours (log-log)*

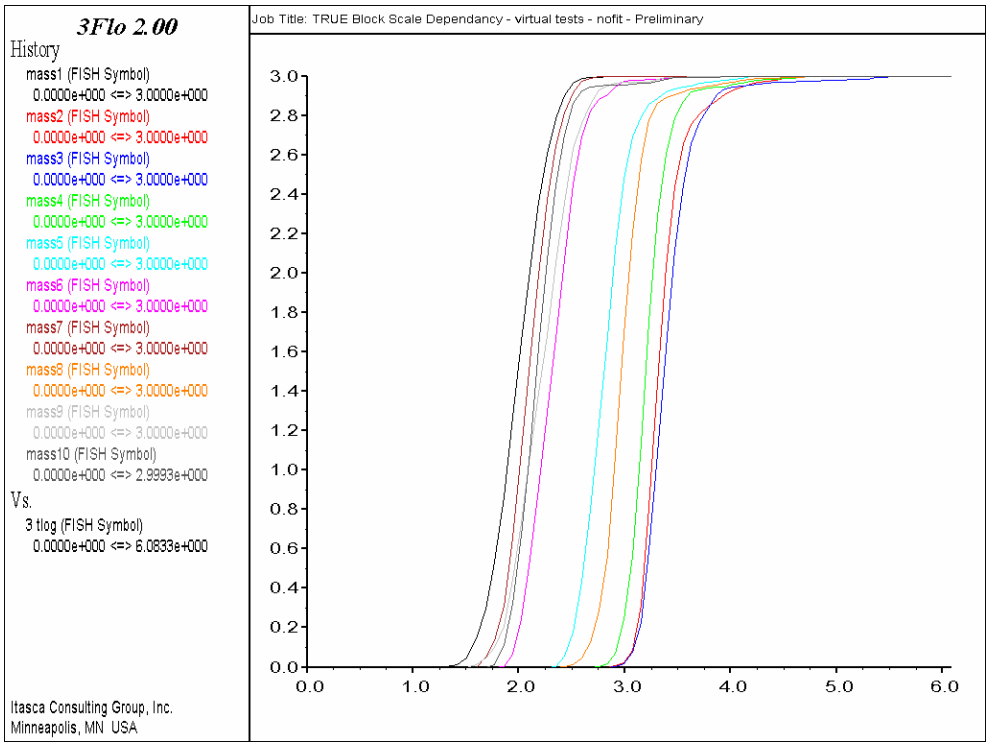

Figure 5-13 : *Preliminary Characterisation stage model – Forward simulations Cumulative mass arrival in pumping well for the 10 synthetic tracer tests vs log (time in hours)*

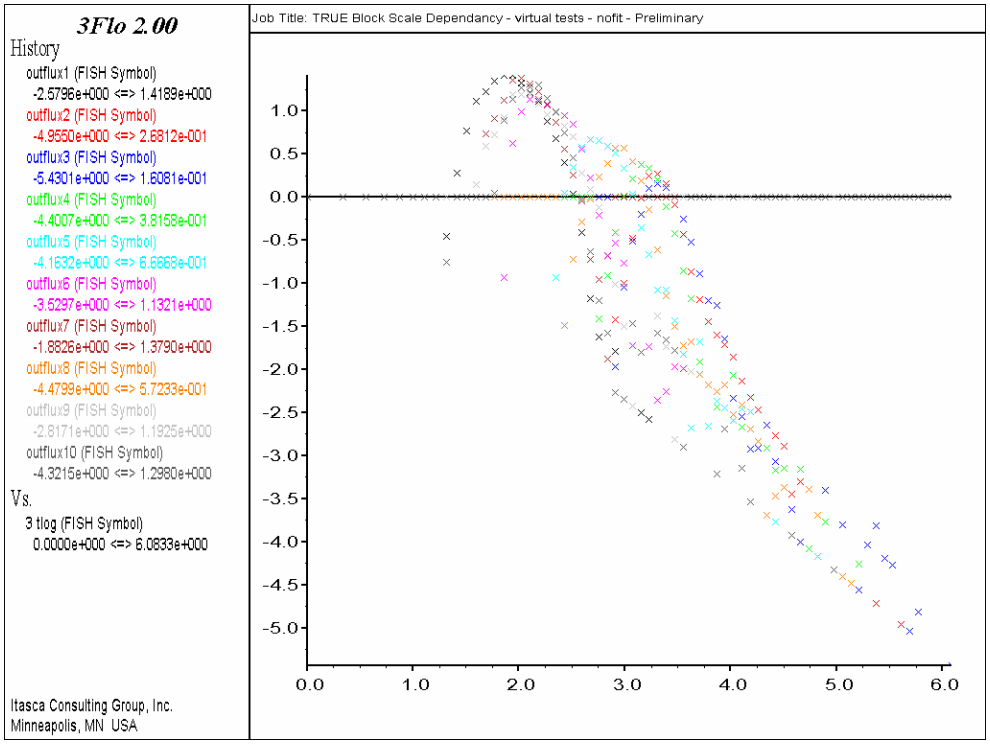

Figure 5-14 : *Preliminary Characterisation stage model – Forward simulations Mass flux (mg/h) for the 10 synthetic tracer tests vs time in hours (log-log)*

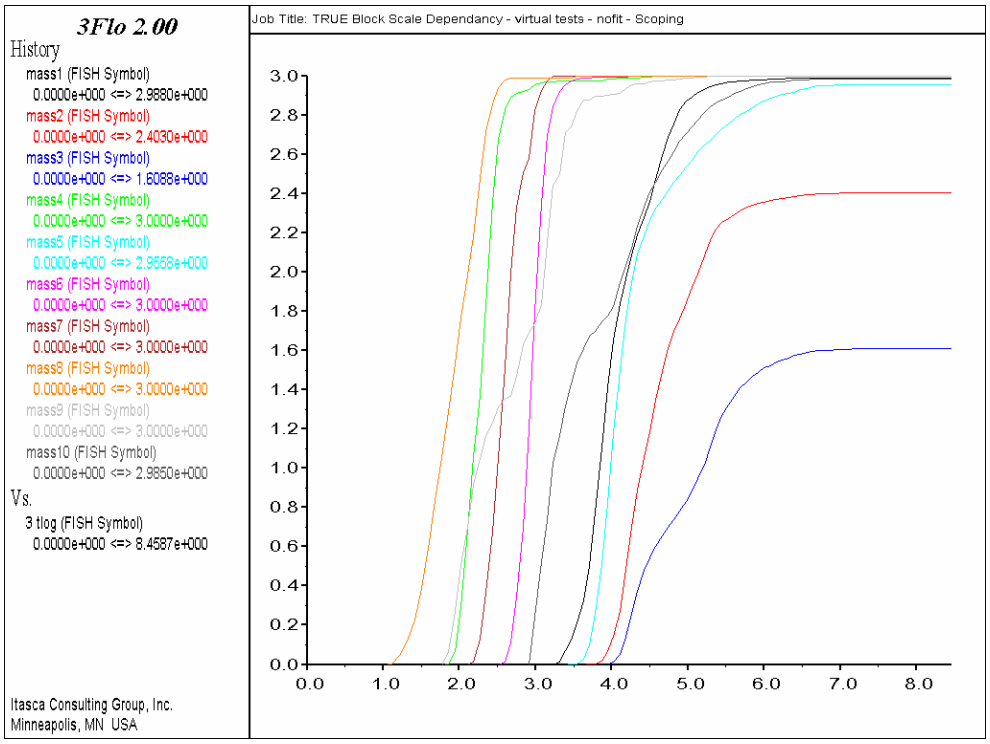

Figure 5-15 : *Scoping Characterisation stage model – Forward simulations Cumulative mass arrival in pumping well for the 10 synthetic tracer tests vs log (time in hours)*

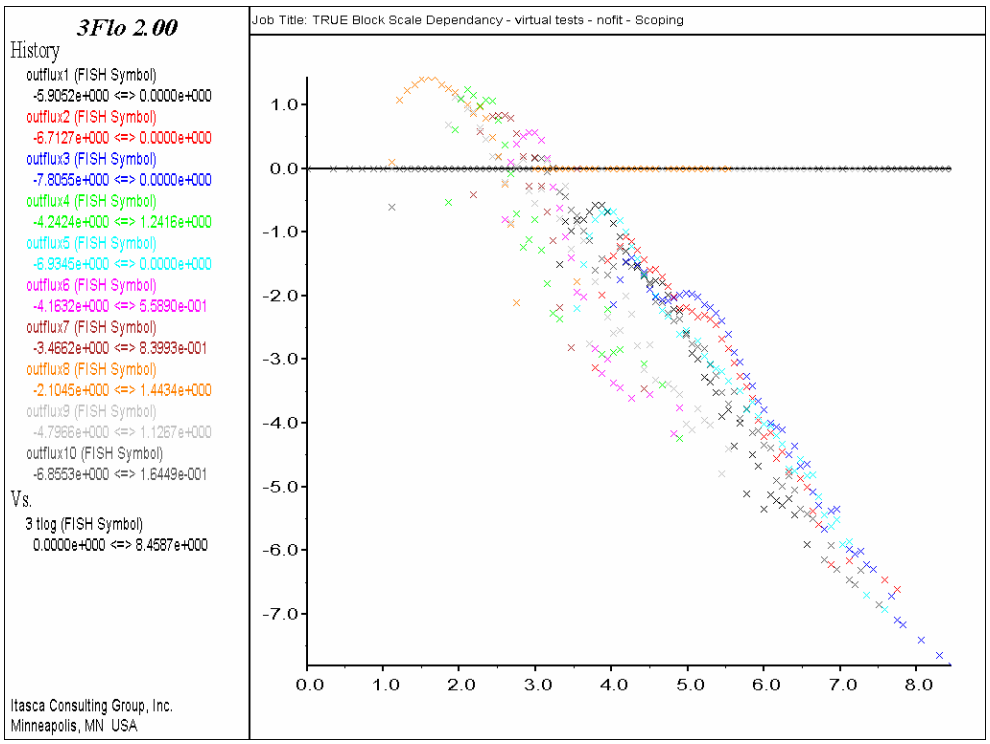

Figure 5-16 : *Scoping Characterisation stage model – Forward simulations Mass flux (mg/h) for the 10 synthetic tracer tests vs time in hours (log-log)*

6. Conclusion

Four successive numerical models of the TRUE Block Scale volume were constructed, corresponding to four successive stages of the characterisation process: Scoping, Preliminary Characterisation, Detailed Characterisation (March 1999 model), and current knowledge (March 2000 model). Three tracer tests, from stage B-2 of the tracer test stage were simulated. The models take into account both structures, specified deterministically, and stochastic background fractures, with conditioning when data are available.

Twelve "forward" simulations (three tracer tests per model) were carried out, using the properties specified by the hydro-structural models available at each stage, choosing the injection points, in the earlier models, to represent the real injection points as closely as possible. In these tests, we could see how the variation of the transport path geometry, from model to model, progressively looses similarity between the test responses, until the Scoping Characterisation model response has very little to do with the tracer migration based on March 2000 model response.

The transport parameters of the March 2000 model were calibrated simultaneously to the three tests, by changing the properties of three structures, # 13, 19 and 23. This resulted in a significantly improved, if not perfect, fit between the simulated and measured tracer breakthrough. On the other hand, using the new properties in the other older models essentially did not improve their response, which still were degraded when going back in time.

Ten "synthetic" injection points were simulated. These "synthetic" points do not correspond to any real experimental result, but comparing the behaviour of the tracers injected there from model to model shows that the four successive hydro-structural models are clearly very different in their response to tracer tests performed in the area of interest, while the change in properties imposed during calibration has a small influence on the overall response.

In this work, we could see clearly how, in the TRUE Block Scale site, the response to tracer tests is strongly conditioned by the hydro-structural model used. Because most of the tracers travel along a limited number of interpreted deterministic structures, proper knowledge of their geometry is a requisite for being able to represent the actual in situ network behaviour realistically.

Bibliography

ANDERSON P., LUDVIGSON J-E, WASS E. & HOLMQVIST M. (2000a) : TRUE Block Scale Project - Interference Tests, Dilution tests and tracer Tests, Phase A, *Swedish Nuclear Fuel and Waste Management Company, Äspö Hard Rock Laboratory, SKB International Progress Report IPR-00-28*.

ANDERSON P., WASS E., HOLMQVIST M. & FIERZ T. (2000b) : TRUE Block Scale Project - Tracer Test Stage – Tracer Tests, Phase B, *Swedish Nuclear Fuel and Waste Management Company, Äspö Hard Rock Laboratory, SKB International Progress Report IPR-00-29*.

ANDERSON P., BYEGARD J., DERSHOWITZ B., DOE T., HERMANSON J., MEIER P., TULLBORG E-L, WINBERG A. (2002a) : TRUE Block Scale Project – Final Report 1. Characterisation and model development. *Swedish Nuclear Fuel and Waste Management Company, Aspö Hard Rock Laboratory, SKB International Progress Report IPR-02-13*.

BILLAUX D. (1990) : "Hydrogéologie des milieux fracturés. Géométrie, connectivité, et comportement hydraulique ». *Thèse de doctorat, Ecole Nationale Supérieure des Mines des Paris, Document BRGM 186, Orléans, France.*

BILLAUX D. and GUERIN (1993) : Connectivity and the Continuum Approximation in Fracture Flow Modeling, *Proceedings of the Fourth Annual International Conference on High Level Radioactive Waste Management. pp. 1118-1122 Vol. 2, American Society of Civil Engineers, New-York.*

DOE T. (2001) : TRUE Block Scale Project - Reconciliation of the March'99 structural model. *Swedish Nuclear Fuel and Waste Management Company, Äspö Hard Rock Laboratory, SKB International Progress Report IPR-01-41*.

HERMANSON J., FOLLIN S. & WEI L. (2001a) : TRUE Block Scale Project – Structural analysis of fractures traces in boreholes KA2563A and KA3510 and in the TBM tunnel. *Swedish Nuclear Fuel and Waste Management Company, Äspö Hard Rock Laboratory, SKB International Progress Report IPR-01-70*.

HERMANSON J., & AL. (2001b) : TRUE Block Scale Project – Sept'98 Structural Model, *Swedish Nuclear Fuel and Waste Management Company, Äspö Hard Rock Laboratory, SKB International Progress Report IPR-01-42*.

WINBERG ANDERS (ED.) (1999) : TRUE Block Scale project - Scientific and Technical Status. Position report prepared for the second TRUE Block Scale review meeting, Stockholm November 17, 1998*, Swedish Nuclear Fuel and Waste Management Company, Äspö Hard Rock Laboratory, SKB International Progress Report IPR-99-07*.

Appendix

3FLO
3D Flow and Transport code in porous and/or fractured media

NAME, VERSION and ORIGIN OF THE CODE

3FLO, Version 2.0

Developed by ITASCA Consultants S.A., France

GENERAL DESCRIPTION

3FLO is a software applied to the 3D simulation of flow and transport in porous and/or fractured media. *3FLO* can solve various types of problems :

- Flow in fracture networks, represented by a 3D network of pipes, or one-dimensional channels.
- Flow (saturated or not) in porous media :
  - ✓ Using classical (Galerkine) 3D Finite Elements, or
  - ✓ Using Mixed-Hybrid 3D Finite Elements.
- Flow in interacting fractures and porous media.
- Pollutant transport, simulated by the particle tracking method.
- Geochemistry, coupled or not with solute transport, taking into account most types of reactions.
- Mathematical morphology, for analyzing the geometrical properties of fractured media.

3FLO can also be used to perform fracture network statistical studies (i.e. : orientation, size, transmissivity, etc... distributions). It also provides a complete logic to process geometrically fracture and pipe networks, in order to "trim" them. For example, a command can be used to discard all dead-ends (useless if the problem at hand is only steady-state).

FEATURES of *3FLO*

FISH macro-language

One unique feature of ITASCA codes is the FISH macro-language. This language can be used to create new variables, meshing procedures, particle detection procedures, specifically designed graphical output, to develop any type of statistical distribution for use in fracture generation or other, and so on.

Fracture generation, and assignation of conductivities

3FLO generates a 3D network of pipes on any assembly of planes:

- Generation of a network of flow planes, with any shape, and detection of their intersections,
- On each plane, generation of a network of regularly spaced or Poisson distributed channels,
- Connection of the channels from one plane to another, through the fracture intersections, to constitute the pipe network.

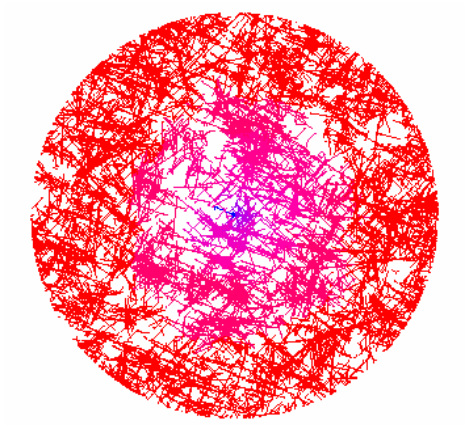

A 3D fracture network

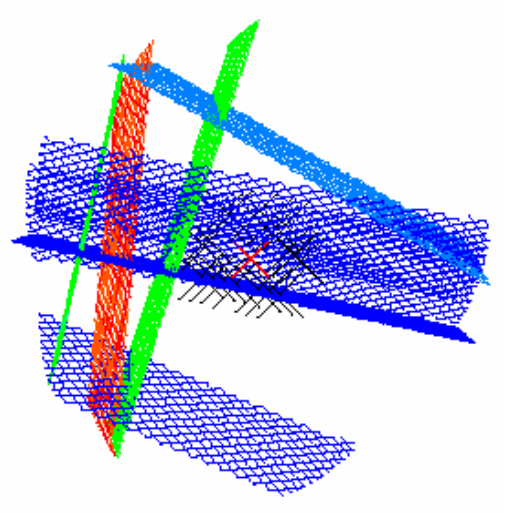

Color-coded conductivities of fractures

Once a network is built, one can assign to each pipe a conductivity taken from a statistical distribution (constant, uniform, normal, lognormal -truncated or not-, or any other distribution to be programmed in *FISH)*.

An aperture map known in an image format (pixels) can also be simulated using a grid of pipes.

The Mathematical Morphology module can quantify the geometrical properties of the space between the fractures (size, shape, connectivity distributions, and so on).

3D mesh generation

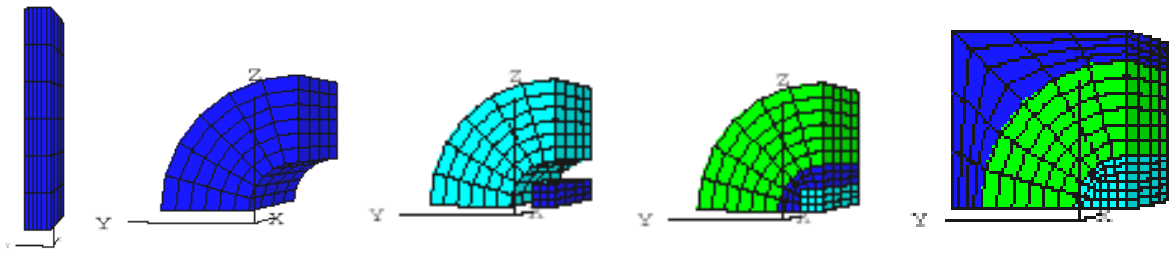

Successive steps to obtain a desired 3D geometry

3FLO's power lies in applying to its basic hexahedron or tetrahedron shapes the *FISH* macro-language. Using it, one can reshape, duplicate, join, delete, and so on, the basic building blocks, and thus create a 3D "jigsaw puzzle" that fills the final geometry of the model.

Flow simulations

3FLO computes steady or transient flow in :

- ✓ 3D fracture networks,
- ✓ 3D porous media (steady or transient flow, saturated or not),
- ✓ 3D fracture networks coupled with porous media.

The flow equation is solved in 1D classical Finite Elements for fractures, and in 3D Mixed-Hybrid Finite Elements for porous media. These elements are more precise than classical (Galerkine) 3D elements, and allow a proper computation of face fluxes. This helps minimizing solute transport computation errors. For example, flow and transport problems are solved without difficulty in models with permeability contrasts of 10^7.

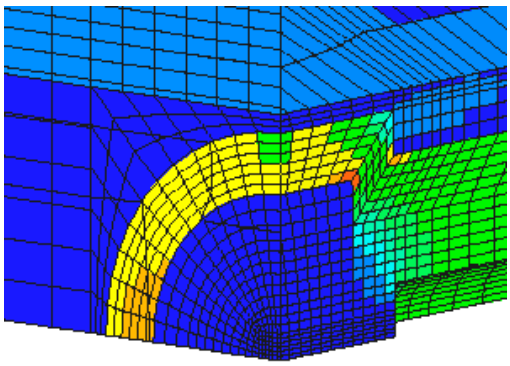

Average flow velocities in a nuclear waste storage model. Permeability contrast is 10^7 between plug (blue) and periphery (yel-green)

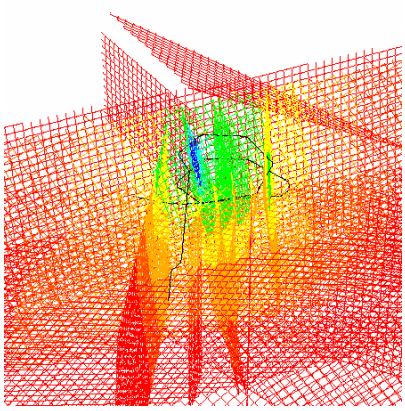

Heads due to the excavation of the access drift to the Äspö (Sweden) underground laboratory

Solute transport

3FLO simulates solute transport using the Random Walk method. In 3D fracture networks, flow is one-dimensional everywhere in pipes, except at intersections. Dispersion is therefore only longitudinal, and is "completed" by the full mixing occurring at intersections. In 3D elements, once the flow field is known, the movement of a particle can be separated in :

- ✓ a longitudinal displacement along a flow line, simulating advection and longitudinal dispersion, and
- ✓ two orthogonal transversal displacements simulating transversal dispersion.

Diffusion can also be represented.
Solute transport may be simulated in "mixed" model, with both fractures and a porous medium. 1D-3D interaction may then receive special treatment.

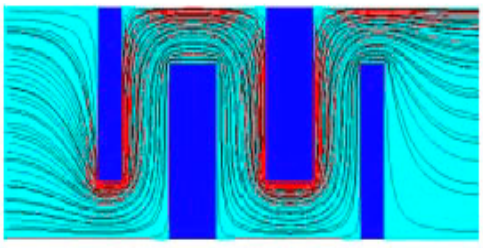

Particle tracks in a theoretical validation example. The permeability ratio between the two materials is 10^7

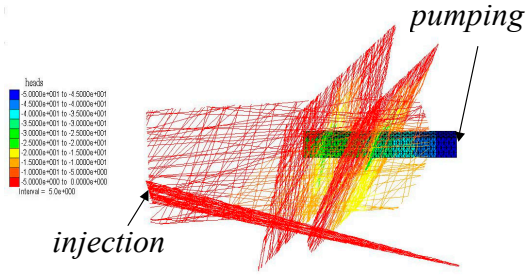

Heads in a coupled fractures-and-continuum model

Geochemistry, and coupling with transport

3FLO can account for most types of reactions: precipitation, dissolution, adsorption, oxydo-reduction, kinetics.

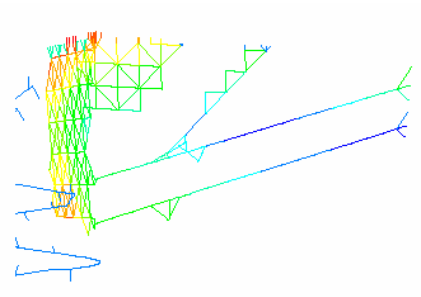

pH in a fracture network